Investigation of Factors affecting Warping of Triboard

A thesis

Submitted in fulfilment

Of the requirements for the degree

Of

Masters of Engineering

In

Chemical and Process Engineering

By

Rahul Sharma

UNIVERSITY OF CANTERBURY

2016

ABSTRACT

Warping is a common phenomenon found in wood products and is defined simply as a distortion from "flatness". The loss of bound water in the wood products causes the product to shrink and 'bow' or 'cup' which occurs if the shrinkage is uneven. Wood warping is an unwanted phenomenon for customers and results in huge losses for New Zealand wood industry in an order of millions of dollars per year. This Masters Project is focused on studying a particular type of wood composite known as Triboard which is manufactured by JNL based in Kaitaia, New Zealand. Triboard is a three-layered panel with a strand board in the core and two MDF fibre layers in the surfaces. JNL has been having issues with warping of this product for some time. In this project, the objectives are to conduct a study to better understand and quantify the factors which cause the Triboard warping, and subsequently to reduce the warping of this product.

The experiment was designed to investigate the effects of certain variations in the recipe which were adhesive loading on strands and fibres, moisture content in strands and fibres, hot press temperature and fibre thickness. 27 Triboard samples were made at AICA in New Plymouth, and fibre and strands were supplied JNL, Kaitaia. A base recipe for the control board was used first to make a board of control.

Preliminary tries were first conducted to determine the hot press platen temperature in the control recipe which was found to be 170^0C. Other parameters in the control recipe were as follows: Board thickness 21 mm (a 3mm MDF layer on each of the outer surfaces, a 15 mm strand layer in the core); MUF solution loading on fibres: 18.2% (solid loading 12%); –––pMDI solution loading on strands 4.5% (solid loading 3%). Following this, 4 sets of experiments were conducted to investigate effects of resin loading (Set A), moisture content of MDF fibres and strands (Set B), hot press platen temperature (Set C) and thickness of MDF fibre layers (Set D). Moisture content gradient, modulus of elasticity of MDF layers and strand layers, and gradient of strain/stress were measured for each sample board. The criteria for assessing board warping is the difference between maximum and minimum stresses, and the asymmetrical distribution of the stress (quantified as the difference between two surface stresses).

Set A had 9 samples each with variations in adhesive loading both in fibres (MUF from 15.2% to 22.8%) and in strands (pMDI from 4% to 5.3%). The results show that the moisture content at the surface layers (5% to 6.5%) were much lower than that in the core layers (9% to 10%). The average moisture content changed from 7.1% to 8.3% depending on the resin loading. Triboard sample A7 with the lowest resin loadings (15.2% MUF, 5.3% pMDI) was observed to have the lowest average moisture content of 7.10% dry basis while sample A3 with highest resin loadings (22.8% MUF, 4.53% pMDI) had the highest moisture content of 8.30%.

From the results of large slices, Triboard sample A6 with highest MUF loading on fibres (22.8%) and lowest pMDI loading (4%) was found to be the most stable with the lowest stress difference and most symmetrical stress distribution. For this sample, the difference between the maximum stress and the minimum stress was 5.45 MPa and the asymmetrical stress distribution gave a value of 0.48 MPa. However, sample A9 with 22.8% MUF loading and 5% pMDI loading was the most unstable having a stress difference of 11.66 MPa and stress asymmetry of 6.68 MPa. The same tests were done on small slices in the same way as for large slices to check if they agree. According to strain measurement on small slices, A6 sample maintained the most stable with the least stress difference (9.84 MPa) and most asymmetrical stress distribution (-3.95 MPa). **Therefore, it is most likely that the high MUF loading on MDF fibres improves the board stability, but the pMDI loading on the strands within the tested range has less impact.**

Set B examined the effects of moisture content of fibres (from 10% to 15%) and strands (from 9% to13%) during preparation. Varying moisture in fibres was a very difficult job and so only 6 samples were prepared. The average moisture content of samples for this set was found to increase with added moisture to the fibres and the strands. With increase in fibres and strands moisture contents, moisture contents of the boards at surfaces changed from 4.5% to 6.7% while the core moisture contents changed from 9.5% to 13.8%. The average moisture content changed from 7.18% to 10.19%. Sample B2 with fibre moisture content of 12% and strand moisture content of 9% showed the lowest stress difference (2.83 MPa) and stress asymmetry (2.83 MPa) while sample B6 with fibre moisture content of 15% and strand moisture content of 13% had the most stress difference (29.28 MPa) and the most stress asymmetry (22.88 MPa). **This concludes that control of the moisture contents of fibres and strands is very important. Moisture content of**

strands should be controlled at 9% or lower while maintaining the fibre moisture content at 11-12%. The small sliced samples gave different results however, based on the stress/strain gradient through the board thickness, these results are less reliable due to significant moisture loss during long time and storage and slicing.

Set C investigated the effect of hot press temperatures. Results from large slices suggest that average moisture content decreased with increase in hot press temperature. Sample C1 (hot press temperature of 160 ^{0}C) had the highest moisture content of 7.47% and sample C3 (pressed at 180 ^{0}C) had the lowest average moisture content of 6.71%. Large slices show that **the most stable board was sample C3 (with hot press temperature of 180°C) which had the maximum stress difference of 5.83 MPa and stress asymmetry of -2.63 MPa. Sample C1 was the most unstable board with maximum stress difference of 13.07 MPa and stress asymmetry of 13.07 MPa.** This is probably due to residual stresses being relieved at high temperatures. Once again, the results from small slices do not agree with the above results which are less reliable.

Set D examined the effect of varying fibre layer thickness in both top and bottom layers. The thickness of MDF layers was varied between 2-3.5 mm. Results from the large slices show that the average moisture content did not change significantly with varying the fibre thickness from 6.79% to 7.64%. It is found that sample D4 (2 mm MDF fibre layer on the top and 2.5 mm on the bottom) to be the most stable with the maximum stress difference of 5.39 MPa and stress asymmetry of 1.11 MPa, respectively. Sample D6 (2 mm MDF on the top and 3.5 mm on the bottom) was found to be the worst with maximum stress difference and stress asymmetry of both 12.34 MPa. Results from small slices show a slightly different result. Sample D5 (2mm MDF on the top; 3 mm MDF on the bottom) was the most stable with maximum stress difference and stress asymmetry of both 2.27 MPa. Sample D3 (3mm MDF on the top; 3mm MDF on the bottom) was the most unstable board with difference of maximum stress of 21.49 MPa and asymmetric stress of 15.18 MPa. Therefore, it is suggested that **the MDF fibre layer on the top should be 0.5 to 1 mm thinner than the MDF layer on the bottom for the 21 mm thick Triboard.**

Acknowledgements

I would like to thank my supervisor Professor Shusheng Pang for his immense amount of time and constructive advice throughout this project. It was a very valuable learning experience.

Many thanks to Mrs. Hilary Kearns for organizing my trips to JNL and AICA and also supplying material for the experimental work.

I am thankful for the financial support from JNL Ltd., New Zealand and Callaghan Innovation through the Fellowship Fund.

I would like to acknowledge the following people for their support without which this investigative study of Triboard would not be possible:

1. Philip Marsh
2. Carol Cowling
3. Chris VanKooten
4. David Waite
5. Jackie Nairn
6. Jeny Collins
7. Kevin Tait
8. Kirsty Galvin
9. Trevor Pearson
10. Wiremu Still
11. Danny O' brien

A special acknowledgement to Ron Mallet for the immense hard work in sawing of the boards and to SCION for letting us borrow a multi-saw machine for small slices. Also to Alan Poynter based in Model Structures Laboratory at University of Canterbury for showing me how to use an Instron machine for 3-point bend testing and advice on results.

TABLE OF CONTENTS

List of Figures

List of Tables

List of Abbreviations

EMC Equilibrium moisture content

FSP Fiber saturation point

JNL Juken New Zealand based in Kaitaia

MC Moisture content

MDF Medium density fibreboard

MOE Modulus of elasticity

MOR Modulus of rupture

MUF Methylene urea formaldehyde

pMDI Polymeric di-isocyanate

RH Relative humidity

CHAPTER 1

INTRODUCTION

Wood occurs naturally as an organic composite of cellulose fibers embedded in a matrix of hemicellulose and reinforced with lignin. Wood has been a major source for fuel and construction material for almost as long as humans have been around. Continual progress in wood technology over many years has given rise to specialised engineered wood products for application with requirement of specific performance. This project focuses on the investigating the reasons for the warping of Triboard product manufactured by JNL situated in Kaitaia. Triboard is produced from the combination of a core layer which is similar to strand board and two layers of fibres on the surfaces which are similar to fibreboard (MDF).

Imported from its homeland in California, radiata pine had its debut in New Zealand in 1850s where it proved to have a fast growth rate while also being versatile in all types of soils including coastal sands, heavy clays, gravels and even volcanic ash deposits. As of now, New Zealand has 89% of this species of the 1.8 million hectares of plantation forests (NZ Ministry of Agriculture and Forestry, 2007). Figure 1-1 provides a distribution of plantations across New Zealand (Arbor Resources Ltd, 2015). From Figure 1-1 it is found that Central North Island leads the number of plantations (577,385) in New Zealand.

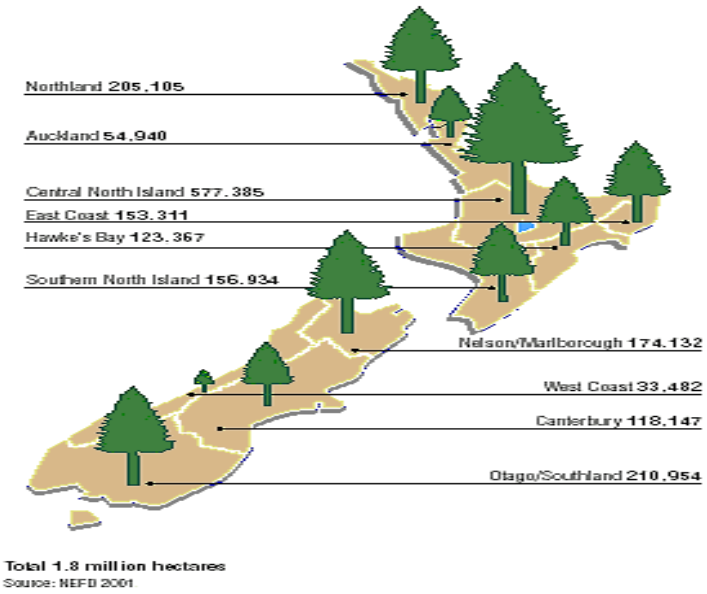

Figure 1-1: Distribution of plantations forest in New Zealand

1.1 BACKGROUND OF PROJECT AND EFFECT OF WARPING ON COMPANY

Triboard has a wide variety of applications such as panel housing, structural walls, floors, fire rated doors and inter – tenancy walls, solid core doors, bracing panels, bench tops and shelving. About 60% of production at JNL is shipped to WoodOne in Japan. JNL has conducted investigation into the warping of Triboard and concluded that there is minimal difference between warp observed at JNL and WoodOne, indicating the fact that the warping begins at the mill before transportation. This is a concerning problem for customers. The warping of Triboard is a serious problem since customers could lose interest in the company's products and this could result in substantial losses for industry. The customers may demand replacement for the original Triboard product and there is no sure way to tell if the replacement will warp or not. Also, this does not allow the company to keep a guarantee on it manufactured wood panels. Warping can be of many types and this would depend on the axis (Longitudinal, Radial or Tangential) around which it takes place. (Figure 1-2).

The major factors causing warping in Triboard is believed to be the residual stresses which are, in turn, induced by uneven shrinkage or swelling of board when it loses or gains bound water (inside the cellular structure) below the Fiber Saturation Point (FSP). FSP is defined as the point where the wood cell structure is filled with bound water while no free water exits in the cell lumen cavities which is about 30% moisture content at room temperature. If the moisture is not evenly distributed within the board, stresses are generated within the board causing distortion and warping.

Figure 1-2: Types of warping observed in wood panels (after Wikipedia)

There are five different types of warping for a piece of solid wood displayed in Figure 1-2 namely, (1) bow which is distortion along the length of the panel, (2) crook which is distortion along the length in the direction of the edges, (3) kink which is the result of a knot in the tree, (4) cup which is distortion causing only the edges to be raised and (5) twist, where the two edges twist on opposite sides of the plane. It is suspected that JNL's Triboard product may be experiencing bowing and twisting of panels since the other three types of distortions have not been observed. The next section highlights some important investigations conducted.

1.2 WORK CONDUCTED PRIOR TO COMMENCEMENT OF MASTERS PROJECT

JNL Triboard mill at Kaitaia has two production lines, one being a continuous production line and the second line is a batch production line in which a number of boards are made in each batch. Boards produced in both lines have warp issues. Boards from Line 2 are stacked in a pack (still at high temperature) and it has been observed that the boards on top and bottom layers behave differently from the rest of the stack.

Before this Master project commenced, JNL had conducted initial investigations. In addition, Pang et al. (2014) had performed a preliminary analysis and recommended some further trials at the Triboard manufacturing mill. Then JNL performed some mill trials on effect of fibre layer thickness on the Triboard warping.

Pang's investigation highlights the first investigative study conducted on warping of the Triboard product. The observations were:

a. Fibre moisture content before mat forming was around 11% and that for the strands were 8%. The overall board moisture was 5.6-6% after hot pressing.
b. After a batch of boards are stacked in a pack from Line 2, the top board/master board was observed to have a high degree of warping around the edges. This was not surprising since the entire top fibre layer area is exposed which promotes faster cooling resulting in shrinking. Also a cup/twist type distortion was observed.

Following this, a test for residual stress was conducted by making slices of fibre and strand from freshly made 24 mm Triboard in addition to a new set of slices being made for oven drying at 105^0C which would provide a moisture gradient. The slices examined for residual stress were examined for effect of the surrounding environment. This was done by keeping one set in a plastic bag and another set in the office overnight. Figure 1-3 shows bowing type of distortion in

the fibre layers. The difference in bowing in the slices left in the plastic bag and that left outside is significant. The set left in ambient conditions showed much worse bowing in comparison to the one left in plastic bag although it should not go unnoticed that there was almost no warping in the strand core and warping was concentrated in the top and bottom fibre layers. This is indicative of the fact that the moisture levels in the set left in ambient conditions were not in a state of equilibrium but rather had much higher moisture levels than equilibrium state which caused it to lose moisture and shrink in an attempt to get closer to EMC. Equilibrium Moisture Content (EMC) is known as a state of no gain or loss of moisture within the board and is discussed further in Chapter 2 where the literature is reviewed. Pang concluded from his investigation that the main reason for warping is a combination of moisture diffusion and residual stresses induced during hot pressing. Since the core strand is much thicker, it will assume a state of compression while the surface fibre layers being much thinner, assumes a state of tension. These could be reduced by achieving a balance between those two quantities.

Figure 1-3: Comparison of bowing between slices kept in ambient conditions and those wrapped in plastic bags

JNL has done a study in conjunction with WoodOne in Japan to try and counteract the effects of warping in Triboard by varying the fibre thickness on top and bottom layers. The three trials they have done are presented here (Interim Report #2: Warp Investigation):

Trial 1

21 mm thickness (3x packs) made with +/- 10% fibres and all other steps in production maintained constant. This trial indicated that average warp can be controlled by fibre thickness. The results of this trial are displayed in Table 1-1.

Note: Pack C is control pack which has no changes associated with it.

Average Warp excludes top and bottom board of the pack.

Table 1-1: Trial 1 results (After Interim Report #2)

Pack #	MDF 1	MDF 2	Average Warp
A	-2 kg	+2 kg	-3.4 mm
B	+2 kg	-2 kg	1.1 mm
C (Control)	0 kg	0 kg	-2.9 mm

So far, JNL has been experiencing warping in Triboard that has been negative (edges bowing down). Trial 1 results clearly display it is possible to change the direction of warping from negative to positive (edges bowing up) by having more fibre thickness on top layer. Pack C which is a control shows that equally thick fibre layers (with no extra addition on either side) have tendency to warp negatively as well.

Trial 2

Following the results of Trial 1, fibre addition was applied by +2 kg on top layers with no change to layer 2 and the warping was measured for Pack B. The results are displayed in Table 1-2.

Table 1-2: Trial 2 results (After Interim Report #2)

Pack #	MDF 1	MDF 2	Average Warp
1	+ 2 kg	0 kg	0.9 mm
2	+ 2 kg	0 kg	0.9 mm
3	+ 2 kg	0 kg	0.2 mm
4	+ 2 kg	0 kg	0.8 mm
5	+ 2 kg	0 kg	2.3 mm
6	+ 2 kg	0 kg	0.5 mm

Samples from Trial 2 were sent to WoodOne for further evaluation. Two packs were sent to WoodOne, Pack #032447180 and #032447181 and two sides of each pack were analysed for warping. Figures 1-4, 1-5 and 1-6 pertain to Pack #032447180 Side A. Plotting these profiles allowed the analysis of a board's behaviour in a pack. The aim was to investigate the degree of warp at three different conditions of the board: before wrapping, at WoodOne in Japan and after lamination. The boards tested were the Top 10, Middle 20 and Bottom 10 in a pack all having an additional +2 kg of fibre on top layer.

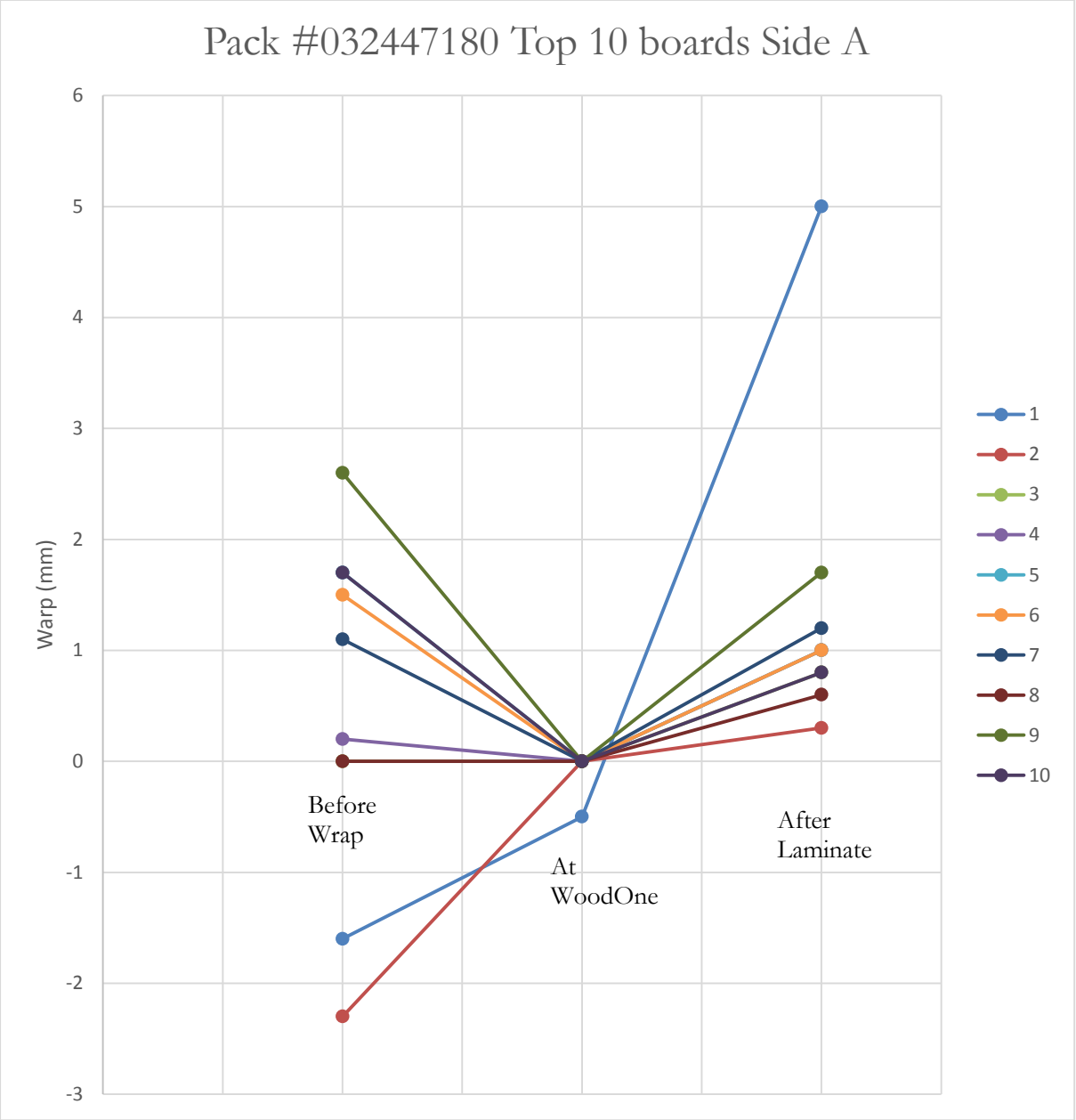

Figure 1-4: Pack #032447180 Side A Top 10 board warp profile after addition of +2kg fibre on top layer (After Interim Report #2)

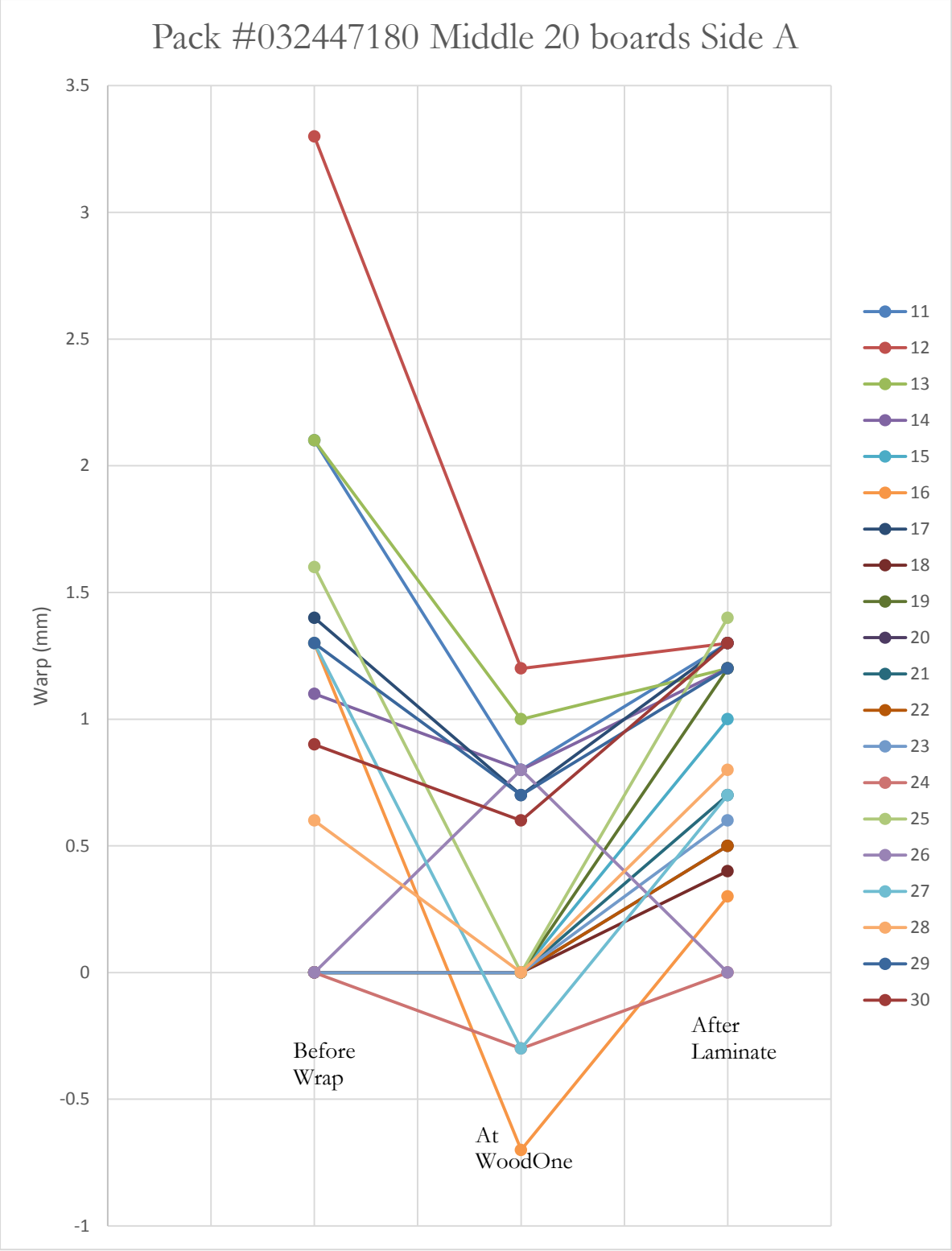

Figure 1-5: Pack #032447180 Side A Middle 20 boards warp profile after addition of +2kg fibre on top layer (After Interim Report #2)

Figures 1-4 and 1-5 show that there is a positive warp increase from the point where it is measured in WoodOne till after lamination. Figure 1-6 is contrasting however, and shows that there is a positive increase when measured at WoodOne and then a decrease after lamination.

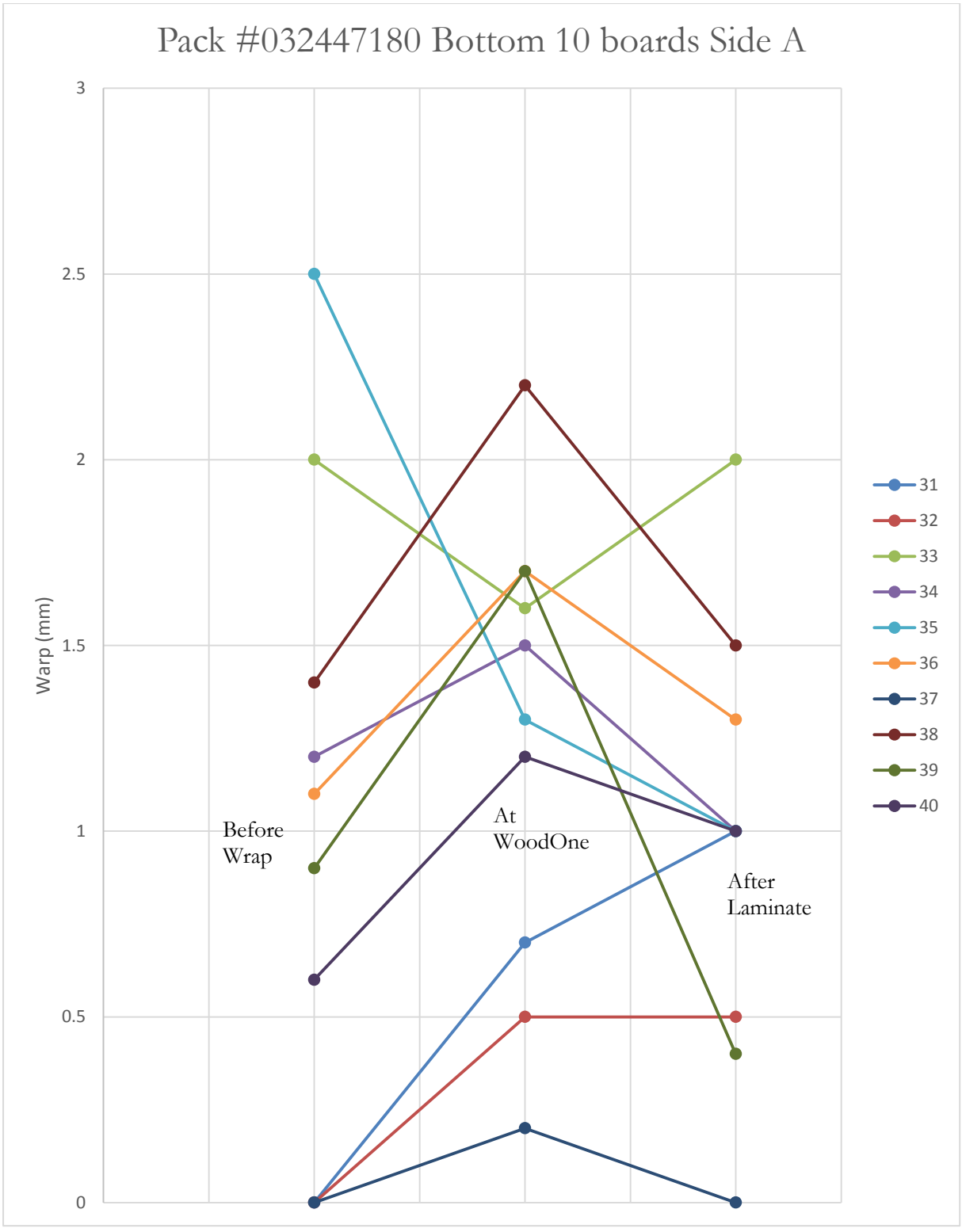

Figure 1-6: Pack #032447180 SIDE A Bottom 10 boards warp profile after addition of +2 kg fibre on top layer (After Interim Report #2)

Table 1-3 shows the Average warp and Standard deviation of warp at each point of measurement. Standard deviation is seen to decrease meaning that the warping amount is getting closer to the average warp value of the board after each step.

Table 1-3: Average warp and standard deviation of warp at different points in measurement for Pack# 032447180 Side A (After Trial Report)

Pack #	Triboard (Before Wrap), 11/12/14	At WoodOne, 24/2/15	After Laminate, 25/2/15	Warp Sensor (Cut Board), 3/3/15
032447180 Side A	Average: 0.86mm Std. Dev: 1.05	Average: 0.44mm Std. Dev: 0.68	Average: 0.89mm Std. Dev: 0.47	No reject

Note – Numerical results do not include warp measurement values from top and bottom board.

As can be seen in the profiles there is very little correlation between the position of a board in a pack and the amount it warps. The only significant observation from these profiles is that the tendency to warp negatively is reduced as lower boards are investigated. Warp measurement results from Pack #032447180 Side B are shown in Figures 1-7, 1-8 and 1-9.

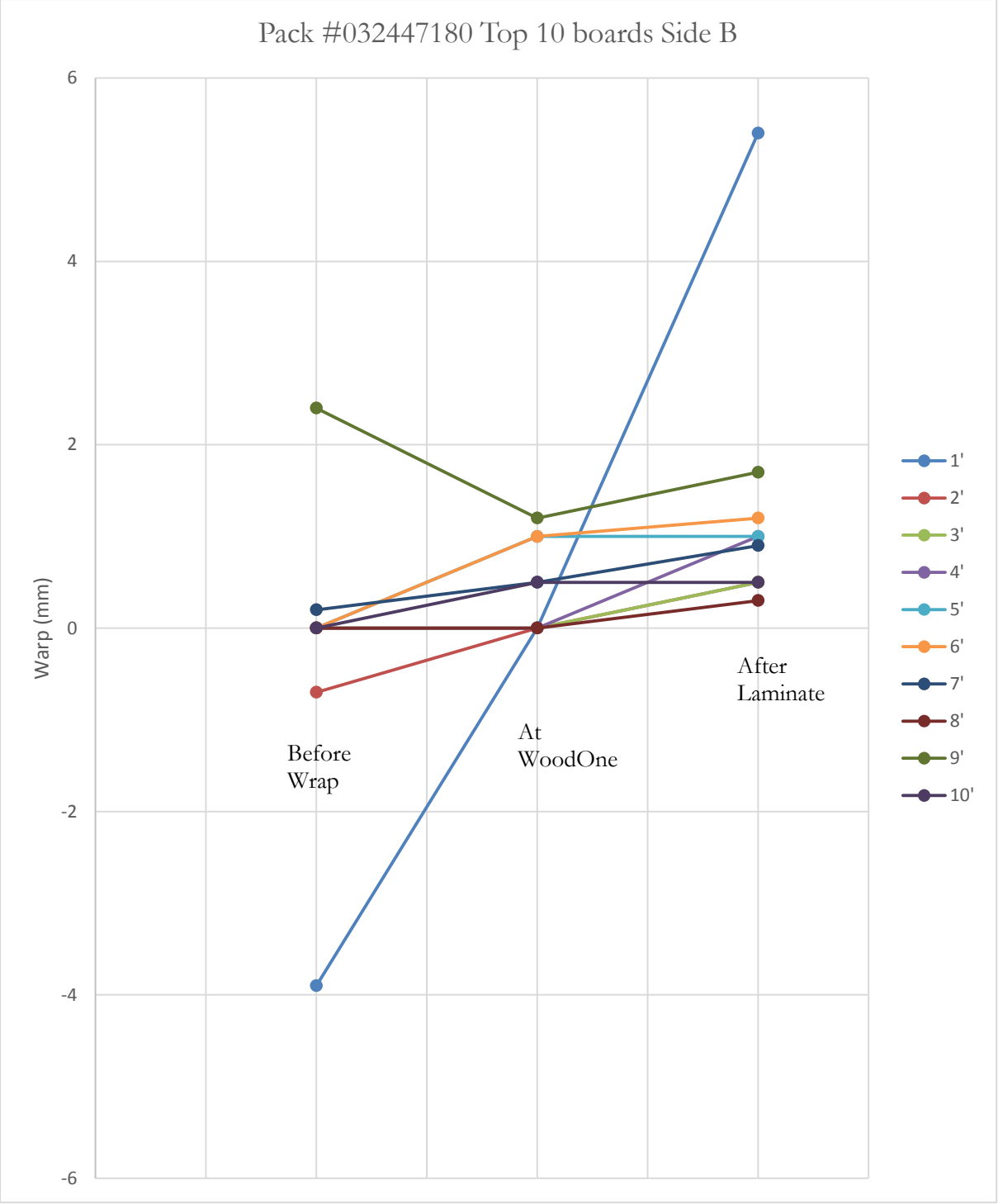

Figure 1-7: Pack #032447180 Side B Top 10 board warp profile after addition of +2kg fibre on top layer (After Interim Report #2)

Side B was also measured in the same manner to calculate average warp and standard deviation. Figure 1-7 shows similar profiles to those seen for top 10 boards of Side A in Figure 1-4 with only the top 2 boards showing negative warp.

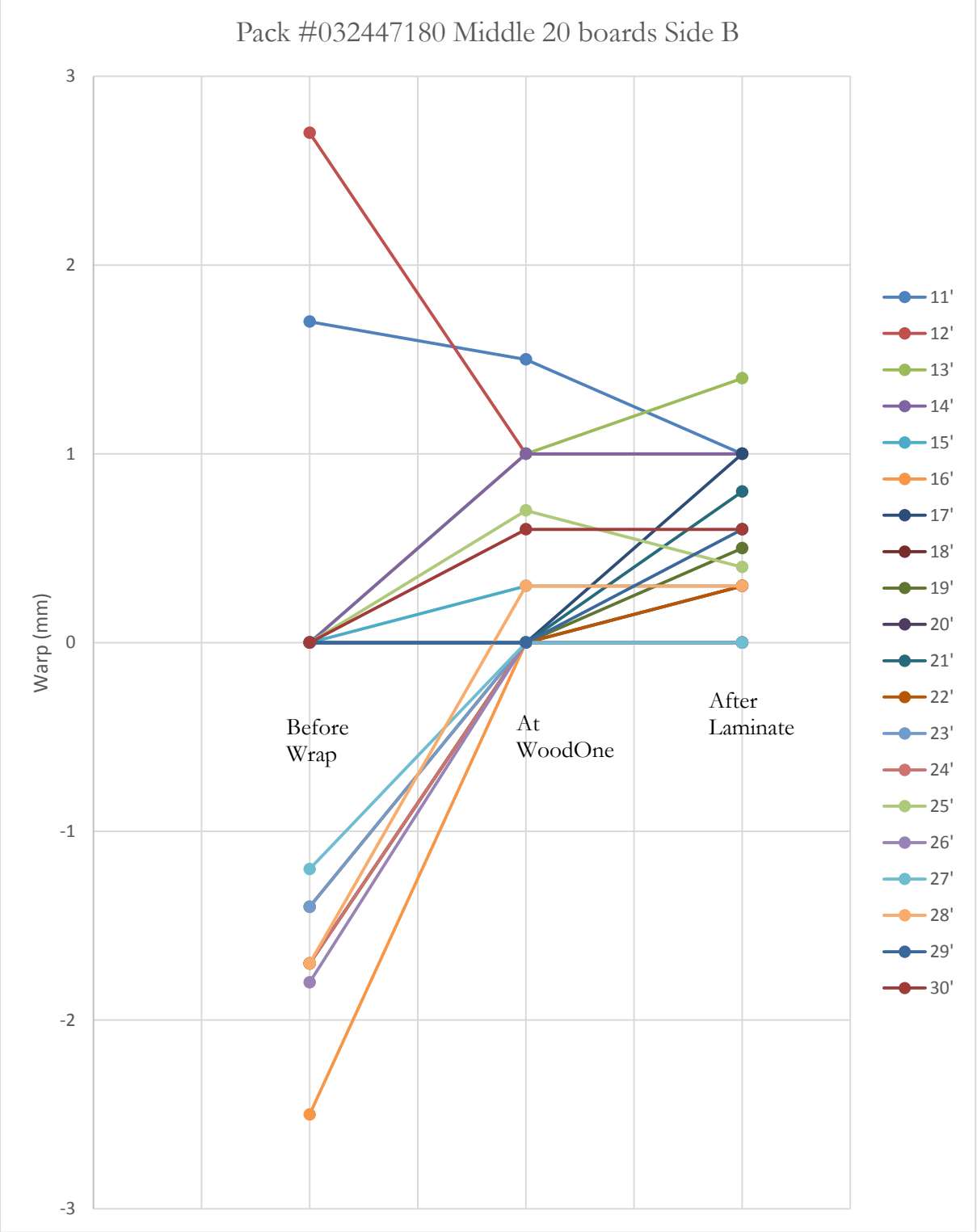

Figure 1-8: Pack #032447180 Side B Middle 20 board warp profile after addition of +2kg fibre on top layer (After Interim Report #2)

Figure 1-8 shows the Side B of the middle 20 boards of the pack. This is contrasting with Figure 1-5 where a majority of the boards were decreasing in warp when measured at WoodOne. Side B

shows that there is a tendency for warp to increase after wrapping at WoodOne. Also Side B maintains warp level after lamination.

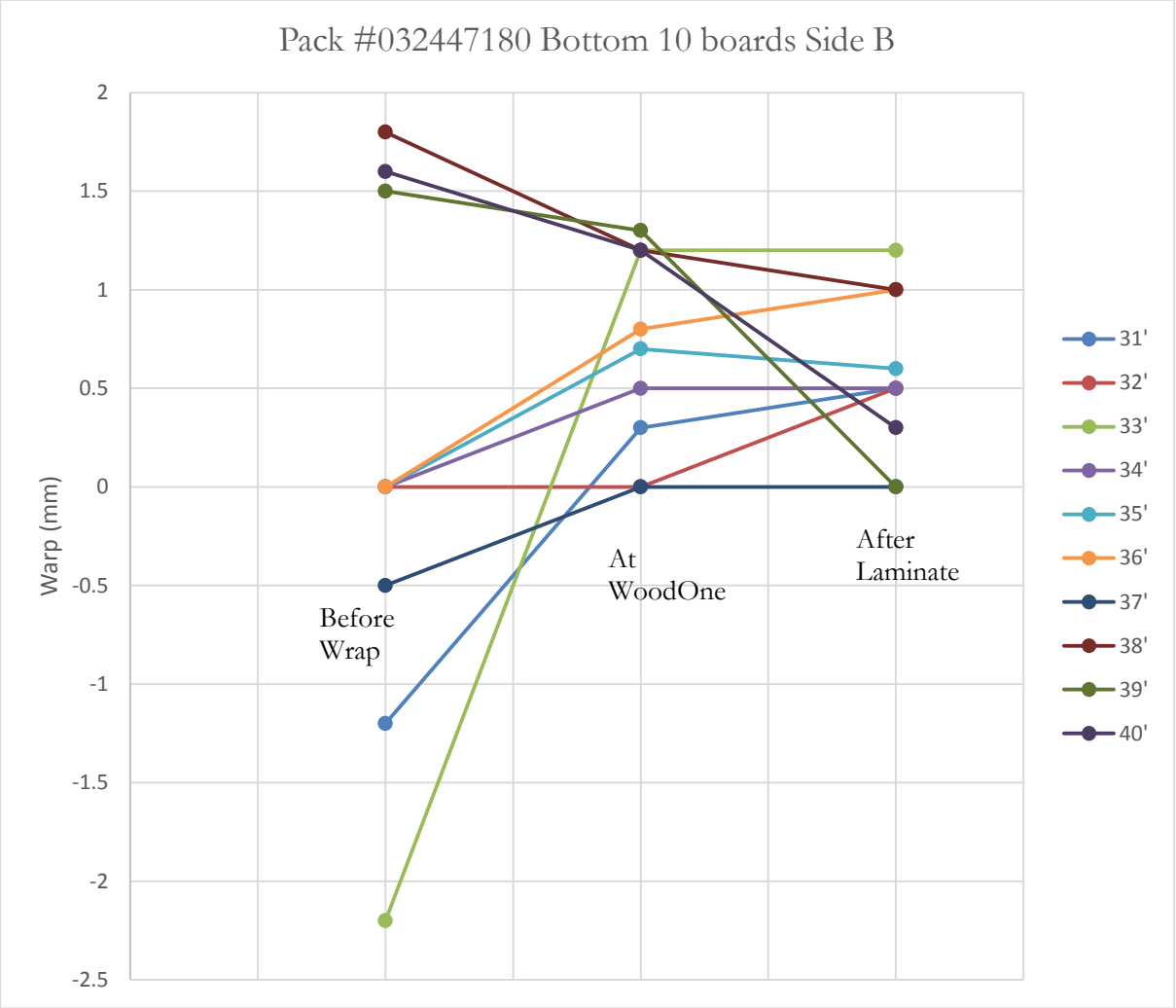

Figure 1-9: Pack #032447180 Side B Bottom 10 board warp profile after addition of +2kg fibre on top layer (After Interim Report #2)

Table 1-4: Average warp and standard deviation of warp at different points in measurement for Pack# 032447180 Side B (After Trial Report)

Pack #	Triboard (Before Wrap), 11/12/14	At WoodOne, 24/2/15	After Laminate, 25/2/15	Warp Sensor (Cut Board), 3/3/15
032447180 Side B	Average: -0.25mm Std. Dev: 1.19	Average: 0.44 mm Std. Dev: 0.49	Average: 0.59mm Std. Dev: 0.45	No reject

JNL also observed that some boards in the pack showed a different "bow tendency" to the surrounding boards and concluded that the degree of warping was independent of the position of a board in the pack.

A warp sensor was used by WoodOne which is a sensitive instrument to measure small deviations of a board from a flat plane. Table 1-5 shows the warp measured from Pack# 032447181 which was another pack with the same addition of +2kg fibre on top layer of Triboard. This pack's results displayed higher warping but was still not rejected by the warp sensor used. This pack confirmed that average warp and standard deviation of warp increased positively every step. However, this pack also showed much higher levels of warp than the first pack.

Table 1-5: Warp measurements from JNL and WoodOne's measurement of warping when +2 kg is added to top fibre layer Pack# 032447181 Side B (After Trial Report)

Pack #	Triboard (Before Wrap), 11/12/14	At WoodOne, 24/2/15	After Laminate, 25/2/15	Warp Sensor (Cut Board), 3/3/15
032447181 Side A	Average: 0.16 mm Std. Dev: 1.56	Average: 1.1 mm Std. Dev: 0.69	Average: 1.2 mm Std. Dev: 0.52	No reject
032447181 Side B	Average: 0.69 mm Std. Dev: 1.55	Average: 1.2 mm Std. Dev: 0.61	Average: 1.1 mm Std. Dev: 0.61	No reject

Conclusions from these studies were:

i. The uneven amount of moisture diffusion across the board after exposure to ambient surroundings is a key factor. This causes the Triboard to distort and warp.
ii. Stress development in Triboard during hot pressing needs investigating. The hot pressing step is responsible for relieving the internal stresses in the board but it requires an optimisation between press temperature and press time to achieve a sufficiently relieved board.
iii. Fibre layer balance could be used to provide additional balance to the board and thus prevent warping.
iv. A board's position in a pack did not affect its degree of warping.
v. Boards were already warped before shipping to WoodOne in Japan since there was no significant difference when warping was measured for the same boards at WoodOne.

1.3 PROJECT OBJECTIVES

The objectives of this project is to understand the fundamentals of warping, and to plan and design experiments which would include varying the recipe with variations of certain parameters:

1. Adhesive loading in fibre layers and strand.
2. Moisture levels of fibre layers and core strand.
3. Hot press temperature.
4. Fibre layer thickness on both top and bottom layers.

These experiments would be conducted at AICA's New Plymouth laboratory. The results would be used to plot moisture and stress profiles which would be helpful in calculating a board's symmetrical stability and stress difference which are the main factors in determining if a board is likely to warp. Using those results a comparison can then be made between company's current recipe and those which gave the best results from experiments.

1.4 REFERENCES

1. Arbor Resources Ltd. (2015) Available online at: http://www.arborresourcesnz.com/plantation-radiata-pine
2. Interim Report #2; Warp Investigation, Juken New Zealand Ltd., Triboard Mill.
3. NZ Ministry of Agriculture and Forestry, 2007, "Situation and outlook for New Zealand agriculture and forestry" Available online: http://maxa.maf.govt.nz/mafnet/rural-nz/statistics-and-forecasts/sonzaf/archive/sonzaf-2007.pdf .
4. Pang S., Kearns H., O'Brien D., (2014) *Report to JNL on Preliminary Investigation on Triboard Warping*
5. Trial Report: Uneven Fibre Layers on 21 mm Triboard (016 code), Juken New Zealand Ltd., Triboard Mill.
6. *Wood Warping*, Wikipedia (2016) Available online: https://en.wikipedia.org/wiki/Wood_warping#/media/File:Wood_warping.png

CHAPTER 2

LITERATURE REVIEW

This chapter will first look at wood properties of radiata pine and then moves progressively on to the processing of engineered wood products including strand and fibre preparation with the production of Triboard which will be discussed in a separate section. The fundamental relationships involving moisture content gradients and stress induced in wood panels is also reviewed. A separate section describes the work done by other researchers in the field of wood warping. Finally, the scope for the thesis will be discussed.

Wood can be classified into two different types, namely softwood and hardwood having different cellular structures and properties which are described in this chapter. The names are not to be confused with the "hardness" property of the wood. If we examine the specific gravities (defined as the ratio of the density of a material to the density of water) of softwoods and hardwoods, certain amount of overlap can be observed. Lewin and Goldstein (1991) classify them in their specific density ranges:

Softwoods: 0.29 - 0.60; Hardwoods: 0.32 – 0.81

Thus, it is entirely possible to come across softwoods that are 'harder' than some hardwoods and hardwoods that are 'softer' than some softwoods. One quality that is present in all wood is anisotropy. In material science, isotropy is defined as having identical values of a specific property in all directions. This property is commonly seen in metals and their alloys. In contrast, anisotropy is the property of a body where properties are directionally dependent. In a wood specimen, one can see the 'lines' going in one direction which signifies the direction of the grain and thus also its strength which is in direction of the grain. Mechanical properties of anisotropic materials are much different depending on the axes of interest. Figure 2-1 illustrates the three material axes of wood with respect to grain direction and growth rings (Green Gold Industrial Co., Ltd.).

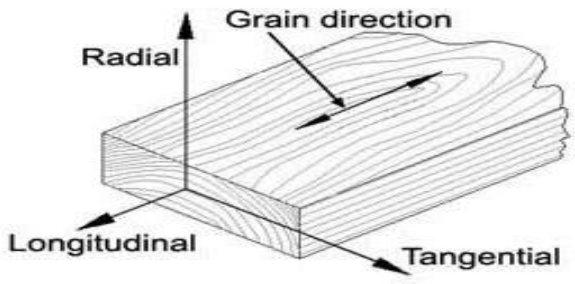

FIGURE 2-10: Three principal axes of wood

2.1 Wood Properties

As mentioned previously, radiata pine was introduced in 1850's in New Zealand and currently dominates 89% of the plantations. This species is a softwood which comes from gymnosperm trees having the characteristic needles, cones and seed-production mechanism.

Rook (1975) did a study of this species and concluded that the ability for Radiata Pine to thrive in New Zealand was mainly due to its continuous growth regardless of the weather conditions. Main factors include day-length (New Zealand's low latitude), Low night temperature (Slows down metabolic activity), Moderate day temperature (higher rate of food production) and frost tolerance (better resistance compared to other species).

2.1.1 Growth rings, Sapwood and Heartwood

A growth ring is defined as a result of new addition of wood radially between the existing wood and the bark of the tree, this being coined the term "secondary growth". Even though the growth of Radiata Pine is favoured by New Zealand's temperate weather conditions although after a season, the rate of food production (carbohydrate) slows down hence slowing down the growth. In the early season, growth is rapid and less dense wood is produced known as "earlywood/springwood" having thin walls and large cell cavities.

In contrast, much denser wood is formed late in the season called "latewood/summerwood" and this has the characteristic thick walls and small cell cavities. Since the bulk of the strength is present in the walls and not the cavities, it is the latewood that provides the strength to the tree. These characteristics of the tree are illustrated in Figures 2-2 and 2-3.

Figure 2-12: Cross section of a pine trunk (The Encyclopaedia of New Zealand)

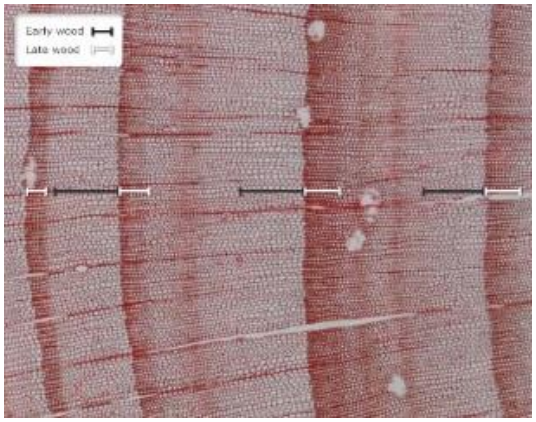

Figure 2-11: Growth rings in a cross section of a pine log (The Encyclopaedia of New Zealand)

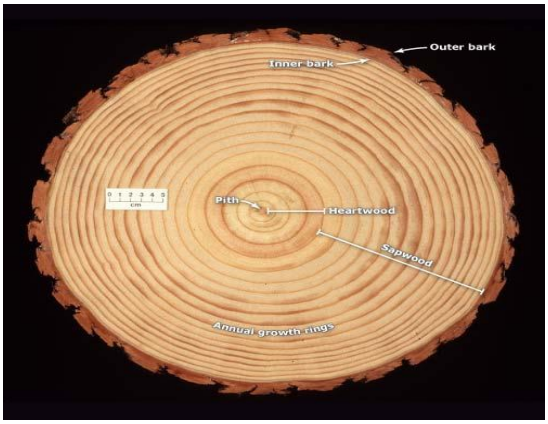

Figure 2-3 also shows the sapwood and heartwood. Sapwood is the live wood in the tree and functions as a conductor of water from the roots to the leaves and storage which acts as a reserve supply for the season. Radiata Pine has much more sapwood which can be seen in the characteristic creamy white zone in the cross-sectional figure. In contrast, heartwood is much darker in colour and "its cells are dead and physiologically inactive" (Butterfield, 1993). The driving force behind Heartwood formation is not clear in current literature but the colour change is thought to be due to the "enrichment of the cells by various extraneous chemicals" which also "permeate both the cell wall and lumen" (Butterfield, 1993). These are called extractives and provide extra resilience to attack from fungi and insects (Butterfield, 1993). Table 2-1 provides a breakdown of the percentages, nature and role of each compound present in wood.

Table 6: Chemical constituents of wood (After Lewin and Goldstein, 1991)

	% Composition	**Polymeric nature**	**Polymerization Degree**	**Molecular building blocks**	**Role**
Cellulose	45-50	Liner molecule crystalline	5,000-10,000	Glucose	Framework
Hemicellulose	20-25	Branched molecule amorphous	150-200	Primarily non-glucose sugars	Matrix
Lignin	20-30	Three-dimensional molecule	100-1,000	Phenol propane	Matrix
Extractives	0-10	polymeric	-	Polyphenols	Encrusting

Heartwood begins to form between the ages of 12 and 15 years. This is concluded by counting rings from the pith. However, Cown (1989) showed that trees did not show a large amount of heartwood even after reaching the mature age of over 30 years (Figure 2-4). Bamber (1960) states that the function of the heartwood is to keep the "amount of sapwood at an optimum thus conserving the nutritional balance in the living part of the tree", thus reinforcing Cown's volume occupancy data in Figure 2-4.

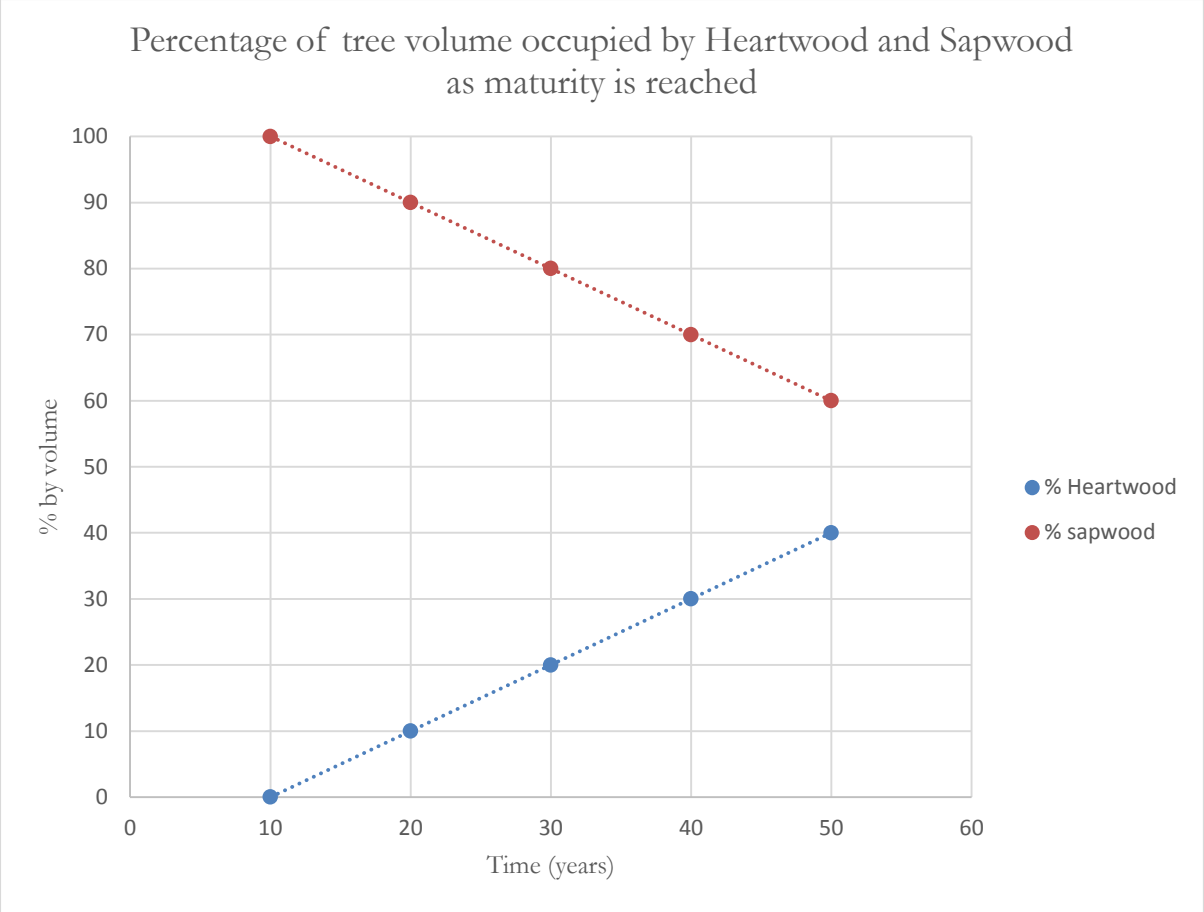

Figure 2-13: Heartwood and sapwood percentages in radiata pine (Adapted from Cown, 1989)

For the determination of sapwood and hardwood in Radiata Pine, Anonymous (1954) used bendizine and Bamber (1960) used aqueous/methanolic ferric chloride. Cummins (1972) however used azo-dye-para-amino-NN-dimethyl aniline which gives a "strong red-purple colour" on reacting with heartwood and is favourably inert with softwood.

2.1.2 TRACHEIDS

The anatomy of Radiata pine, being a softwood is much simpler than Aspen, a hardwood. The microstructure has three principle orthotropic directions namely, longitudinal, radial and tangential. Tracheids (elongated cells) act as carriers of water and mineral salts. The longitudinal tracheids are constructed of earlywood tracheids (hexagonal) and latewood tracheids (rectangular) which differ in length, radial diameter, wall thickness and pitting, the earlywood tracheids being shorter than latewood tracheids (Bamber and Burley, 1983). Figure 2-5 shows a scanning electron micrograph of a block of Radiata pine highlighting the tracheids.

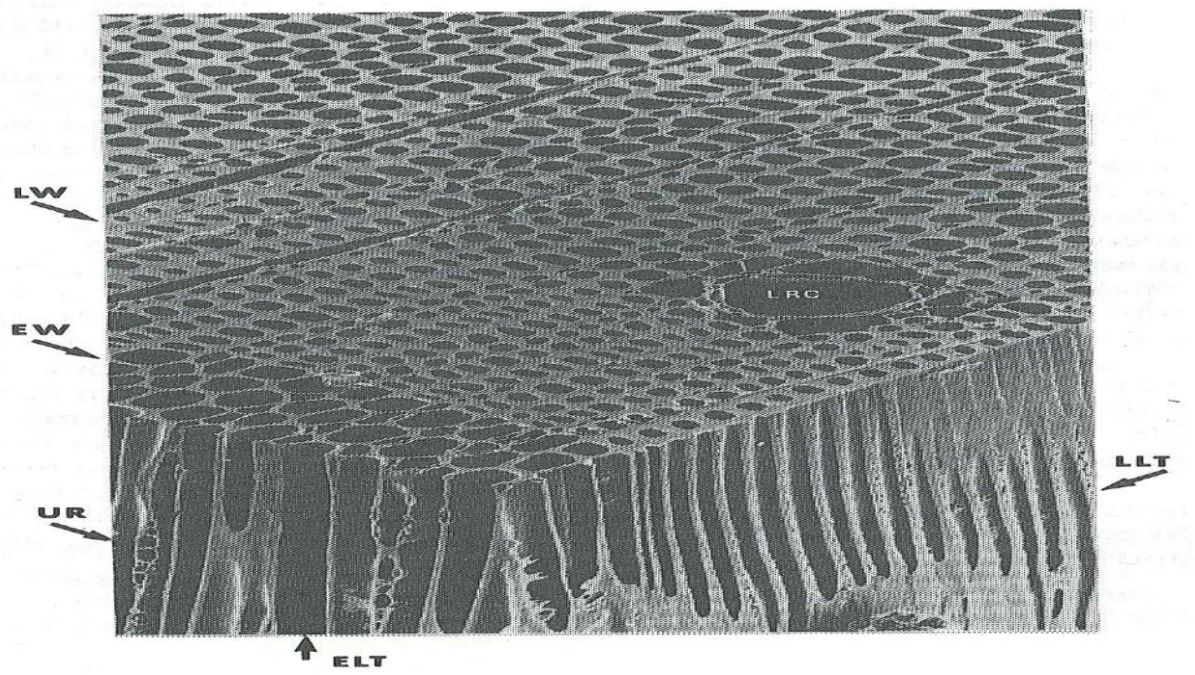

Figure 2-14: A 100x magnification of radiata pine softwood (After Bamber and Burley, 1983)

In Figure 2-5, the labelled abbreviations are as follows:

LW: Latewood; **EW**: Earlywood; **LRC**: Longitudinal Resin Canal; **UR**: Uniseriate Ray;

ELT: Earlywood Longitudinal Tracheid; **LLT**: Latewood Longitudinal Tracheid

Table 2-2 provides the dimensions of longitudinal tracheids of earlywood and latewood. Earlywood has a diameter more than three times bigger than latewood while the cell wall thickness is less in earlywood.

Table 7: Radial dimensions of longitudinal tracheids (After Bamber and Burley, 1983)

	Earlywood		**Latewood**	
	Diameter (mm)	Cell Wall Thickness (mm)	Diameter (mm)	Cell Wall Thickness (mm)
Pinus Radiata	0.045	0.003	0.013	0.005

Kininmonth and Whitehouse (1991) give the length of a longitudinal tracheid as ranging between 0.73mm - 4.78mm. These observed dimensions make the tracheid much longer than wider having the lumen (open space) in the middle for conduction of mineral salts and water up the tree stem.

2.1.3 BORDERED PITS

An important feature of the tracheid cell wall are pits which allows the transfer of fluids from one place to another. There are three types of pits that exist on cell walls:

- Bordered pits: between tracheids
- Half-bordered pits: between parenchyma cells and tracheids.
- Simple pits: between parenchyma cells

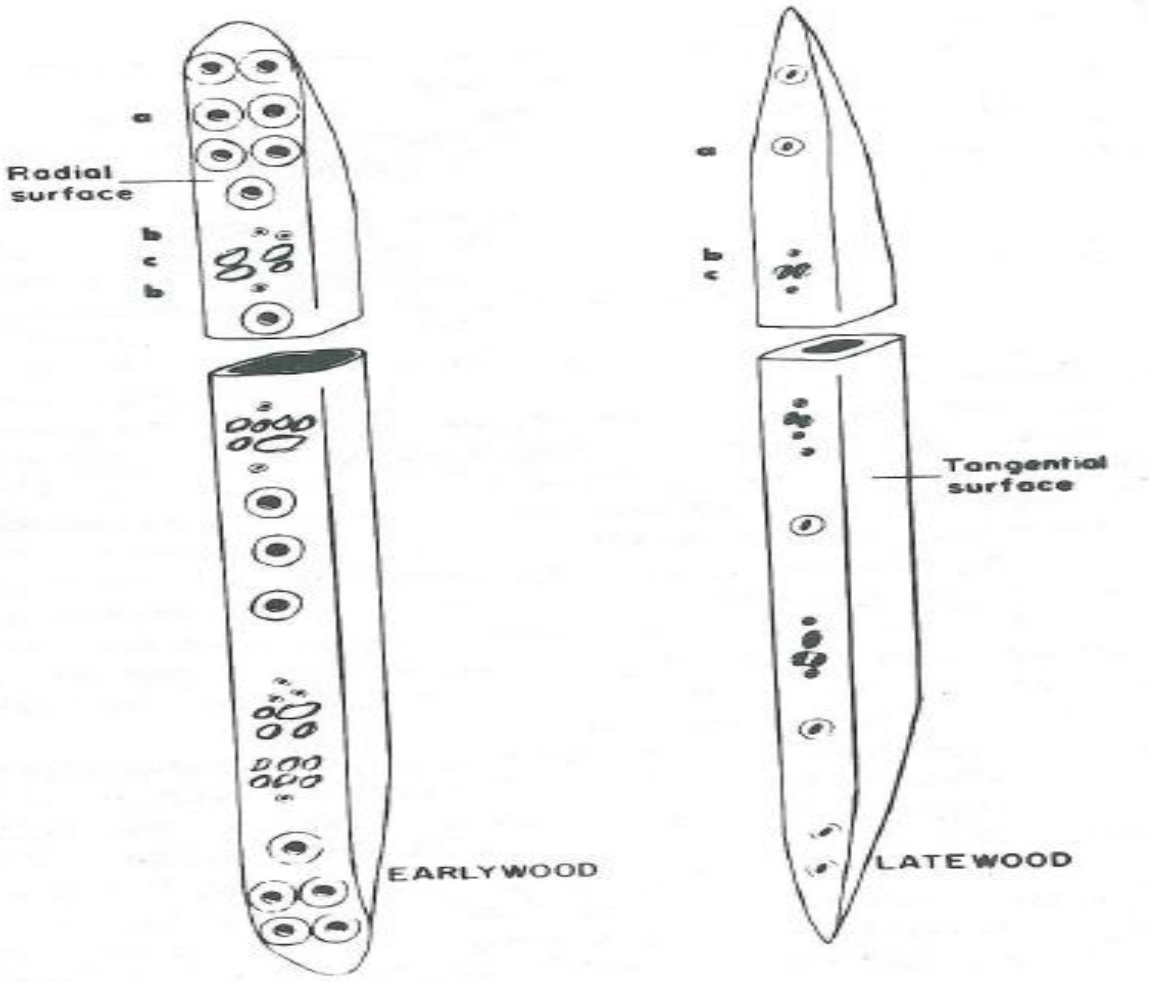

Figure 2-15: Isolated earlywood and latewood longitudinal tracheids (After Howard and Manwiller, 1969)

Figure 2-6 shows bordered pits on earlywood and latewood longitudinal tracheids. It is noticeable that the latewood section has much less tracheids than the earlywood section.

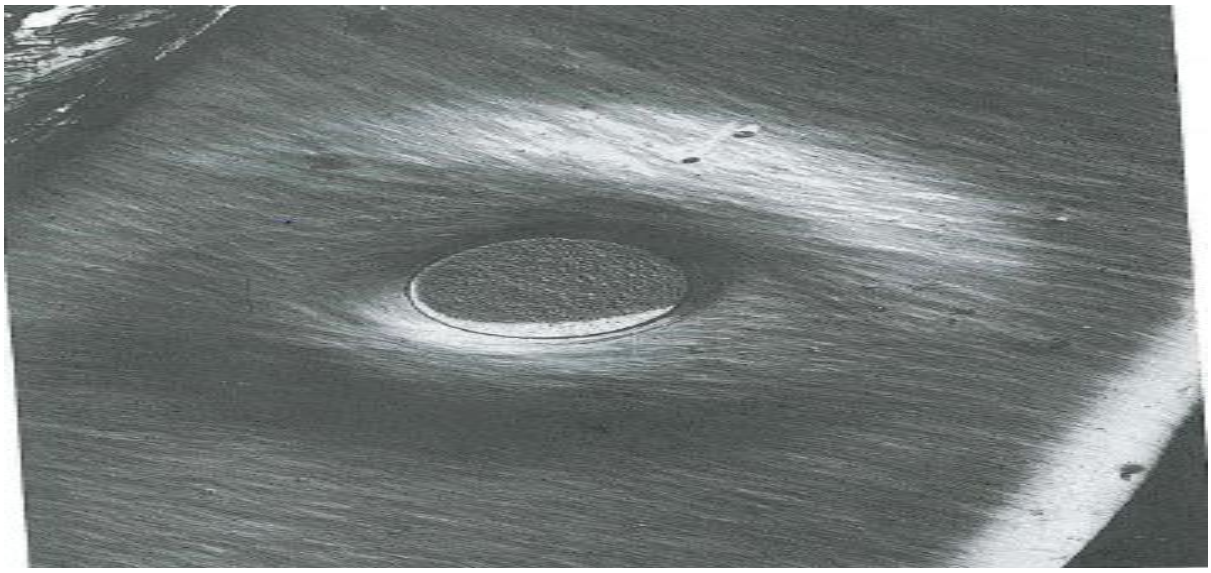

Figure 2-16: Bordered pit as seen from cell lumen (After Lewin and Goldstein, 1991)

Figure 2-7 shows the pit as seen from the lumen (open space) of a tracheid. The circular (black) opening is called the pit aperture and the outer lining is called the pit border. If a pit border is removed, the pit membrane is exposed displaying two important regions of the pit, torus which is the central nonperforated area and margo which is the outer perforated area (Lewin and Goldstein, 1991). The margo region is much thinner than the torus and all liquid flow occurs conveniently through this opening and transfers out the aperture into the lumen of adjacent tracheids. For this mechanism to be successful, the pit has to be open/in an unaspirated condition. However, due to pressure reduction in the capillary action due to wood drying where air enters the water conducting pathways, the pit becomes closed/aspirated. This action "confines the air embolism to a small area" and water transfer is still ongoing in the rest of the stem (Lewin and Goldstein, 1991).

2.1.4 Resin Canals

Resin canals function as intercellular spaces which take in resin (complex organic substances) secreted by parenchyma cells and are lined with thin-walled epithelium. Resin canals only occupy a very small percentage of the wood (1% volume basis) and occur as a result of "cellular differentiation by the breakdown of columns of thin-walled parenchyma cells in response to the hydrostatic pressure of the resin bleeding from neighboring epithelial parenchyma cells"

(Butterfield, 1993). Traumatic resin canals can also form as a result of injury to the tree through natural causes like wind, frost, insect or fungal attack. These tend to form in earlywood and the pitch pockets develop around 40mm wide, 100mm long, and 5mm thick (Butterfield, 1993).

2.2 IDENTIFYING HARDWOODS

Hardwoods are derived from angiosperms commonly known as flowering trees. They are much more complex structure in comparison to softwoods. For instance, the function of conduction of water/sap and mineral salts in addition to support is done by tracheids (Section 2.1.2) in softwoods but in hardwoods, different cell types carry out these functions. Vessel elements (also called pores) carry out the function of sap conduction and their size and arrangement in the earlywood/latewood are used to classify hardwoods into three types –

1. Ring-porous – The earlywood pores form rings
2. Diffuse-porous – no clear earlywood ring arrangement and all same size.
3. Semi-Ring-Porous – Decrease in size from earlywood to latewood

For identification of hardwoods, another factor to take into consideration is the pore diameter and frequency which is classified in Tables 2-3 and 2-4:

Table 8: Pore diameter and size (The Wood Database)

Size	**Diameter (µm)**
Small	<50
Medium	50-100
Large	100-200
Very Large	>200

Table 9: Pore frequency (The Wood Database)

Relative Frequency	**Vessels/mm^2**
Very few	<5
Few	5-20
Moderately numerous	20-40
Numerous	40-100
Very numerous	>100

Note – Pore frequency is only a measure for diffuse-porous woods.

2.3 PROCESSING OF THE ENGINEERED WOOD

As mentioned before, Triboard is a composite manufactured from two different forms of raw wood material, namely strands in the core and fibres near the surfaces. The contrasting yet similar individual process to manufacture Strand board and Fibreboard are explained employing Process Flow Diagrams.

2.3.1 STRAND BOARD PREPARATION PROCESS

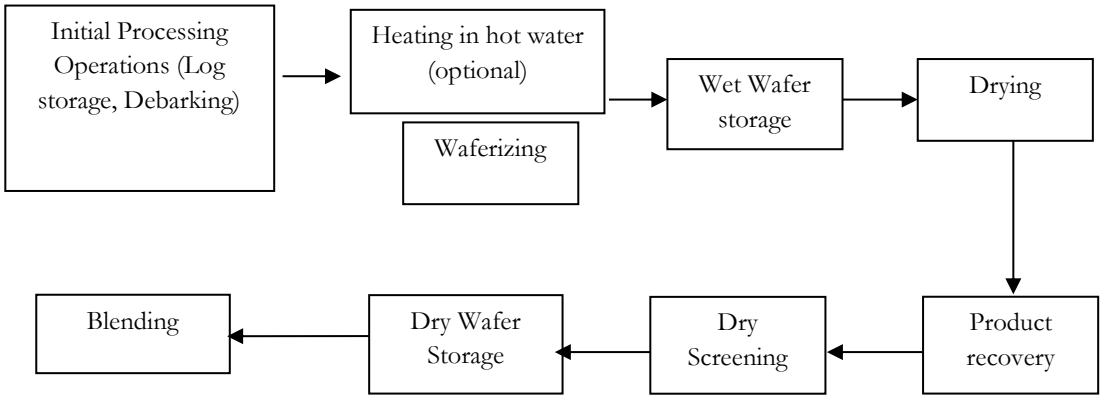

Figure 10: Processing flowchart for strandboard

A stepwise breakdown of each step is as follows:

- **Initial Processing Operations:** This involves storing freshly cut logs, debarking which is the process of removing bark form wood using a debarker as shown in Figure 2-9. The **b**ark can be used in the mill's energy supply.

- **Optional heating and Waferizing:** In northern regions, heating is a pre-treatment process where logs are prepared for stranding by maintaining them in a hot pond at a temperature between 18 and 43 degrees Celsius for thawing. After debarking the logs are cut into precise lengths of 3.8 cm wide by 7.6 cm to 15 cm long by 0.07 cm thick (Haygreen and Bowyer, 1989). No wood is wasted here.

Figure 2-17: Industrial size log debarker (IEM Ltd.)

- **Drying:** Triple-pass rotary drums fired by wood residue are often used for strands drying in OSB manufacturing. The drying medium at the dryer entrance is at a temperature of around 540 °C or lower to dry the strands to target moisture content of 4 - 8% (dry basis) to compensate for moisture gain through addition of additives. A typical rotary drum dryer is displayed below in Figure 2-10.

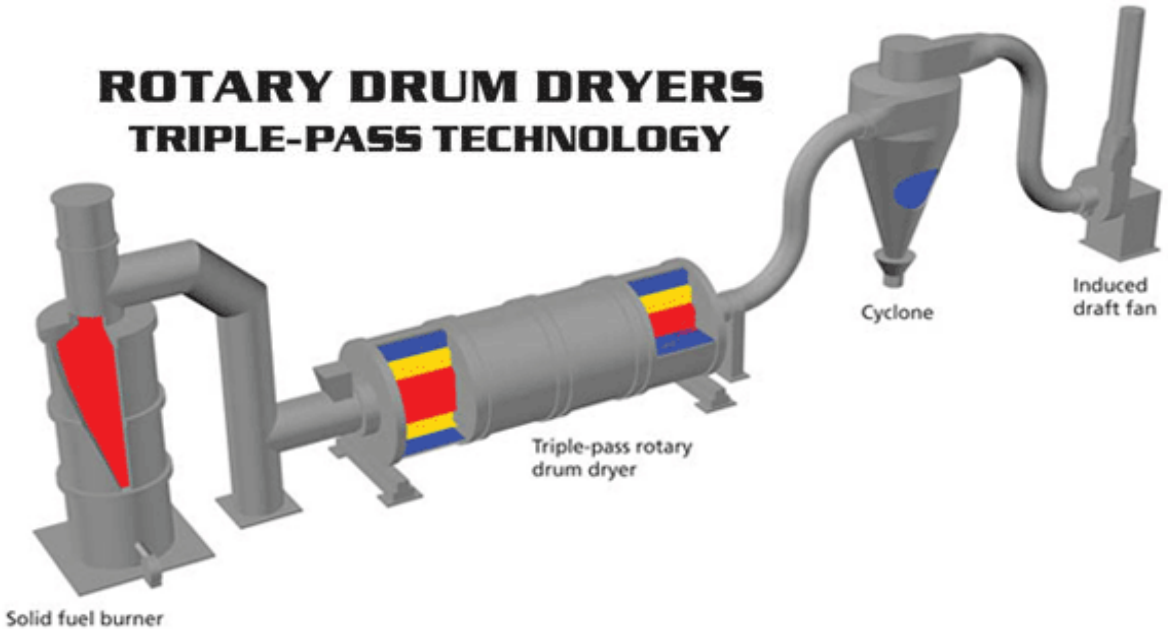

Figure 2-18: Rotary dryer for drying wood strands (Worldwide Recycling Equipment)

- **Screening:** The dried strands are moved through pneumatic flow pipe from the dryer and screened to remove fines. It is necessary to remove fines from the strands as their adhesive absorption is much more than the strands. The cyclone also separates the strands by surface area and weight. The screened strands are stored and the undersized

material is used as fuel for heating the drying medium. The dried strands are then conveyed to the blender, where the adhesives are injected which is a mixture of resin, wax, water and other additives (Wood Products Industry).

- **Screening:** The dried strands are moved through pneumatic flow pipe from the dryer and screened to remove fines. It is necessary to remove fines from the strands as their adhesive absorption is much more than the strands. The cyclone also separates the strands by surface area and weight. The screened strands are stored and the undersized material is used as fuel for heating the drying medium. The dried strands are then conveyed to the blender, where the adhesives are injected which is a mixture of resin, wax, water and other additives (Wood Products Industry).

- **Dry Wafer Storage and Blending:** The stored screened strands are stored and the undersized material is used as fuel for heating the drying medium. The strands are then conveyed to a blender, where the adhesives are injected which is a mixture of resin, wax, water and other additives. Figure 2-11 shows a short retention time blender used in OSB manufacture. The most commonly used resins for OSB are phenol-formaldehyde (for outdoor applications) and urea formaldehyde (for indoor applications) (Wood Products Industry). Additionally, fungicide may be added in the blending process as a preservative.

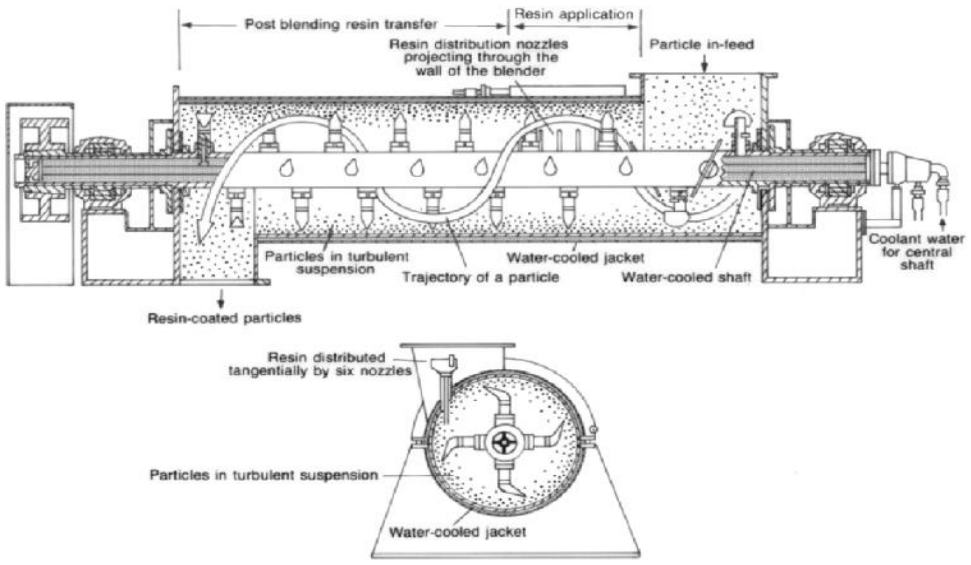

Figure 2-19: Short retention time blender for strands (After Walker, 2006)

2.3.2 FIBRE PREPARATION PROCESS

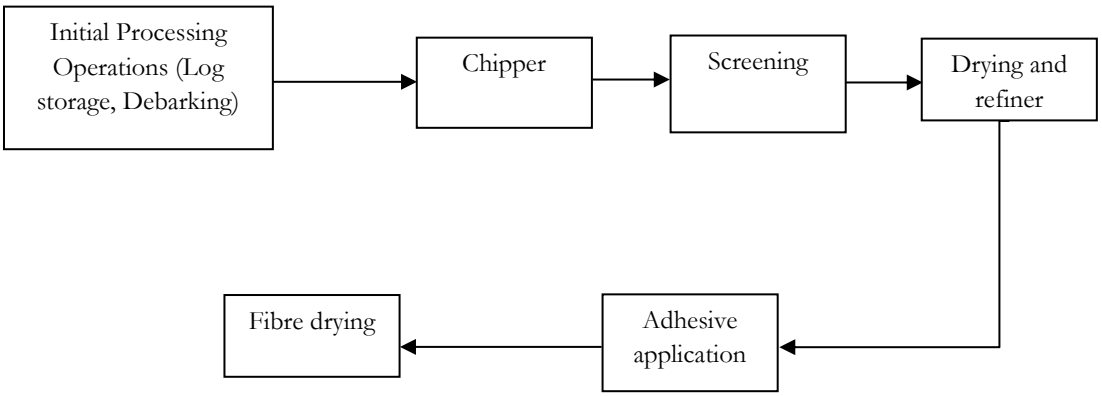

Figure 2-20: Processing flowchart for fibres

Figure 2-12 provides a stepwise breakdown of the process. These are explained below:

- **Initial processing operations:** Radiata pine logs are cut and stored where they are fed in a debarking machine to remove the bark.

- **Chipping and Screening:** After log debarking, chips are made in a chipper which creates chip and eventually become fibre. Those chips have to be washed and pre-heated with steam for softening the lignin (Walker, 2006). Chips also have to go through screening for separation into oversize and undersize chips. If chip geometry is not necessary to control, hammer-milling or drum chippers may be used for chipping.

- **Refiner:** The chips are refined for a higher quality furnish into suitable fibres. The refiner is essentially a pair of rotating large discs with knives that cut the chips into fibres while steam pressure and centrifugal force provide a radial force (Forestry Insights).

- **Adhesive application:** Urea Formaldehyde (UF) resins are used for MDF processing as the most common resin but phenolic, melamine and isocyanates may also be used. Similar to the OSB processing, a short-retention blender may be used or resin injection is done via a blowline system. In the blowline case, fibers from the refiner are first blended and then discharged to the dryer (Wood Products Industry).

- **Fibre Drying:** The target moisture content to achieve for the mat before entering the hot press is 10-12%. To achieve this, modern dryers can operate as high as 850C. A short residence time tube dryer quickly evaporates moisture from the surface.

2.4 Processing of Triboard

The prepared strands are placed between two fibre layers and the next steps are outlined:

Hot press: Those triple layers are then moved on to the next stage which is hot pressing. A multi-opening press is more common in modern industries. This type of press contains individual slots where multiple boards can be loaded at a time and the press closed for desired resin cure temperature and time. A benefit of using multi-opening press is that all boards are pressed alike and similar density profiles in the boards are produced Figure 2-13 shows such a press. Cross-directional strands formed in the previous section are pressed under high temperature and pressure to form a dense structural panel. A critical temperature has to be reached and held in the pressing step to make sure the adhesive is cured (to reach desired properties) and also make sure the board is not overheated.

Figure 2-21: Multi-opening vertical hot press (Trade Belt)

- **Cooling:** The board is quite hot as a result of hot pressing and needs to be cooled down to a lower temperature and to reach its 'maximum properties'. Cooling parameters are designed such that the board receives symmetrical cooling and balances out its stresses and be ready for sanding. This is achieved by using a Star Cooler which has multiple slots arranged in a "cooling wheel" which allows heat loss to ambient surroundings. (Walker,

2006). Figure 2-14 shows such a cooler. Another reason for cooling is to prevent hydrolysis occurring within the board which is also a problem in hot pressing. The dynamic parameters which are constantly changing within the board are temperature, moisture distribution and vapor pressure. The parameters do not cease changing even after leaving the press. These dynamic changes also result in asymmetrical stress changes which 'warps' the panel.

Figure 2-22: Cooler for hot pressed boards (Shandong Tengfei Mechanical and Electrical Technology Co., Ltd.)

- **Sanding and Cutting:** Modern sanders are 'wide-belt sanders' which are used to dimension the board at high speed and also give a board a high quality finish as opposed to older drum sanders which were wrapped around with sandpaper and had very limited contact with the board. Now the panel needs to be cut to size. The most common trimming systems available in all board manufacturing industries is known as the two-pass trimming system. It is composed of a first-pass with two side saws for edge trimming, a perpendicular corner transfer to a second-pass with two saws. This system was modified when additional saws were added to the trimming system (Maloney, 1993). This type of line is particularly useful to break large panels down to sizes that are easier to manage and further cutting. A new saw that has been observed in use is particularly useful for cutting to length continously pressed boards as they leave the press. For cutting continuously pressed boards a new saw has been developed which can be seen in

Figure 2-15. This saw momentarily stops the board with clamps so that a 'cut-off' can be made (Maloney, 1993).

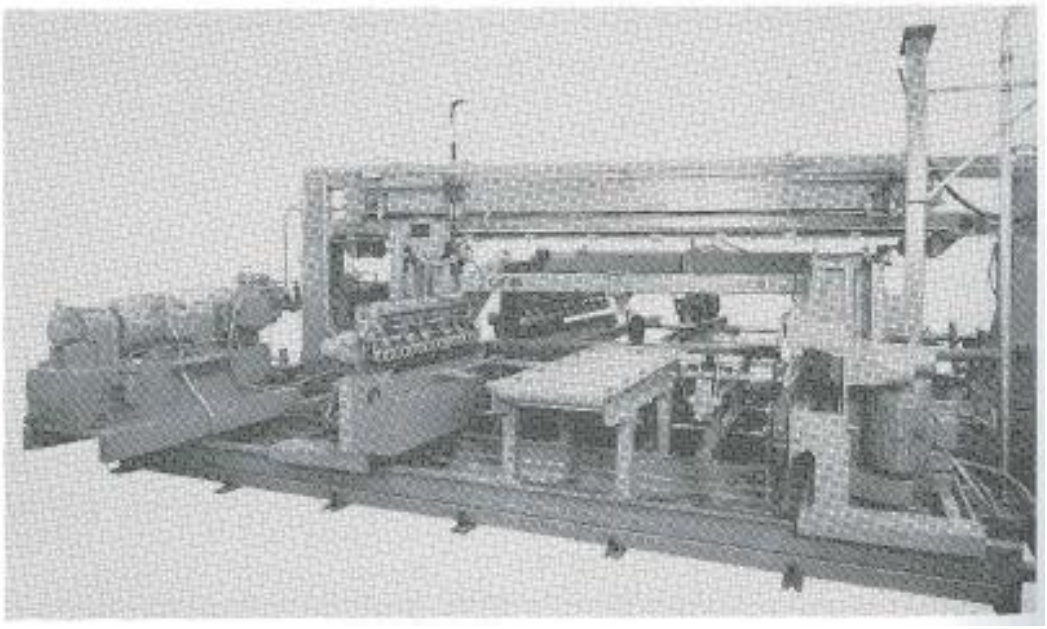

Figure 2-23: Trimming unit for large pressed boards (From Maloney, 1993)

2.5 Exploring fundamental relationships in literature

2.5.1 Relationships between Equilibrium Moisture Content and Relative Humidity

It is very important to see relationships between moisture, stress and warping in wood. Moisture content is an important quantity measured in this project which would help in creating profiles for each sample that is prepared in the laboratory. A term called "shrinkage intersection point" is of particular importance since it determines the moisture content at which the properties of wood start to change and it was found to be 30% for Radiata Pine (Harris, 1961). Since heartwood has higher content of extractives, it has a lower shrinkage intersection point in comparison to sapwood. Another important property to consider is Equilibrium Moisture Content (EMC). This value is dependent on a number of factors:

1. Whether sample is gaining or losing moisture
2. Atmospheric conditions for e.g. drying temperature
3. Species and within species variability

Orman (1955) approximated the EMC for radiata pine as follows:

$$\log Y = 0.997 \log X + 0.012$$

Where

Y = Equilibrium Moisture Content

X = Generalised Equilibrium Moisture Content

Also Bramhall and Wellwood (1976) tabulated general equilibrium moisture content values at different temperatures. These were graphed and are shown in Figure 2-16. This makes it possible to calculate the EMC for Radiata Pine at a range of temperatures.

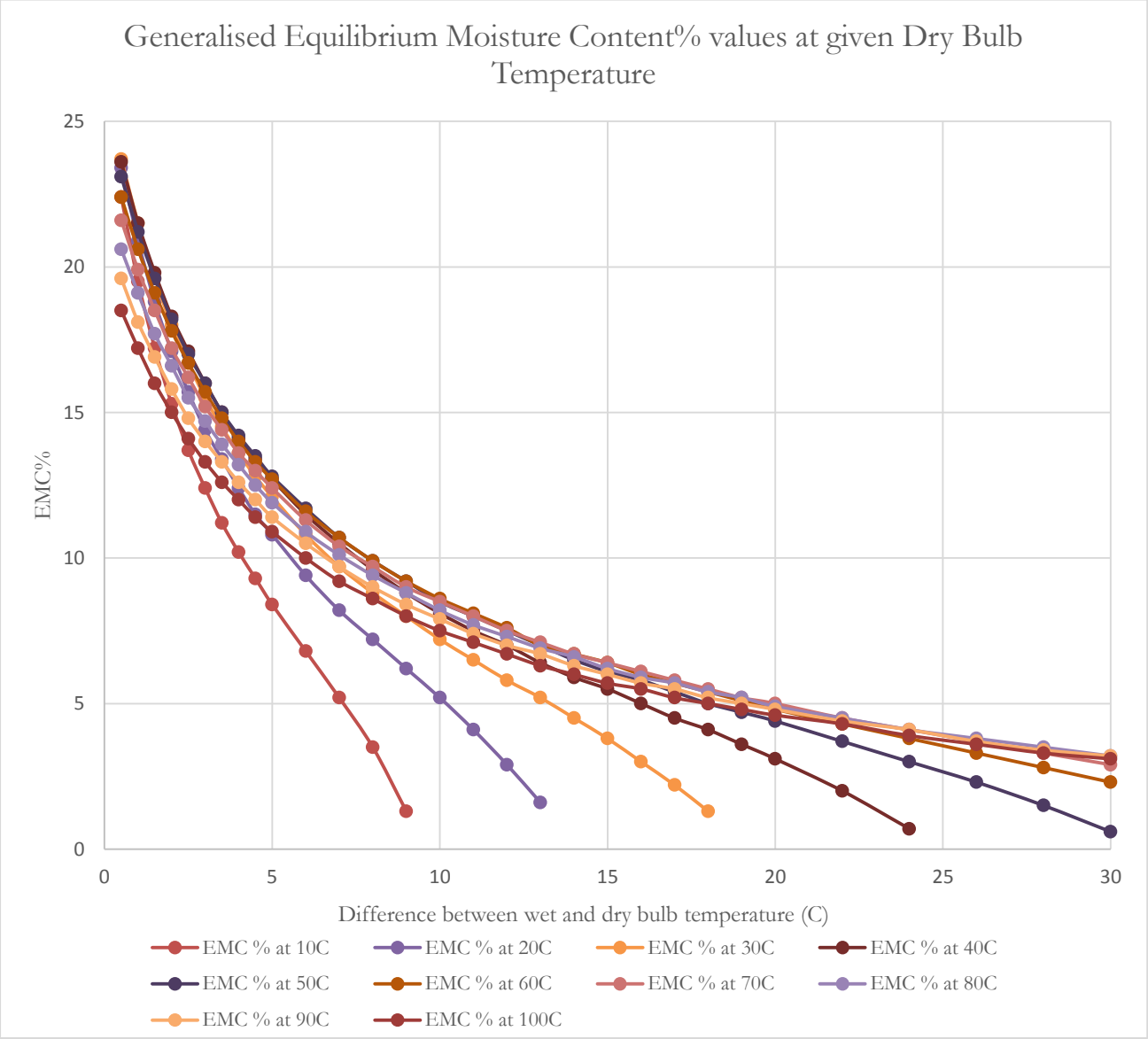

Figure 2-24: Generalised equilibrium moisture content for radiata pine (Adapted from Bramhall and Wellwood (1976))

Applying Orman's relation to the generalised EMC profiles in Figure 2-16, new profiles can be plotted which are shown in Figure 2-17. Using those graphed solutions, it is possible to get coordinates for any temperature specific EMC profile.

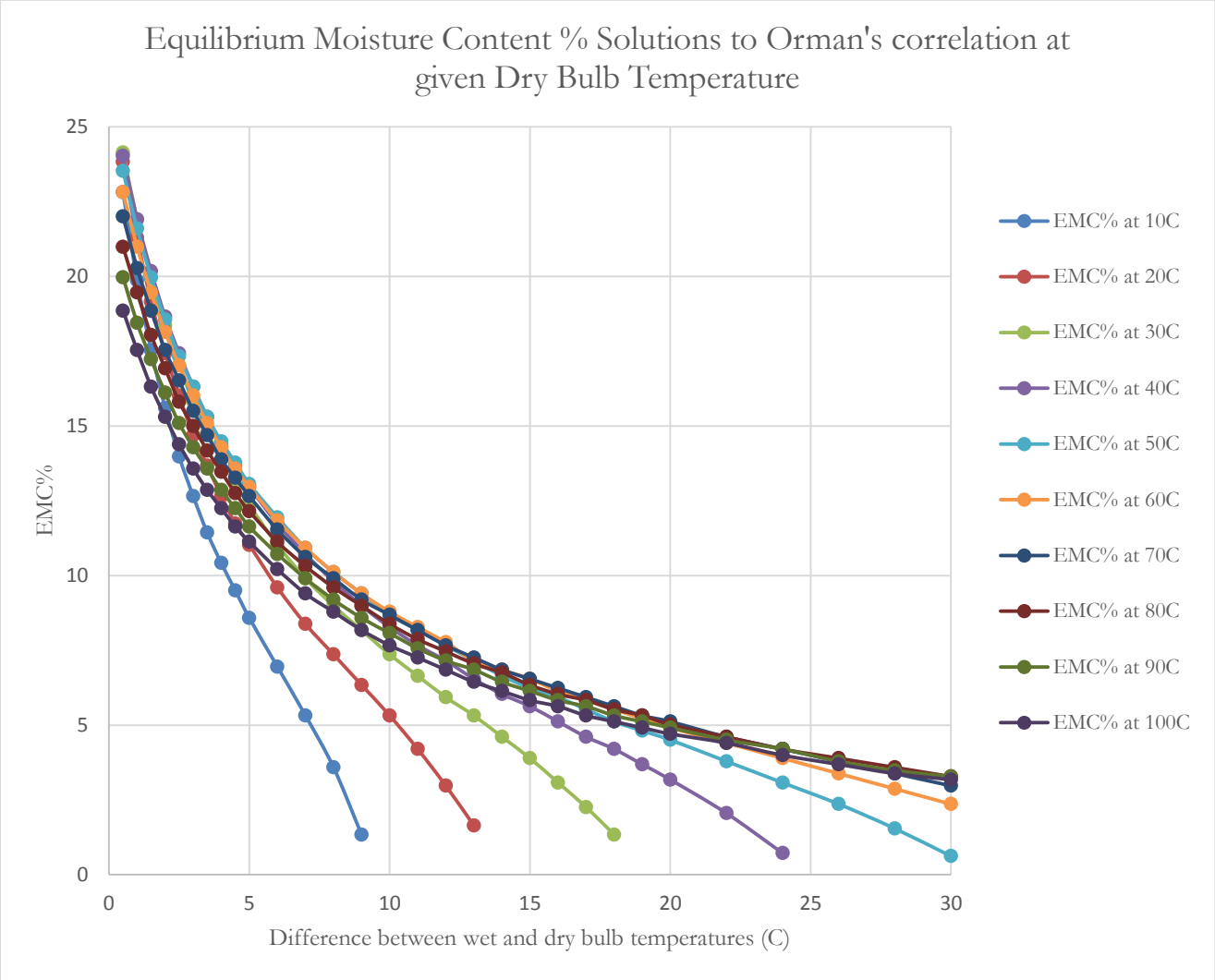

Figure 2-25: Equilibrium moisture content% solutions to Orman's correlation for radiata pine

It is also possible to see the relationship between Equilibrium Moisture Content and Relative Humidity as shown in Figure 2-18. This figure is also obtained from Bramhall and Woodwell's (1976) recorded data. Relative humidity is defined as follows:

$$\psi = \frac{partial\ pressure\ of\ water\ vapour}{saturation\ vapor\ pressure\ of\ water\ at\ same\ temperature}$$

It can be seen in the figure that as the dry bulb temperature decreases, EMC profile is reduced. As the relative humidity increases, EMC increases. It is possible to approximate these profiles to polynomial functions. As the degree of the function increases the closer it gets to the original

data since there are more terms present in higher order functions which compensate for the errors in approximation. This comparison is shown in Figures 2-19, 2-20, 2-21 and 2-22 up to a 5th order approximation where the data fits almost exactly on the polynomial curve.

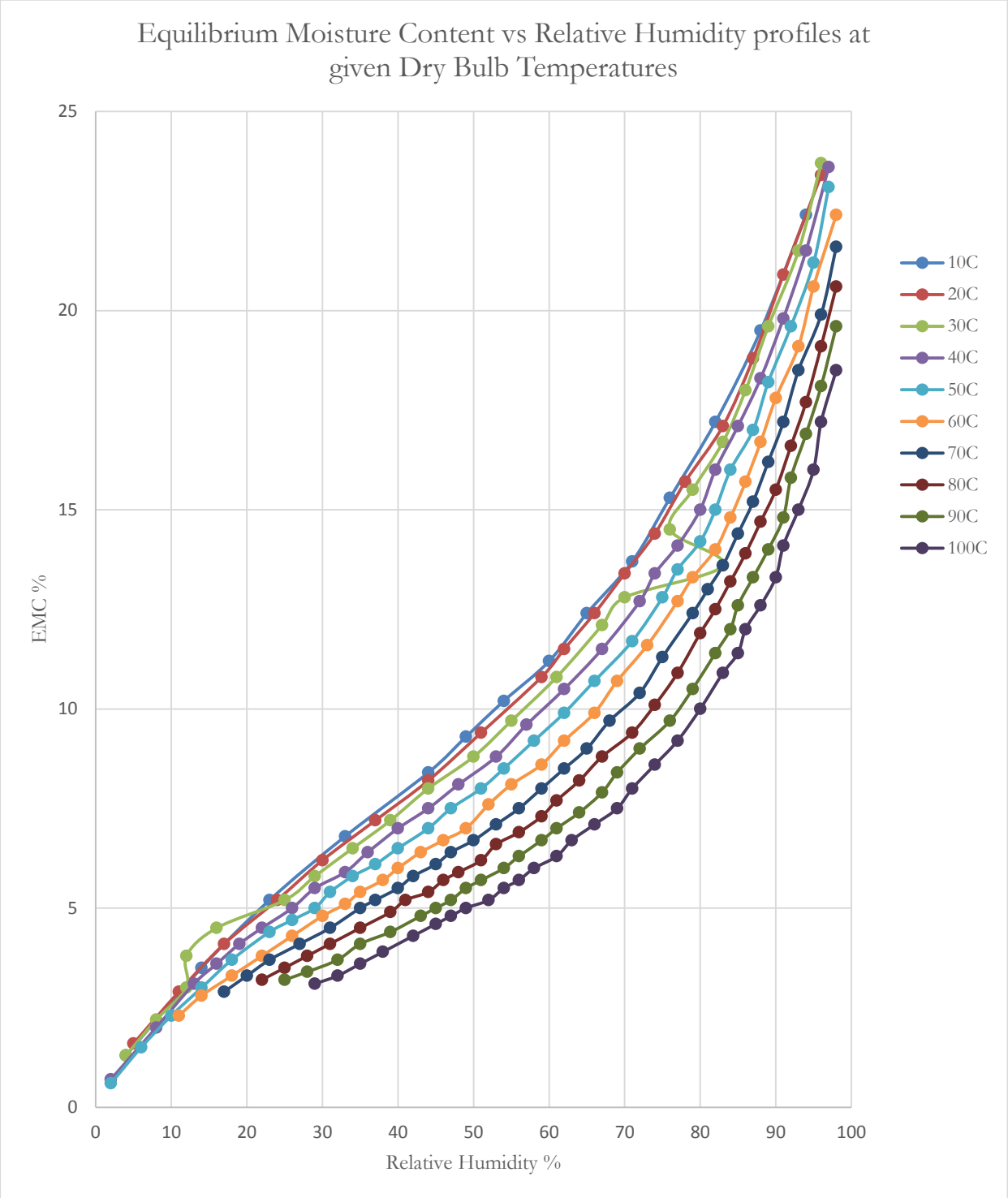

Figure 2-26: Equilibrium moisture content - relative humidity relationship (Adapted from Bramhall and Woodwell (1976))

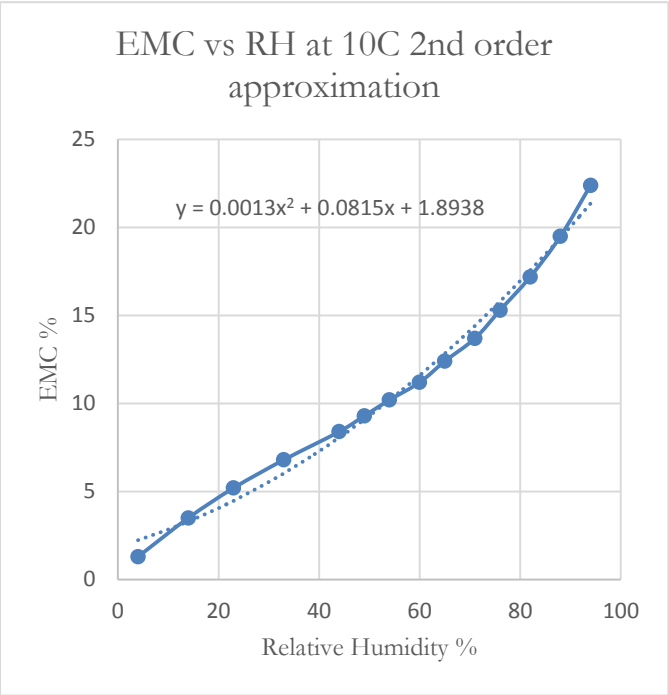

Figure 27: 2nd order approximation for Bramhall and Wellwood's EMC and RH data

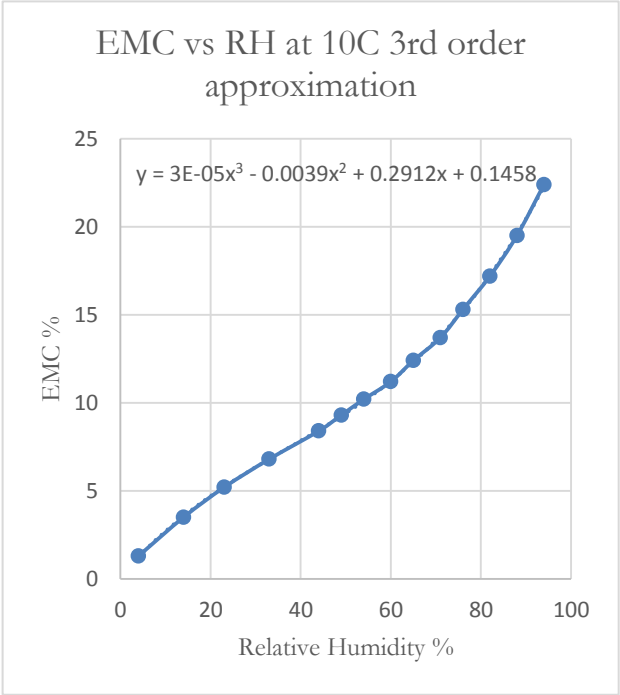

Figure 2-28: 3rd order approximation for Bramhall and Wellwood's EMC and RH data

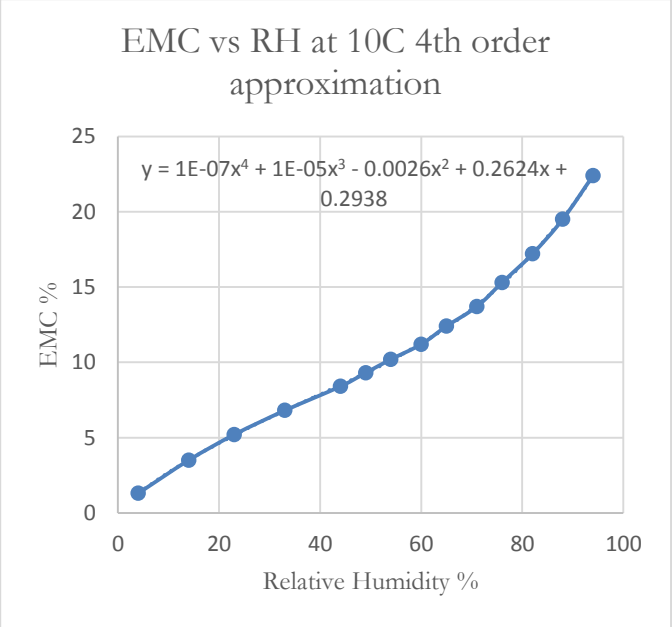

Figure 30: 4th order approximation for Bramhall and Wellwood's EMC and RH data

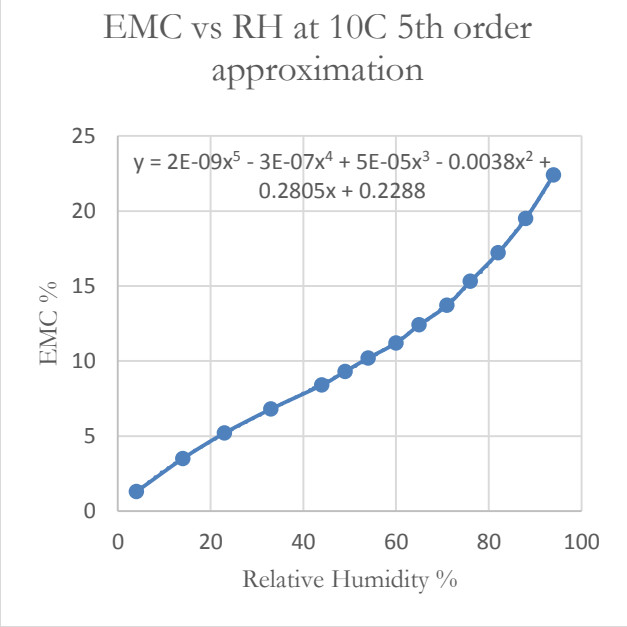

Figure 29: 5th order approximation for Bramhall and Wellwood's EMC and RH data

Kollman (1959) described the hysteresis effect of adsorption. Hysteresis, generally speaking, is a phenomenon that occurs when a systems output is dependent on its history of inputs. Orman (1955) displayed that in the case of moisture movement in wood, this effect is reduced as "moisture changes cover a narrower range". Figure 2-23 show how adsorption and desorption effects within wood forms a loop.

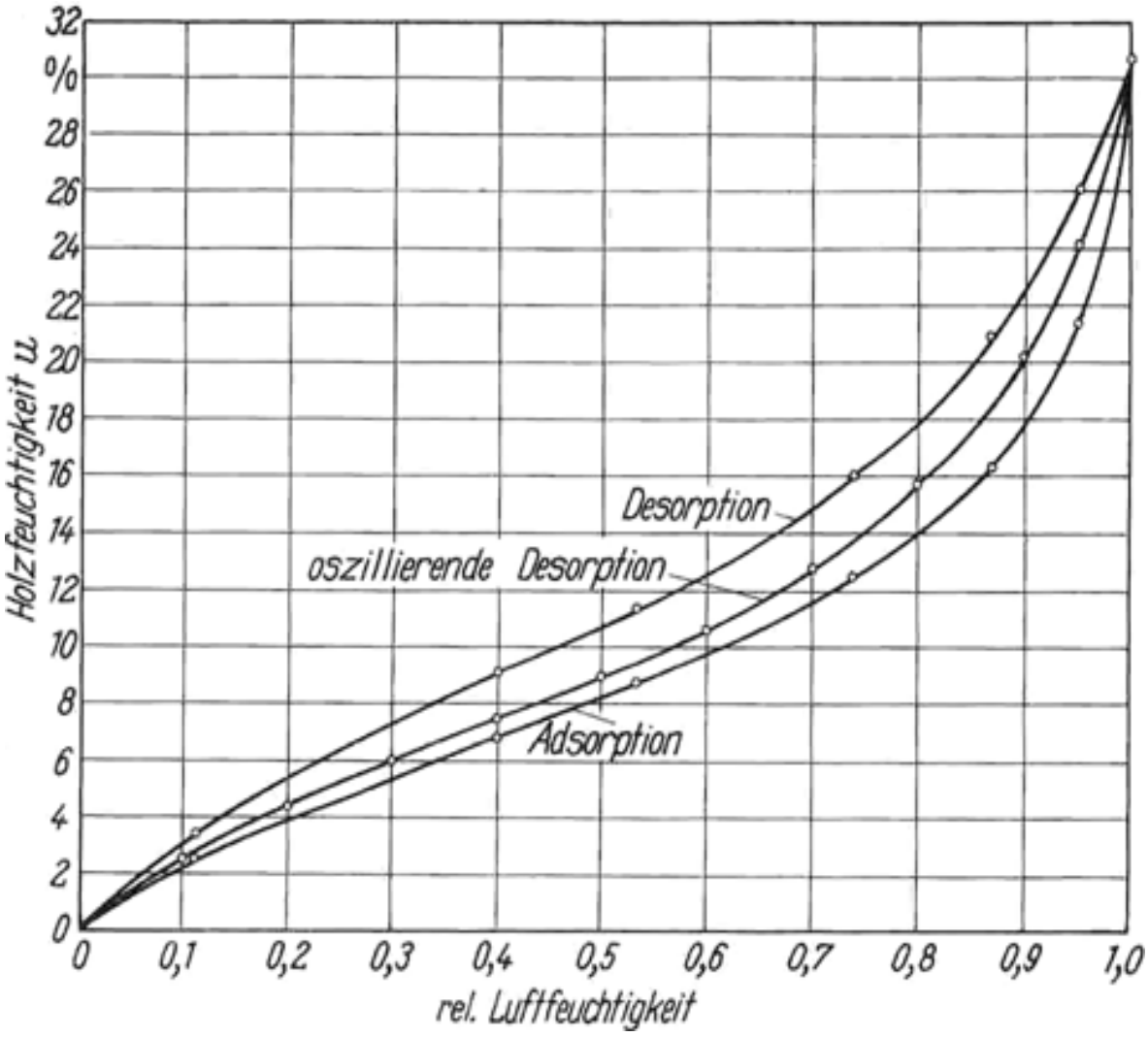

Figure 2-231: Moisture Content vs. Relative humidity hysteresis effect (after Kollman (1959))

A more analytical approach was taken by Pang (1994). The method of non-linear least squares regression analysis was applied to Cunningham and Sprott's (1984) correlation and the resultant prediction equation for Equilibrium Moisture Content for Radiata Pine is as follows:

$$X_e = \frac{18}{W}\left[\frac{K_1 K_2 \psi}{1 + K_1 K_2 \psi} + \frac{K_2 \psi}{1 - K_2 \psi}\right]$$

Where,

X_e = Equilibrium Moisture Content

ψ = Relative Humidity expressed as a decimal

K_1, K_2 and K_3 are temperature dependent coefficients defined mathematically as follows:

$$K_1 = 9.864 + 0.04773T_C - 5.012*10^{-4}\ T_C^{\ 2}$$

$$K_2 = 0.7196 + 1.698*10^{-3}T_C - 5.553*10^{-6}\ T_C^{\ 2}$$

$$W = 187.6 + 0.6942T_C - 0.01853T_C^{\ 2}$$

Since Equilibrium Moisture Content is expressed as a multivariable function of Relative Humidity and Temperature, simulations for this were done and the profiles produced are shown in Figure 2-24. Noticeable difference in the profiles obtained from Bramhall and Woodwell's data and Pang's Least Squares approach on Cunningham and Sprott's (1984) equations is that the profiles in Figure 2-24 are smoother and there are no deviations which can be seen in the profile at 30C in Figure 2-18. This is where the application of Least Squares regression was useful since this method minimizes the sum of the squares of errors giving a better fit solution.

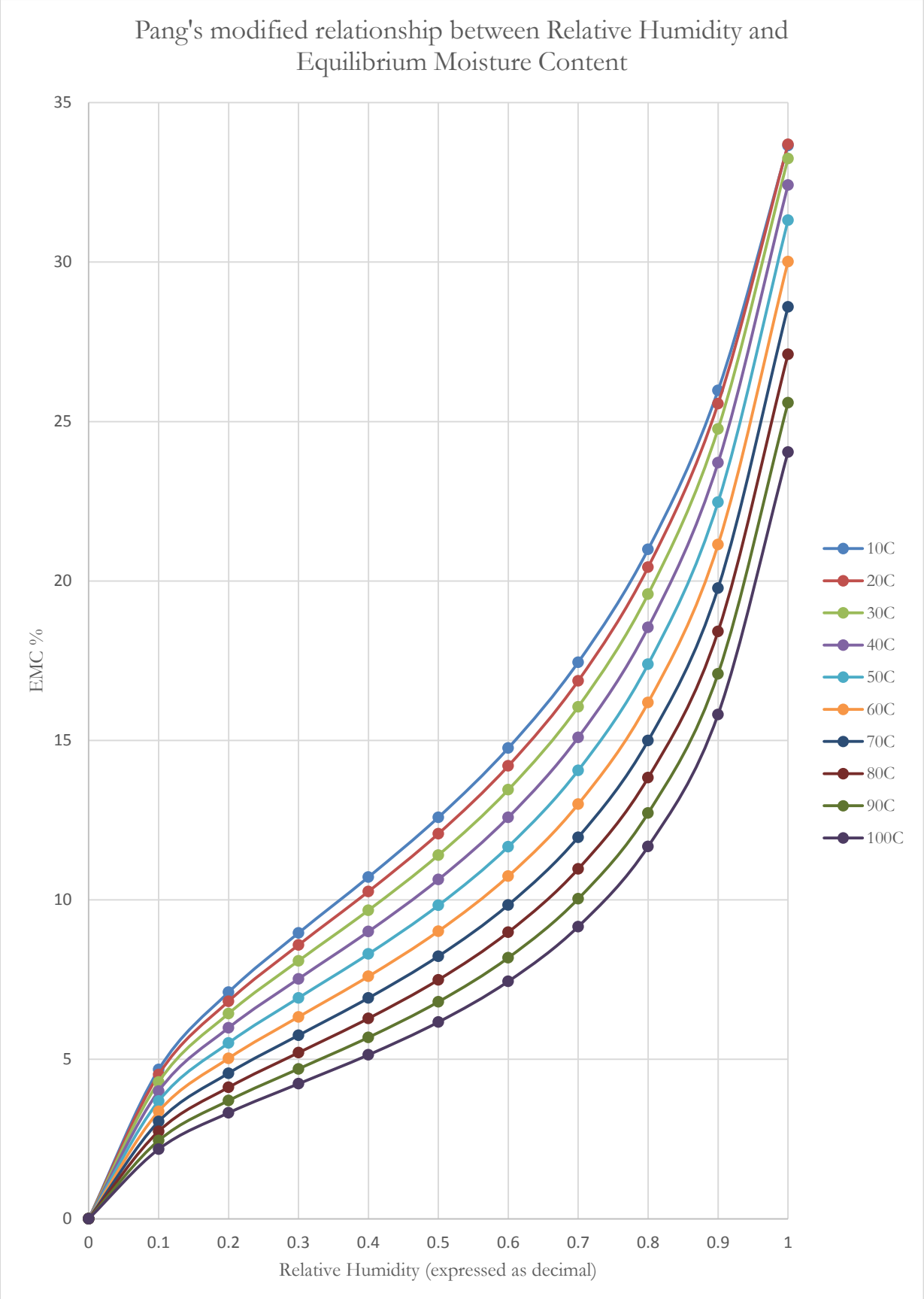

Figure 2-32: Pang's modified correlation for RH and EMC obtained using least squares regression (After Pang, 1994)

2.5.2 MOISTURE CONTENT AND TEMPERATURE GRADIENTS IN BOARDS

The hygroscopic nature of wood makes it dimensionally unstable when being exposed to varying humidity or liquid water. As the moisture is absorbed by the wood, there is an increase in volume which may also be generated when the wood unevenly loses moisture causing uneven shrinkage. This dimensional instability of boards (in general) is thought to be the result of residual stresses which are generated in the panel during the hot pressing and possible curing of the adhesives.

The mechanism of moisture transfer can be explained as follows. The hot platen is the heat source for the board hot pressing. As soon as it touches the board surface, the water that is bound in the cellular structure and that in the adhesive/resin evaporates (Gupta, 2007). The vapor pressure in the surfaces of the outermost layer consequently increases and gives rise to a vapor pressure gradient through the board thickness (high towards the surfaces and low in the core). As the vapor migrates to other areas of the board which are cooler, it condenses and latent heat is released consequently. According to Gupta, this results in a "relatively rapid temperature rise along with an increase in the moisture content". With continuing of the hot pressing, the transferred heat in the core starts to evaporate the moisture and a front of evaporation appears which moves gradually towards the central plane (Gupta, 2007). Through this mechanism across the board, temperature and moisture gradients develop indicating that in the process heat and mass transfer are coupled.

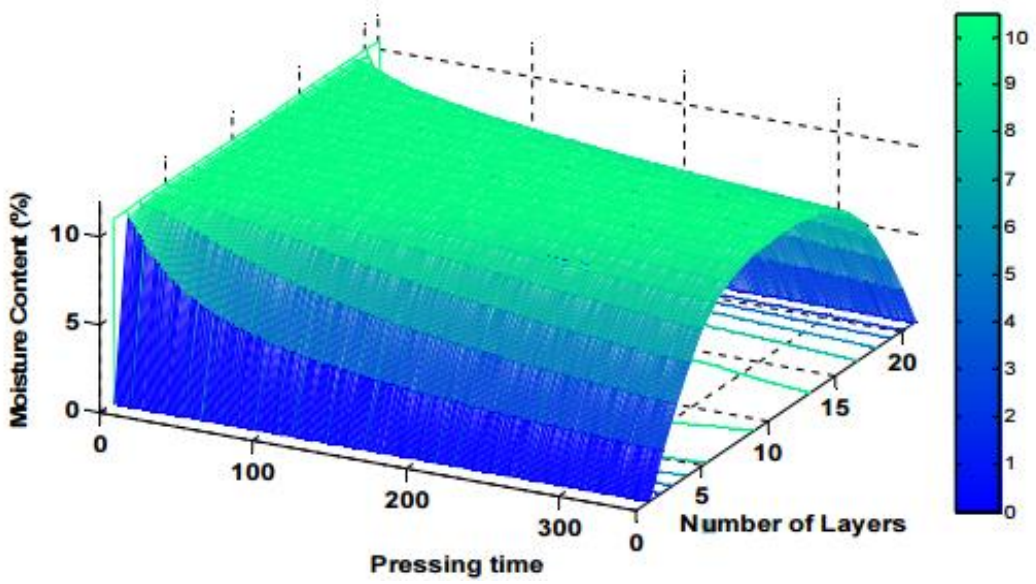

Figure 2-33: Moisture content gradient in MDF board during hot press (After Gupta (2007))

Figure 2-25 shows an example of moisture content gradient development with pressing time in MDF which was predicted from a mathematical model by Gupta. The moisture content at the surface is reduced to a very low level as the hot platen touches the board surface. This also depicts that the maximum moisture content is concentrated at the center (core). Gupta also applied his mathematical model to predict temperature gradient with pressing time and the results are shown in Figure 2-26. The results suggest that the core temperature increases at a much slower rate in comparison to the top surface layer which reaches the hot plate temperature quickly.

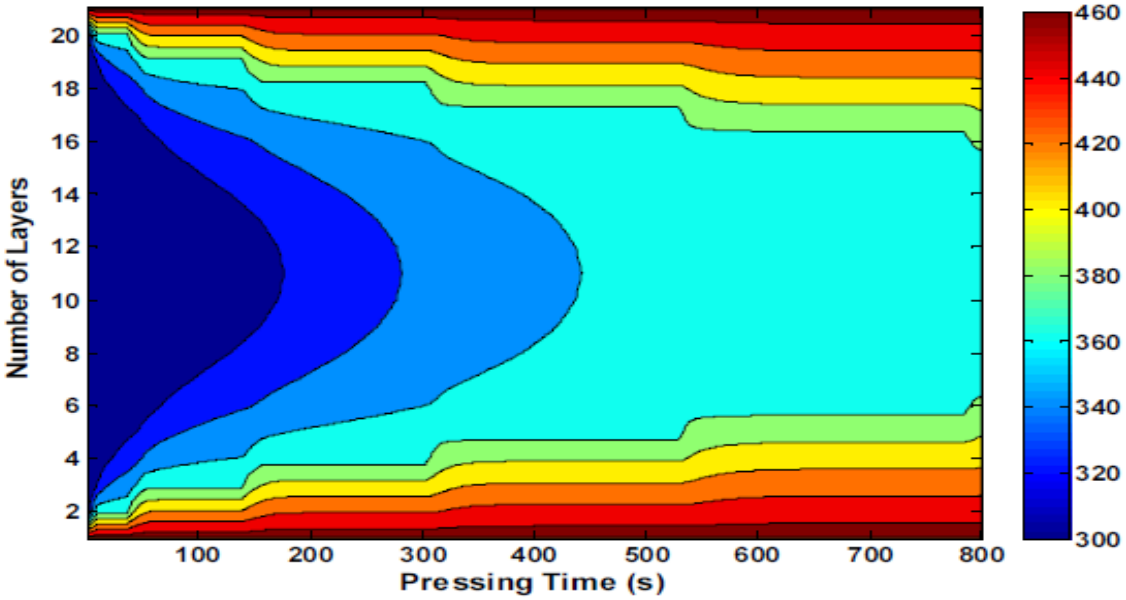

Figure 2-34: Temperature profiles in a MDF board during hot pressing (After Gupta (2007))

Costa and Carvalho (2007) estimated physical and transport properties employing correlation available in literature and concluded that thermal conductivity, steam diffusivity and permeability had a significant effect on the heat and mass diffusion phenomena in MDF through experiments. These properties were considered to be time dependent. The equations used in their study were taken from previous studies such as Siau (1984) which gave an expression for calculation of specific heat for moist wood, Humphrey (1982) which provided an expression for thermal conductivity with correction for temperature and moisture content terms, Suzuki and Kato (1989) which gave an expression for porosity in MDF, Stanish et al. (1986) who provided the "semi-empirical equation" for air interdiffusion coefficient calculation and Hata et al. (1990) who calculated the effective diffusivity of steam in air within a board. These correlations in addition to thermodynamic relationships gave enough information to solve the three

dimensional Partial Differential Equations which rise from the Energy and Mass balances (solved by using the methods described by Patankar (1980) and Spalding (1972)). The main conclusions from Costa and Carvalho's were that the temperature gradient at the surface formed a "plateau" and gas/steam pressure decreased since the surface was losing vapor at a much faster rate than gaining. Also, during pressing, the temperature profile was observed to be linear over the horizontal surface meaning that the vertical temperature profile while mass transfer profiles were observed to be linear in the vertical direction.

2.5.3 Stress and Strain development

Stresses are introduced into wooden boards due to the effect of hot pressing since it gives rise to moisture content gradients and temperature gradients. These stresses can have serious consequences on the stability of the board and it is therefore important to be able to measure those stresses and strains. Figure 2-27 shows a moisture content profile for a Sitka Spruce flakeboard which is similar to MDF. Humphrey (1990) showed that the moisture content was concentrated in the centre of the MDF since the surface layers are closest to the platens and at high temperature resulting in decrease in moisture from the surface. This means that the board will have to reach equilibrium with the atmosphere which is cooler resulting in a decrease in temperature/moisture content and contractions in the board.

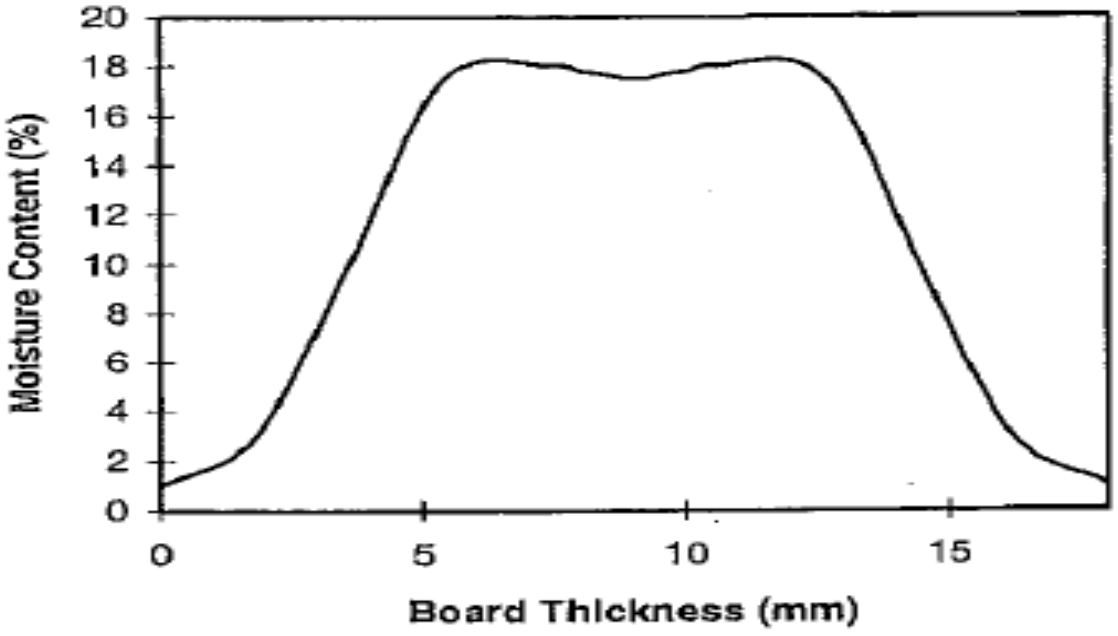

Figure 2-35: Moisture content as a function of board thickness of Sitka spruce flakeboards after hot pressing (After Humphrey (1990))

The residual stress development equation used by Houts et al. (2000) is shown below.

$$\varepsilon_i = \frac{\sigma_i}{E_i} + \alpha_i(\Delta T_i) + \beta_i(\Delta M_i)$$

Where:

Subscript i = layer number

ε= Strain

σ = Stress

E = Young's Modulus (Also varied with relaxation modulus)

β = Coefficient of linear moisture expansion

α = Coefficient of linear thermal expansion

ΔT = change in temperature

ΔM = change in moisture content

Values for change in Temperature and Moisture Content were determined by Kamke and Cassey (1988a, 1988b), Kayihan et al. (1981), Kayihan and Johnson (1983) and Humphrey (1990, 1991). Houts et al. (2000) used two destructive methods namely, dissection and hole-drilling methods to measure residual stresses. About 20 layers were used to investigate the effects of temperature and moisture content one by one. The residual stress distribution is obtained from their results is shown in Figure 2-28 and the conclusion was that the model was very effective at measuring residual stress on the outer board surface. The change in moisture content had more effect than other parameters.

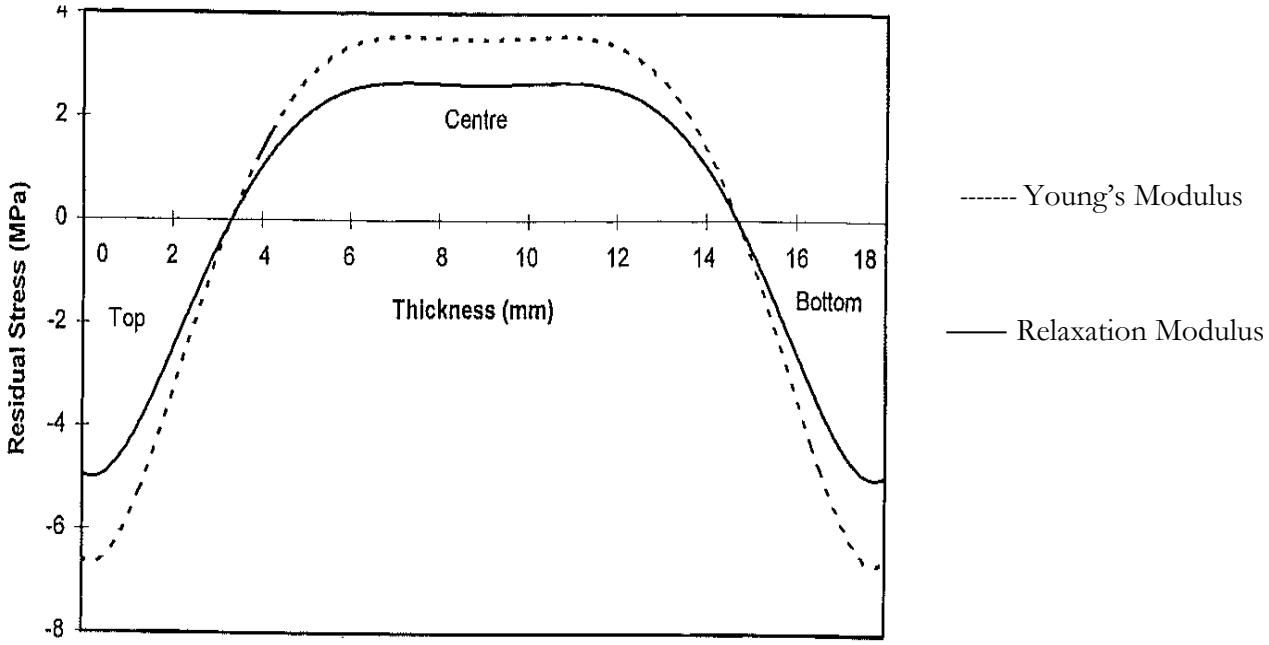

Figure 2-36: Residual stress distribution for a 18mm thick board using young's modulus and relaxation modulus (After Houts et al. (2000))

Pang (2000) also conducted studies of residual stresses in MDF which was a follow-up study after the drying model developed by Pang (1996). Radiata pine boards were dried in a tunnel dryer after which they were cooled and steam conditioned at 100 ^{0}C and maximum relative humidity. Average moisture content, moisture content gradient, temperature profile and stress distribution within the boards were measured. The model in differential equation form is as follows:

$$d\varepsilon = \left(\frac{\partial \varepsilon_X}{\partial t} + \frac{\partial \varepsilon_\sigma}{\partial t} + \frac{\partial \varepsilon_{MS}}{\partial t} + \frac{\partial \varepsilon_C}{\partial t} + \frac{\partial \varepsilon_T}{\partial t}\right).dt$$

Where:

ε = Total strain

ε_X = Strain due to moisture shrinkage

ε_σ = Strain that is induced by stress

ε_{MS} = Mechano-sorptive strain

ε_C = Creep strain

ε_T = Temperature induced strain

t = Time

Pang's study concluded that the stresses were not effectively relieved if the board kiln drying was stopped too soon and processed. Overall the model was in very close agreement with experiment results but more data and further improvements are needed.

2.6 RELATED RESEARCHES ON WOOD WARPING

Warping has been observed in other studies on wood. Gereke et al. (2009) conducted a study on hygroscopic warping of cross-laminated solid wood panels which were made from Norway spruce and were exposed to different climate conditions between 65% and 100% relative humidity at both faces. Cup deformation was observed in addition to increasing relative thickness of the outer layer and "annual growth ring orientation was found to have significant influence in the magnitude of cup formation". The simulation prepared by the team took into account elastic strain, moisture-induced swelling and mechano-sorptive strain and was well in agreement with the test results. Bader et al. (2007) and Popper et al. (2004) did similar work on three layered solid wood panels made of Spruce. Bader et al. worked on calculating water vapour diffusion and thermal conductivity in those samples and concluded that the voids cause a "slight decrease of the coefficient of thermal conductivity". Bader's study was also in agreement with Gereke's in that the orientation of the growth rings was a contributing factor in determining some physical properties. Popper et al. tested spruce panels' water vapour diffusion for both wet and dry climatic conditions. The conclusion of this study was that diffusion was much more restricted in dry conditions (RH ranging from 100% to 65% at 20^0 C) than wet conditions (RH ranging from 0% and 65% at 20^0 C). Another observation made was that the type of adhesive was not a factor that affected the results but rather the "number of glue layers per panel thickness" as it contributed to the water vapor resistance to diffusion.

Cai and Dickens (2003) calculated Modulus of Elasticity, Linear Expansion, Poisson's ratio among other quantities for veneer composites under influence of a moisture gradient and created a two-dimensional warping model. They concluded that Poisson's ratio had "the potential to increase warp" and shear modulus had no effect while the relationship of Modulus of Elasticity and Linear Expansion was highly complicated with warp. The most interesting observation was that density had a linearly negative relationship with warp since "self-weight" of the panel provided the necessary torque required to counteract warping. Ganev et al. (2003) did a similar

study on MDF panels and found contradicting results to Cai and Dickens when relating panel density to warp. Ganev's finite element model method found that as the average panel density increased, the level of warp increased consequently as a result of "effect of density on the expansion properties". They also concluded that the panels with a sharper density profile experienced higher strain profiles which allowed warp to be more severe on those panels.

A more analytical approach was chosen by Xu and Suchsland (1995). Noriss' (1964) equation used for calculation of warp is displayed below:

$$W = \frac{L^2}{8} \frac{\frac{\sum_1^n \alpha_i E_i (S_i^2 - S_{i-1}^2)}{\sum_1^n E_i (S_i^2 - S_{i-1}^2)} - \frac{\sum_1^n \alpha_i E_i T_i}{\sum_1^n E_i T_i}}{\frac{2\sum_1^n E_i (S_i^3 - S_{i-1}^3)}{3\sum_1^n E_i (S_i^3 - S_{i-1}^3)} - \frac{\sum_1^n E_i (S_i^3 - S_{i-1}^3)}{2\sum_1^n E_i T_i}}$$

This equation was tested for the values of E_i (Modulus of Elasticity) and α_i (expansion value for given exposure interval of layer i) which were thought to be inaccurate due to deformations in the longitudinal direction being a mix of elastic and inelastic and not purely elastic which is the basis of the equation. Other terms in the equation are as follows:

W = Deflection at center span of laminated beam (mm)

T_i = Thickness of layer i (mm)

S_i = Sum of thicknesses $\sum T_i$ (mm)

L = Length of beam (mm)

Xu and Suchsland experimentally modified the values for Modulus of elasticity and expansion and used the numerical value obtained from the equation to compare with measured warp of various types of wood beams that were manufactured fresh in laboratory conditions at various moisture contents. This modification was coined the term "inelastic approach". When compared, Xu concluded that these modifications allowed for a better estimation of warping and that for plywood the expansion value should be modified "for the cross-grain direction by reducing the tabulated value to one fourth" while no such change was required for MDF and particleboards since they showed more elastic behaviour.

As mentioned previously, Equilibrium Moisture Content, Relative Humidity and Temperature are major factors to consider when studying warping since they greatly affect the structural integrity of a wood panel by controlling the driving force for the moisture diffusion. Wu (1998)

used Nelson's (1983) isotherm models based on Gibb's free energy to determine a relationship between EMC and Relative Humidity. The model used was as follows:

$$\frac{RH}{100} = exp\left\{\left(-\frac{W_w}{R\,.T}\right)\ exp\left[A\left(1.0 - \frac{EMC}{M_v}\right)\right]\right\}$$

Where

RH = relative humidity in percent;

W_w = molecular weight of water;

R = universal gas constant;

T = absolute temperature (K);

A = natural logarithm (ln) of Gibbs free energy per gram of sorbed water as RH vanishes;

M_v = a material constant which approximates the fiber saturation point for desorption (%).

EMC = Equilibrium Moisture Content

Wu experimented on commercially available oriented strandboard, particleboard, medium-density fibreboard, hardboard, high pressure laminate, aspen and southern pine by testing equilibrium moisture content at various relative humidities. Nelson's model worked quite accurately for all these types of wood types showing that M_v values were "considerably lower" for HPL, hardboard and MDF in comparison to other types. Another quantity considered was hysteresis which is defined as the ratio of adsorption to desorption moisture contents. This was seen to vary between 0.77 and 0.85 for all types of sample.

2.7 SCOPE OF THESIS

The literature examined in this Chapter has been chosen carefully to justify that further study in the field of wood warping through examining fundamental properties like Moisture Content, residual stress and strain is required. To date, a study on Triboard product made by a company is missing in literature and this thesis will hopefully scratch on the surface of the problem that is warping of Triboard.

This project is focusing on investigating the reasons for warping in JNL's Triboard product and all experimentation was carried out at AICA in New Plymouth and University of Canterbury in Christchurch. The experiments were designed so that many variations in JNL's current recipe could be examined and a trend could be predicted based on the results.

The experiment set up has been discussed in Chapter 3 while Chapter 4 shows the results and discusses possible trends obtained from 3-point bend mechanical testing and high temperature drying of Triboard samples. Chapter 6 contains conclusions drawn from results and possibility of experiments that could help with further work on Triboard.

2.8 REFERENCES

1. Anonymous (1954) *Color Tests for differentiating heartwood and sapwood of certain oaks, pines and Douglas-fir*. U.S.D.A, Forest Products Laboratory, Tech. Note No. 253.
2. Bader, H.; Niemz, P.; Sonderegger, W. (2006) *Investigation on the influence of the panel composition on selected properties of three-layered solid wood panels*. Holz Roh Werkst (2007) 65:173-181
3. Bamber, R.K. & Burley, J. (1983) *Wood Properties of Radiata Pine* Commonwealth Agricultural Bureaux
4. Bamber, R.K. (1960) *Sapwood and heartwood*. Forestry Commission of New South Wales.
5. Bramhall G., Wellwood R. W. (1976) *Kiln drying of western Canadian lumber*. Canadian Forestry Service, Western Forest Products Laboratory, Information Report: Western Forest Products Laboratory
6. Butterfield, B.G. 1993. The Structure of Wood: An Overview. In Walker, J.C.F. (ed): "*Primary Wood Processing: Principles and Practise"*. Chapman and Hall, London.
7. Cai, Z.; Dickens, J. R. (2003) *Wood Composite Warping: Modelling and Simulation*. Wood and Fiber Science, 36(2), 2004. pp. 174 185
8. Carvalho, L.M.H. and Costa C.A.V. (2007) *Modeling and Simulation of the hot-pressing process in the production of Medium Density Fiberboard (MDF)* Chemical Engineering Communications, 170:1, 1-21, DOI: 10.1080/00986449808912732.
9. Cown, D.J. 1989. *Wood Characteristics of New Zealand Radiata Pine and Douglas fir: Suitability for Processing*. New Zealand Forestry Corporation Ltd. Wellington.
10. Cummins, N.H.O. (1972) *Heartwood differentiation in Pinus species – A modified azo-dye test*. New Zealand Journal of Forestry Science Vol. 2, 188-91.
11. Cunningham M.J. and Sprott T.J. (1984) *Sorption properties of New Zealand building materials*. Research report R43, Building Research Association of New Zealand, Judgeford.
12. E.T. Howard & F.G. Manwiller 1969: *Anatomical characteristics of southern pine stemwood. Wood Science*, 2:77
13. Ganev, S; Cloutier, A.; Gendron, G.; Beauregard. (2003) *Finite Element Modelling of the Hygroscopic Warping of Medium Density Fiberboard*. Wood and Fiber Science, 37(2), 2005, pp. 337-354
14. Gereke, T.; Gustafson, P.J.; Persson, K.; Niemz, P. (2009) *Experimental and numerical determination of the hygroscopic warping of cross-laminated wood panels*. Holzforschung, Vol. 63 pp. 340-347

15. Green Gold Industrial Co., Ltd. *About Wood, Science of Wood* Available at: http://www.ggi-myanmar.com/wood/
16. Gupta, A. (2007) *Modelling and Optimisation of MDF Hot Pressing.* Unpublished Doctoral dissertation, University of Canterbury, Christchurch, New Zealand.
17. Harris, J.M. (1961): *The dimensional stability, shrinkage intersection point and related properties of New Zealand timbers.* Technical paper/ Forest research institute, New Zealand forest service (36), 17.
18. Hata, T., Kawai, S. and Sasaki, H. (1990) *Computer simulation of temperature behaviour in particle mat during hot pressing and steam injection pressing* Wood Science and Technology, 24, 65.
19. Houts J., Bhattacharyya D. and Jayaraman K. (2000) *Determination of Residual Stresses in Medium Density Fibreboard* Holzforschung 54 (2000) Volume 54 176-182.
20. Humphrey, P.E. (1982) *Physical aspects of wood particleboard manufacture* Ph.D. Thesis, University of Wales, U.K.
21. Humphrey, P.E. (1990) *Some physical transformations that occur during the cure of thermosetting adhesive-to-wood bonds* Proc. Wood adhesive in 1990: status and needs, May 1990, Pullman, WA. pp 86-90
22. Humphrey, P.E. (1991) *Pressing issues in panel manufacture: Internal behaviour during pressing and its impact on time minimization, properties and profit.* Proceedings of the Washington State University International Particleboard/Composite Material Series Symposium. Publ. by Washington State University, Pullman, WA. pp. 99-108.
23. Industrial Equipment Manufacturing (2015) Available online at: https://plus.google.com/photos/101011169587362149520/albums/6059327581532488353/6059327774667494466?pid=6059327774667494466&oid=101011169587362149520
24. Insights.co.nz, 'Forestry Insights'. N.p., Retrieved on: 6 Aug. 2015. Available online at: http://www.insights.co.nz/products_processes_f.aspx
25. J.G. Haygreen and J.L. Bowyer, *Forest Products and Wood Science: An Introduction,* Second Edition, Iowa State University Press, Ames, IA, 1989
26. Kamke, F.A. and Cassey L.J. (1998b). *Fundamentals of flakeboard manufacture: internal-mat conditions.* Forest Prod. J. 38 (6), 38-44.
27. Kamke, F.A. and Cassey, L.J. (1988a). *Gas pressure and temperature in the mat during flakeboard manufacture.* Forest Prod. J. 38 (3), 41-43.
28. Kayihan, F. and Johnson, J.A. (1983). *Heat and moisture movement in wood composite materials during the pressing operation – a simplified model.* In: *Numerical methods in heat transfer,* Volume II.

Eds. R.W. Lewis, K. Morgan, and B.A. Schrefler. John Wiley and Sons, New York pp. 511-531.

29. Kayihan, F., Johnson J.A. and Lubon C. (1981) *Preliminary calculations of heat and mass transfer during the pressing operation of wood composite materials during the pressing operation of wood composite manufacture.* In: *Numerical methods in thermal problems,* Volume II, Eds. R. W. Lewis. K. Morgan, B.A. Schrefler. Pineridge Press, Swansea, U.K. pp. 277-188.
30. Kininmonth, J.A. and Whitehouse, L.J. 1991. "*Properties and Uses of New Zealand Radiata Pine: Volume 1-Wood Properties"*. New Zealand Ministry of Forestry, New Zealand Forest Research Institute, Rotorua, New Zealand.
31. Kollman, F. (1959) *Uber die Sorption von Holz und ihre exakte Bestimmung. Holz als Werkstoff* Volume 17, Issue 5, pp 165-171
32. Lewin, M. and Goldstein, I.S. 1991. *Wood Structure and Composition*. Marcel Dekker, Inc. New York.
33. Maloney, T.M. (1993) *Modern Particleboard & Dry-Process Fiberboard Manufacturing* (Updated Ed.). San Francisco: Miller Freeman
34. Nelson, R.M. (1983) *A Model for Sorption of Water Vapor by Cellulosic Materials* Wood and Fiber Science, 15(1), 1983, pp. 8-22
35. Norris, C.B. (1964) *Warpage of laminated materials due to change in moisture content or temperature.* Linear movement of plywood and flakeboards as related to the longitudinal movement of wood. USDA Forest Service Research Note FPL-073.
36. Orman, H.R. (1955) *The response of New Zealand timbers to fluctuations in atmospheric moisture conditions.* Technical paper/Forest research institute, New Zealand forest service (no.8).
37. Pang, S. (1994) *High-temperature drying of Pinus Radiata boards in a batch kiln* Ph.D. Thesis, University of Canterbury, Christchurch, New Zealand.
38. Pang, S. (1996) *Moisture content gradient in a softwood board during drying: simulation from a 2-D model and experimental measurement.* Wood Science and Technology June 1996, Volume 30, Issue 3, pp 165-178, DOI: 10.1007/BF00231631.
39. Pang, S. (2000) *Modelling of stress development during drying and relief during steaming in Pinus Radiata lumber* Drying Technology: An International Journal, 18:8, 1677-1696, DOI: 10.1080/07373930008917806
40. Patankar, S.V. (1980) *Numerical Heat Transfer and Fluid Flow* Hemisphere, New York.
41. Popper, R.; Niemz, P.; Eberle, G. (2004) *Diffusion processes in multilayer solid wood panels.* Holz als Roh-und Werkstoff, Volume 62, Issue 4, pp 253-260

42. Rook, D.A. 1975. *Why does Radiata Pine grow so vigorously in New Zealand?* Forest Industries Review. 7:2-3.
43. Shandong Tengfei Mechanical and Electrical Technology Co., Ltd. *Particle Board Production Line* (TF-2012) Available online at: http://miguel-phil.en.made-in-china.com/product/PqXnzmBTHvpj/China-Particle-Board-Production-Line-TF-2012-.html
44. Siau, J.F. (1984) *Transport Processes in Wood* Series Volume 2 Springer-Verlag Berlin Heidelberg DOI: 10.1007/978-3-642-69213-0
45. Spalding, W.T. (1973) *Predicting equilibrium moisture content of wood by mathematical models* Wood Fiber, 5, 41.
46. Stanish, M. A., Schajer, G.S. and Kayihan, F. (1986) *A mathematical model of drying for hygroscopic porous media* AIChe J., 32(8), 1301.
47. Suzuki, M. and Kato, T. (1989) *Influence of dependent variables on the properties of medium-density fiberboard* Mokuzai Gakkaishi, 35(1), 8.
48. Technology Transfer Network Clearinghouse for Inventories & Emissions Factors *AP 42, Fifth Edition, Volume 1 Chapter 10: Wood Products Industry, Wafer board/Oriented Strand board Final Section* Available online at: http://www.epa.gov/ttn/chief/ap42/ch10/index.html
49. Technology Transfer Network Clearinghouse for Inventories & Emissions Factors *AP 42, Fifth Edition, Volume 1 Chapter 10: Wood Products Industry, Medium Density Fiberboard Final Section.* Available online at: http://www.epa.gov/ttn/chief/ap42/ch10/index.html
50. The Encyclopaedia of New Zealand *Story: Radiata Pine Page 6 – The wood* Available at: http://www.teara.govt.nz/en/diagram/16850/cross-section-of-a-pine-trunk
51. The Wood Database, *Hardwood Anatomy.* Available online at: http://www.wood-database.com/wood-articles/hardwood-anatomy/
52. Trade belt: Pu/PIR Discontinuous for Freezing & Refrigeration Panel, 2015. Available online at: http://plant.tradebelt.com/PUPIR_line02/Hot_Press_Line.html
53. Walker, J.C.F. (2006) *Primary Wood Processing: principles and practise* (2nd Ed.) Dordrecht, The Netherlands: Springer.
54. Worldwide Recycling Equipment Sales, *Deal of the day: Heil 24' Triple Pass Dryer.* Available online at: http://wwrequip.com/blog/equipment-specials/deal-of-the-day-heil-24-triple-pass-dryer/
55. Wu, Q. (1998) *Application of Nelson's Sorption Isotherm to Wood Composites and Overlays.* Wood and Fiber Science, 31(2), 1999, pp. 187-191

56. Xu, D; Suchsland, O (1995) *A Modified Elastic approach to the theoretical determination of the hygroscopic warping of laminated wood panels.* Wood and Fiber Science, 28(2), 1996, pp.194-204

CHAPTER 3

EXPERIMENTS ON FUNDAMENTAL STUDIES

In the cases where stresses in a material/specimen remain even after the source of external force is removed, these stresses are coined the name 'residual stresses'. Depending on the situation of material application, these residual stresses may be desired or undesired. In the Triboard case, residual stresses are undesirable, which is one of the key factors causing board warping when the stresses are not symmetrically balanced.

In the early stage of hot pressing, the board surfaces are first heated up and lose moisture, therefore, the surface layers tend to shrink while the core layers are still cool and retain the original dimension. In this way, the surface layers are stretched while the core is compressed. However, the core thickness is much greater than the surface layers, and the tensile stresses in the surface layers are much greater which stretch the surface layers rather than compressing the core. In the meantime, the adhesive in the surface layers are cured, and the fibres are consolidated. In this way, the surface layers are stabilized at a stretched state. With further hot pressing, the core starts to lose moisture and shrink, but the surface layers have already been set at a stretched state which will resist the core shrinking. A compromise will eventually be reached between the surface layers and the core layer: the surface layers are now in tension and the core in compression. If the surface layers are sliced at this state and the constraints are released, the surface layers will stretch and the core shrink. Evidence for this has been found in Pang's study of the JNL Triboard (Chapter 1). However, this is only a qualitative observation and the exact mechanism for the stress generation during the Triboard hot pressing is still unclear.

Winandy and Krzysik (2007) conducted a study on MDF panels, and deduced that different press platen temperatures and press times had significant impact on appreciable loss in all mechanical properties, with bending strength being the most affected property. Application of adhesive is for the wood particles to hold together firmly through the adhesion force once the adhesive has cured. The adhesion areas also prevent moisture movement due to the consolidated state. The ultimate effect of adhesive on the residual stress and consequently the board warping is not fully understood and no papers or reports have been found in literature. In this chapter the experimental work undertaken at AICA laboratory, New Plymouth will be explained in detail.

3.1 Experimental Objectives

The objectives of the experiments were to investigate the effects of operation conditions including hot press temperature, moisture contents of MDF fibres and strands, resin loading and MDF fibre layer thickness on residual stress and moisture content profiles in Triboard. The stress gradient and symmetry in the Triboard are believed to be heavily contributing to warping. The Triboard samples were made on a small scale lab hot press available at AICA situated in New Plymouth. Test sample preparation and most of the measurements were also performed at AICA. 3-point bend test and high temperature oven drying of samples were conducted at University of Canterbury.

3.2 Experiments for Control Board Manufacturing

3.2.1 Materials

Materials: Radiata pine strands and MDF fibres supplied by JNL Triboard; MUF resin (for fibres); pMDI (for strands) and wax supplied by AICA

Equipment: Lab scale hot press; Circulation Tube conditioner; Mixer for resinating fibres and strands; Mat Pre pressing box; Hot Press; Table Saw at Ron Mallet's wood workshop; Instron Testing Machine at Model Structures Laboratory, University of Canterbury; Multi-saw (borrowed from Scion, Rotorua)

Instrument and sensors: Balance (±0.01g); Length measurement instrument (Digital Vernier caliper) (±0.01mm).

3.2.2 BASE RECIPE FOR TRIBOARD MANUFACTURING

Table 3-11: Base recipe for preparing MDF fibers for control Triboard sample

Components of fibres	by Mass (g)	By percentage of dry fibre mass (1000 g)
Oven dry fibres	1000	-
Moisture	70	7.00%
MUF (Solids)	120	12.00%
MUF (Solution)	182	18.20%
Wax	15	1.50%
Total mass of resinated fibre	1267g	

NOTE: The 182 MUF solution contains 120 g solids. A mass-thickness ratio of 175 g/mm was used for the fibre layers. This ratio was also used in Set D where the thicknesses of the fibre layers was varied. All other boards were using 525 g of fibre which corresponds to 3 mm thickness.

Table 3-12: Base recipe for preparing strand for control Triboard

Components of Strand	by Mass (g)	By percentage of dry strand mass (1700 g)
Moisture	153	9.00%
pMDI (Solid)	50.05	2.94%
pMDI (Solution)	77	4.53%
Wax	26	1.53%
Scavenger	28	1.65%
Total wetting present in dry strand	284	16.70%
Total mass of resinated strand	1984g	

NOTE: The 77g pMDI solution contains 50.05g solids.

Actual use of resinated wet strands: 1663 g

The strand thickness was 15mm making the board thickness for the base recipe at 21mm and the mass-thickness ratio for the strand about 111 g/mm.

3.3 BOARD PREPARATION METHOD

All boards were prepared using the same method except where there is a variation in recipe. This is described per set.

- The fibres and strands were selected separately and then weighed. After this the fibres were conditioned in a circulating pipe system to achieve a uniform moisture content. An example is shown in Figure 3-1.

Figure 3-37: Natural and forced circulation dryer (After Espoir Engineering Pvt. Ltd.)

- MUF solution and wax were measured in beakers as required from the recipe, and then sprayed into the circulation tube to mix with the fibres. Similarly, pMDI solution, wax and scavenger were measured as per required from the recipe, and then sprayed into a mixer to strands. A scavenger is a chemical added to wood panels to reduce the emissions formaldehyde emissions.

- These resinated fibres and strands were collected and weighed as required from the recipe for mat forming in a specially designed box and the mat was prepressed.
- The fibres were laid first at bottom, then strand in the middle and finally another layer of fibre on top as per the experiment set requirements.
- The pre-pressed mat was then covered with a steel plate before it was moved into the hot press which was operated at the required temperature.
- The mat was hot pressed for about 500 seconds depending on the recipe, with Temperatures of two plates and the distance between them (board thickness) were measured and data was logged by a computer. A temperature of 170 ^{0} C was used for pressing of the control boards. An example photo of data logging with temperature curves inside the hot press can be seen below (Figure 3-2).
- The finished board was labelled and packed for sawing and cutting procedures.

Figure 3-38: Data logging during hot pressing for board A1

3.4 EXPERIMENTS FOR MANUFACTURING TEST BOARD SAMPLES

NOTE – Set C was done first as it allowed an idea of which temperature would be the best for hot pressing the boards. 170^{0}C was chosen for hot pressing of other sets as it produced the best cured board.

3.4.1 EXPERIMENT SET A: EFFECT OF ADHESIVE LOADING IN STRANDS AND FIBRES

The resin loadings to fibres and strands were varied from the base recipe in which the MDF fibres had a loading of 18.2% MUF solution and strands had a loading of 4.53% pMDI. The resin loading for the MDF fibres was controlled adequately, however due to the difficulty in accurately loading pMDI in strands, the actual pMDI loadings were different from the plan, although every effort was made to follow the planned loading.

Table 3-13: Recipe variations in manufacturing of set A board samples

Sample Identification	MUF Loading (weight, percentage over oven dry fibre)	pMDI Loading (weight, percentage over oven dry strands)
A1	151.7 g (15.2%)	76 g (4.47%)
A2	182 g (18.2%)	78 g (4.59%)
A3	227.5 g (22.8%)	77 g (4.53%)
A4	151.7 g (15.2%)	68 g (4%)
A5	182 g (18.2%)	75 g (4.4%)
A6	227.5 g (22.8%)	68 g (4%)
A7	151.7 g (15.2%)	90 g (5.3%)
A8	182 g (18.2%)	82 g (4.8%)
A9	227.5 g (22.8%)	85 g (5%)

Note that all loading values are based on solution of adhesive and not solids present in solution.

The adhesive loading (%) is defined as:

$$\frac{Mass\ of\ solid\ resin\ applied\ (g)}{Mass\ of\ dry\ wood\ material\ (g)} \times 100\%$$

Boards are made using the regular methods of laying but the adhesive loading (percent of solid resin applied per unit mass of dry wood materials) is varied between the layers to examine its effect on residual stresses. The resin loadings for the core strands and MDF fibres were investigated in this experiment. For the adhesive to complete curing, the central line of the board needs to reach 135 °C or at least greater than 100 °C for a minute. This was achieved in all the samples made. The adhesive application also prevents moisture diffusion within the board due to the consolidated state.

3.4.2 Experiment Set B: Effect of Fibre and Strand Moisture Content

Table 3-14: Recipe variation on manufacturing of set B board samples

Sample Identification	Moisture in fibre (moisture weight, and oven dry based moisture content)	Moisture in strand (moisture weight, oven dry based moisture content)
B1	100 g (10%)	153 g (9%)
B2	120 g (12%)	153 g (9%)
B3	150 g (15%)	153 g (9%)
B4	110 g (11%)	153 g (9%)
B5	120 g (12%)	221 (13%)
B6	150 g (15%)	221 (13%)

- For manufacturing of this set board samples, moisture contents in fibres and strands before the hot-press were altered over a larger range compared to standard operation at the JNL Triboard mill. Table 3-4 shows these variations.
- **Note** – This set of boards were the most difficult to make, as adding moisture was very difficult and removing water from fibres was even more difficult. A circulation tube conditioner was used for both drying and wetting. Due to this constraint only 6 samples were made in comparison to the originally planned 9.

3.4.3 Experiment Set C: Effect of hot press temperature

Table 3-15: Hot press temperature variation in manufacturing of set C board samples

Sample Identification	Hot Press Temperatures
C1	160^0 C
C2	170^0 C
C3	180^0 C

- In this set, three hot press temperatures were used for manufacturing the Triboard samples. The three platen temperatures were 160 °C, 170 °C and 180 °C as outlined in Table 3-5. Hot press time was not considered as an independent variable as the central line temperature was used as the target to achieve. The core temperature of the board needed to be high enough to cure the adhesive but should not be too high as to overheat the board. Here the target was that the core temperature was held at 100 °C or higher for a minute so that the adhesive can be cured.

- During the hot press, a pair of thermocouple were inserted into the board centre to check and measure the core temperature.

- The base recipe was used to prepare the mats before hot press although some minor variation was noticed between runs as described below.

Note – Resin solution loadings on the MDF fibres and strands are given as follows although it was attempted to maintain these as constants.

C1: MUF loading on fibres: 182g (12%); pMDI loading on strands 88 g (5.2%)

C2: MUF loading on fibres: 182 g (12%); pMDI loading on strands 90 g (5.3%)

C3: MUF loading on fibres: 182 g (12%); pMDI loading on strands 86 g (5.1%)

3.4.4 Experiment Set D: Effect of fibre layer thickness

Table 3-16: Fibre layer thickness/mass variation in manufacturing of set D board samples

Sample Identification	Top Layer Fibre Thickness	Top Layer Fibre Mass (g)	Bottom Layer Fibre Thickness	Bottom Layer Fibre Mass (g)
D1	2 mm	350	2 mm	350
D2	2.5 mm	437.5	2.5 mm	437.5
D3	3 mm	525	3 mm	525
D4	2 mm	350	2.5 mm	437.5
D5	2 mm	350	3 mm	525
D6	2 mm	350	3.5 mm	612.5
D7	2.5 mm	437.5	2 mm	350
D8	3 mm	525	2 mm	350
D9	3.5 mm	612.5	2 mm	350

In this set, effect of varying the MDF layer thickness was investigated. The MDF layer has a minimum limit of 2 mm since thinner than 2 mm would allow the strands to come out during sanding. A mass-thickness ratio of 175 g/mm was used for the fibres as mentioned before. This allowed a better estimation of the thickness layers and made board preparation easier. Table 3-6 shows thicknesses of both layers (top and bottom) and also the corresponding fibre mass for each layer.

Note - Strand thickness remained the same for all samples.

3.5 MEASUREMENTS

3.5.1 SAMPLE BOARD PLAN AND SECTIONING FOR TEST SAMPLES

Schajer (2013) classified measurement methods into two main categories:

1. Relaxation measurement methods
2. Diffraction methods
3. Others including Magnetic, Ultrasonic, Thermoelastic, Photoelastic and Indentation

The measurement required in this project was a combination of layer removal and sectioning methods both of which are relaxation method. This method allows the specimen to be separated from the whole and residual stress to be examined.

Note - Measurement of deformation/warp was not possible since samples made in AICA laboratory were too small to show any visible change.

Once the sample board was made, it was packed and sent to Ron Mallet's workshop for cutting and slicing. The board was trimmed to a square of 330 mm by 330 mm from which the test samples were cut as shown in Figure 3-3.

- The small sections (S1 to S4) cut from the sample board were sliced further in five slices to determine moisture content gradient and strain/stress profile.
- The larger sample FL was sliced for 3-point bend testing to calculate modulus of elasticity (MOE) and modulus of rupture (MOR) while the sample OD was used for oven drying to determine moisture content for each slice and thus allow a plot of moisture gradient to be made.

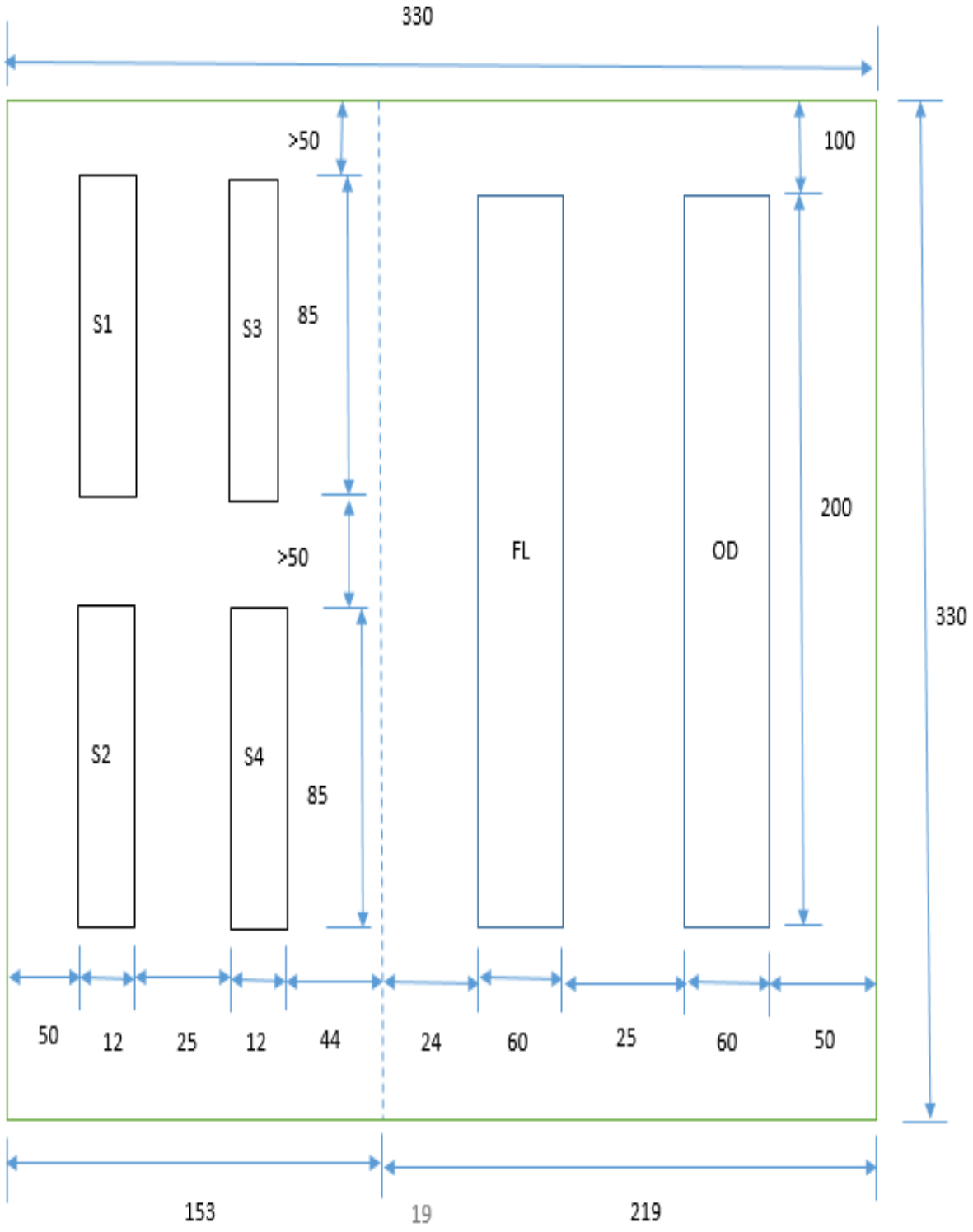

Figure 3-39: Outline of board sectioning plan

Note: Figure is not to scale and only for instructional purposes. All lengths are in millimetres.

After cutting the samples labelled S1, S2, S3 and S4, their actual lengths were measured (L_0) and then sliced in a multi-saw which was sharpened in AICA to get fast slicing. The multi-saw is shown in Figure 3-4.

Figure 3-40: Multi-saw borrowed from Scion, Rotorua

Each slice-cut through the multi-saw produced five smaller slices labelled from top MDF to bottom MDF as 1, 2, 3, 4 and 5 where 1 and 5 were the MDF slices and 2, 3, 4 were the strand slices. The reason for cutting multiple slices is to have more data and get a more accurate average. This was then labelled with their respective board code depending on experiment set. These slices were measured in length after cutting for stress and strain measurement.

3.5.2 Stress, Strain and Moisture Content Measurement

1. After slicing, most of the slices did not maintain their original length (L_0) when residual stresses existed. Slices expanded if they were in compression before the slicing and others contracted if they were in tension before slicing.
2. After slicing, the length and weight of each slice were measured. The final length was denoted L_i, and the changes in length were:

   $\Delta L_i = L_i - L_0$
3. The strain and stress of each slice are calculated by:

   $\varepsilon_i = \Delta L_i / L_0 \quad ; \quad \sigma_i = - \varepsilon_i E_i$

   In which E_i is the modulus of elasticity of the slice

Weights of the slices were taken as soon as they exited the multi-saw and then were sealed in plastic bags to protect from any moisture loss. After measuring the lengths and weights of these slices, they were subjected to 24 hours of oven drying at 103 ^{0}C to determine the oven-dry-weight.

Moisture content distribution (dry basis) was determined as:

$$MC_i(\%) = \left(\frac{W_i - W_f}{W_f}\right) \times 100\%$$

Where:

W_i = Weight of slice before oven drying (g); W_f = Weight of oven-dried slice (g);

The slices obtained from the section OD were used for determination of moisture content gradient and average moisture content only.

The section labelled as FL was for flexural testing to determine modulus of elasticity (MOE) and modulus of rupture (MOR) of strand and MDF fibre layers.

FL and OD sections were separated by using a table saw as shown in Figure 3-5 according to a method below:

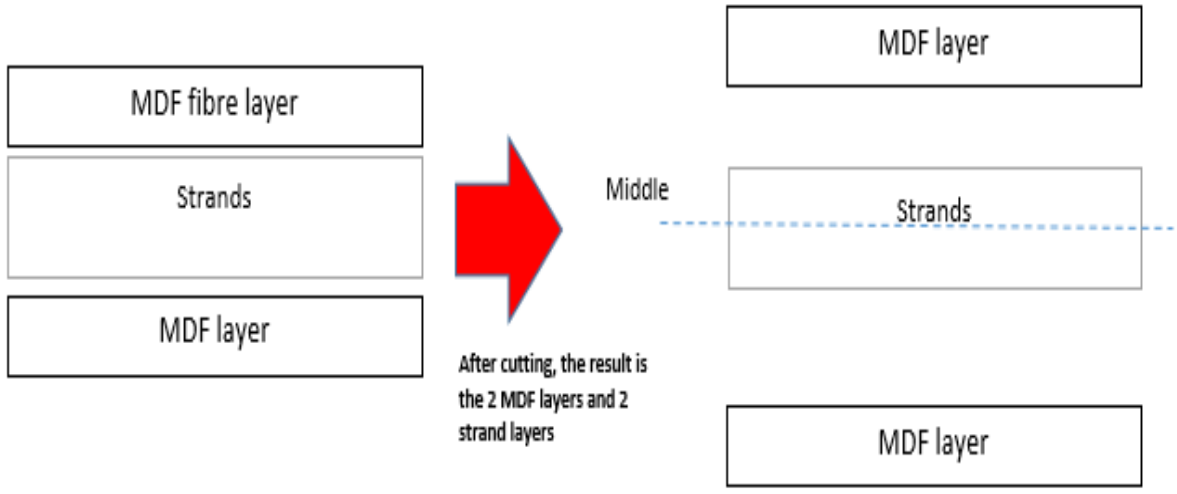

Figure 3-41: Slicing method for larger sections (FL & OD)

1. The section was first cut from the top and then the bottom releasing two MDF layers named 1 and 4 respectively.
2. This left the strand section in the middle which was then sawn from the middle to give two separated strand layers.
3. The upper strand layer was denoted 2 and the one below it was denoted 3.

Each layer was then labelled with the respective board code depending on the experiment set it belonged to (Figure 3-6). So for example for flexural testing from Set B was labelled as:

Top Layer of fibre: B5-FL-1

Second Layer of strand: B5-FL-2

Third Layer of strand: B5-FL-3

Bottom Layer of fibre: B5-FL-4

Figure 3-42: Large slices created from FL section

NOTE – The slices cut from OD and FL sections were also oven-dried after tests for determination of moisture contents. As the moisture loss was more substantial in slicing for small samples, the larger samples sawn from the OD sections are more reliable.

3.6 FLEXURAL TESTING

Yoshihara and Tsunematsu (2006), De Moura et al. (2009) and Forsberg et al. (2010) all had success in implementing three-point bend test in their investigative studies of wood properties which makes three-point bend tests suitable for testing for Modulus of Elasticity (MOE) and Rupture (MOR). Figure 3-7 shows a simple visualization for Three-point bend testing.

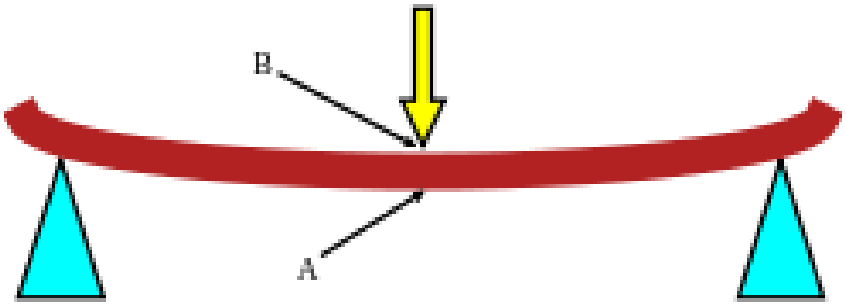

Figure 3-43: Beam under three-point bending (Wikipedia)

Point A experiences tension while point B experiences compression. These mechanisms have been explained as follows:

Tension of a body means that the body is subjected to a pulling force at its opposing ends. This results in tensile internal stresses within the body producing elongation in the direction of the load application (Record, 2004). Wood shows anisotropic features with mechanical properties varying with orientation, namely longitudinal, tangential and radial. The greatest strength and modulus of elasticity are observed in wood along the grain direction (longitudinal) when the tensile force is applied parallel to the grain. Therefore, straight-grained wood specimens are the strongest while cross grain at any angle would reduce the strength and modulus of elasticity of wood since tensile strength perpendicular to the grain is much smaller than those parallel to the grain (Record, 2004).

Compression can be observed in wood specimens when these are under compressive forces no matter the external forces may be applied over the whole surface or part of the surface as seen in Figure 3-8:

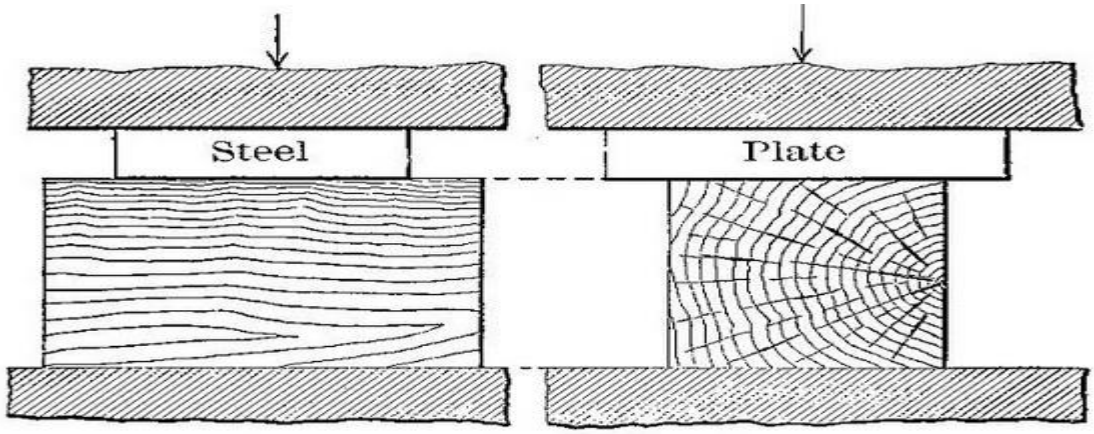

Figure 3-44: Compression scenarios 1(right) and 2 (left) (After Record, 2004)

1. With load acting over the entire area of the specimen.
2. With load concentrated over a portion of the area.

The fibres get compact as a result of the compression across the grain and the load increases irregularly as the density increases (Record, 2004). The irregularities in the load come from the fact that 'the fibres collapse a few at a time, beginning with those with the thinnest walls. In the case of the load being applied only on a specific upper area of the specimen, indentation occurs on the wood through the bearing plate resulting in crushing of the upper fibres (Record, 2004).

Flexural testing equipment was set up in accordance with AS/NZS 4266.5 (Reconstituted wood-based panels - Methods of testing) with a change in the span of the sample tested. Since the sawing of the samples was very difficult and was not perfect, the thicknesses of the samples were not very consistent. AS/NZS 4266.5 required that the span of the sample for 3-point bend testing should be 15 times the nominal thickness of the sample. Also, Yoshihara and Matsumoto (1999) recommended that the span/thickness ratio of specimen to be tested should be more than 20 (Average thickness of the specimens was 4mm). This span requirement was to reduce the effects of shear force on the sample and thus give a more accurate MOE value. Therefore, in the present study, a span of 84 mm was decided for all three-point bending tests. In the MOE tests, the maximum load of 19.31 kg (189.43 N) was applied with a crosshead speed of 2 mm/min. The equipment used is shown in Figure 3-9.

Figure 3-45: Instron machine with data recording software and crosshead speed controller (Model Structures Laboratory, University of Canterbury)

Derivation for MOE of a beam undergoing a three-point bend test is as follows (Roylance, 2000):

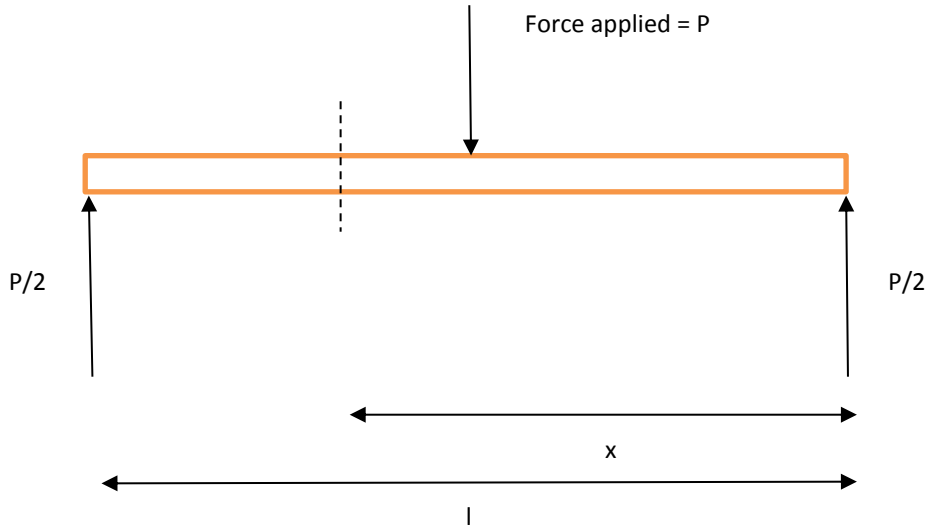

Figure 3-46: Derivation of MOE equation for beam undergoing 3-point bend test for a distance x

$$Bending\ Moment = \ w = \frac{P}{2}\ (l - x)$$

$$Slope = \ \int Bending\ Moment = \ -\frac{P}{4}(l - x)^2 + k$$

where k = first constant of integration

$$Section\ Modulus = \ \delta EI = \ \iint Bending\ Moment = \ \frac{P}{12}(l - x)^3 + kx + c$$

where c = second constant of integration

The two boundary conditions are as follows:

$$At\ x = \frac{l}{2}\ , Slope = 0; At\ x = l, Deflection = 0$$

These give the constants of integration as:

$$k = \frac{Pl^2}{16}\ ; c = \ -\frac{Pl^3}{16}$$

Thus,

$$\delta EI = \frac{P}{12}(l - x)^3 + \frac{Pl^2}{16}x - \frac{Pl^3}{16}$$

At midpoint,

$$\delta EI = \frac{P}{12}\left(l - \frac{l}{2}\right)^3 + \frac{Pl^2}{16}\frac{l}{2} - \frac{Pl^3}{16}$$

$$E = \frac{P\ l^3}{48\delta I}$$

Where

E = Modulus of Elasticity (MOE)

P = Difference between 40% and 10% of maximum load

I = Moment of Inertia

δ = Deflection

l = length of beam

In a similar fashion, the equation for MOR can also be derived: $MOR = \frac{P\,l}{(b\,d^2/6)}$

Where

P = Difference between 40% and 10% of maximum load

l = length of beam

b = width of beam

d = thickness of beam

3.7 ERRORS ASSOCIATED WITH EXPERIMENTATION

The experimental errors in the final results are associated with the accuracies in the various stages of the experiments which are analysed as follows:

1. Time was spent between making board, slicing and testing which induced moisture loss from boards to ambient and moisture transfer within a board. Results obtained from Set A and B are more reliable since they were made, cut, measured for dimensions and packed on the same day. There was one-day delay for sets C and D for measuring dimensions. There was further delay of a week for tests of MOE and MOR samples. These samples were first brought from New Plymouth to Christchurch and then testing for mechanical properties and oven drying began.
2. A saw was used to separate fibre layers and strand. This was not perfect as the MDF layers had some cured strand attached to it.
3. Multi saw blades were sharpened to a high degree after some slicing tests, therefore the slices made before the saw sharpening were overheated losing mass and moisture.
4. Some moisture gain may have occurred in weighing the samples after oven drying.

3.8 REFERENCES

1. AS/NZS 4266.5:2004 Reconstituted wood-based panels – Methods of test*: Method 5: Modulus of elasticity in bending and bending strength.*
2. David Roylance, Department of Materials Science and Engineering MIT, Cambridge, MA 02139 *Beam Displacements* November 30, 2000.
3. De Moura, M.F.S.F., Dourado, N. and Morais, J. (2009) *Crack equivalent based method applied to wood fracture characterization using the single edge notched-three-point bending test.* Engineering Fracture Mechanics, Elsevier, DOI: 10.1016/engfracmech.2009.10.008.
4. Espoir Engineering Pvt. Ltd. (2013) Available online at: http://www.indiamart.com/espoirengineering/process-equipment-division.html
5. Forsberg, F., Sjodahl, M., Mooser, R., Hack, E. and Wyss, P. (2010) *Full three dimensional strain measurements on wood exposed to three-point bending: Analysis by Use of Digital Volume Correlation Applied to Synchrotron Radiation Micro-Computed Tomography Image Data.* Strain, 46(1), 47-60 DOI: 10.1111/j.1475-1305.2009.00687.x.
6. Pang S., Kearns H., O'Brien D., (2014) *Report to JNL on Preliminary Investigation on Triboard Warping*
7. Record, S. J. (2004) *The Mechanical Properties of Wood Including a Discussion of the Factors Affecting the Mechanical Properties, and Methods of Timber Testing.* Retrieved from http://www.gutenberg.org/files/12299/12299-h/12299-h.htm
8. Schajer, G. S. (Ed.). (2013). *Practical Residual Stress Measurement Methods (1)*. Somerset, GB: Wiley. Retrieved from http://www.ebrary.com
9. Winandy J. E.; Krzysik A. M. (2007) *Thermal Degradation of Wood Fibers during Hot-Pressing of MDF Composites: Part I. Relative Effects and Benefits of Thermal Exposure.* Wood and Fiber Science, 39(3), 2007, pp. 450-461
10. Yoshihara, H. & Tsunematsu, S. Mater Struct (2006) *Feasibility of estimation methods for measuring Young's modulus of wood by three-point bending test* 39: 29. doi:10.1617/s11527-005-9015-6
11. Yoshihara, H., and S. Matsumoto (1999). *Examination of the proper span/depth ratio range in measuring the bending Young's modulus of wood based on the elementary beam theory*. Mokuzai Kogyo 54:269-272

CHAPTER 4

RESULTS AND DISCUSSION

4.1 SET A – LARGE SLICES

4.1.1 MOISTURE CONTENT GRADIENT AND AVERAGE MOISTURE CONTENT

Recipe for Set A: The adhesive loading and recipe for this set of experiments are outlined in Table 3-3 (Chapter 3) which are repeated in Table 4-1 for easy analysis.

The results of moisture content gradients and average moisture content shown in this section were obtained from the slices cut from the OD section. As discussed in previous sections, these should give more reliable results for moisture contents as these samples were prepared in shorter time in comparison with smaller slices cut using multi-saw. The moisture content gradient is shown in Figure 4-1 in which the x-axis shows the layer number; 1 being the top MDF fibre layer, 2 and 3 the middle strand layers and 4 being the bottom MDF fibre layer.

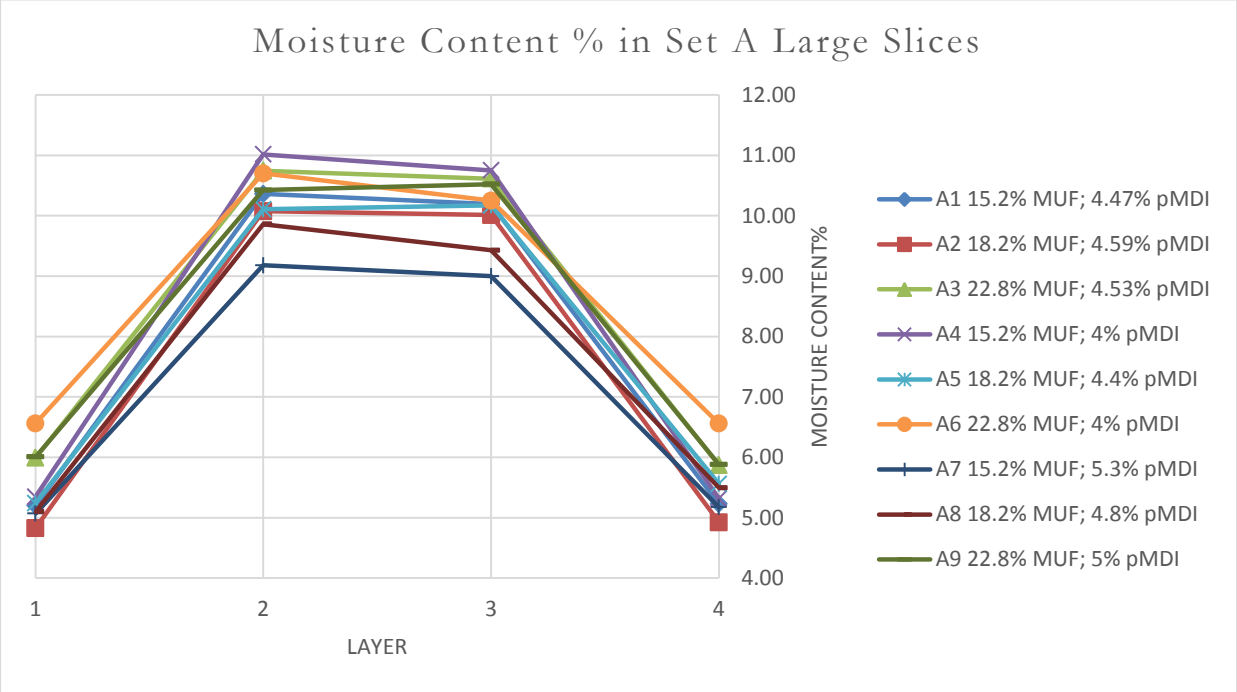

Figure 4-47: Moisture content profile for set A based on large slices

The moisture content gradients show bell curves with the middle strand layers having high moisture content for each board. The adhesive loading does not appear to significantly affecting

the moisture content gradient although A2, A7 and A8 samples show slightly lower moisture content gradients.

However, the average moisture contents changed from 7.1% for A7 board to 8.52% for A6 board as given in Table 4-1. It is interesting to note the general trend that the average moisture content was more strongly related to the adhesive loading for the MDF fibres. All of the boards except for A4 with average moisture content above 8% were those which had MDF fibres with an adhesive loading of 22.8%. Both the MDF fibre adhesive (MUF) and the strand adhesive (pMDI) had similar moisture on the solid resin basis (~50%). Strand moisture distribution was between 8 and 12% and the fibre moisture content was 6%. The dominant influence of MDF fibre adhesive loading on the average moisture content of the board samples can be due to two factors:

1. The initial fibre moisture content was lower than that of strands thus the fibres absorbed more water from the adhesive.
2. With higher adhesive loading on the fibres, the surface layer had high density thus reducing moisture loss during the hot press.

Table 17: Average moisture content in set A board samples based on measured moisture contents of large slices

Sample Identification	MUF Loading (solution weight and percentage over oven dry fibre)	pMDI Loading (solution weight and percentage over oven dry strands)	Average Moisture Content (%) of board samples (dry basis)
A1	151.7 g (15.2%)	76 g (4.47%)	7.74
A2	182 g (18.2%)	78 g (4.59%)	7.46
A3	227.5 g (22.8%)	77 g (4.53%)	8.30
A4	151.7 g (15.2%)	68 g (4%)	8.11
A5	182 g (18.2%)	75 g (4.4%)	7.77
A6	227.5 g (22.8%)	68 g (4%)	8.52
A7	151.7 g (15.2%)	90 g (5.3%)	7.10
A8	182 g (18.2%)	82 g (4.8%)	7.47
A9	227.5 g (22.8%)	85 g (5%)	8.21

4.1.2 Profiles of Strain, Stress and MOE

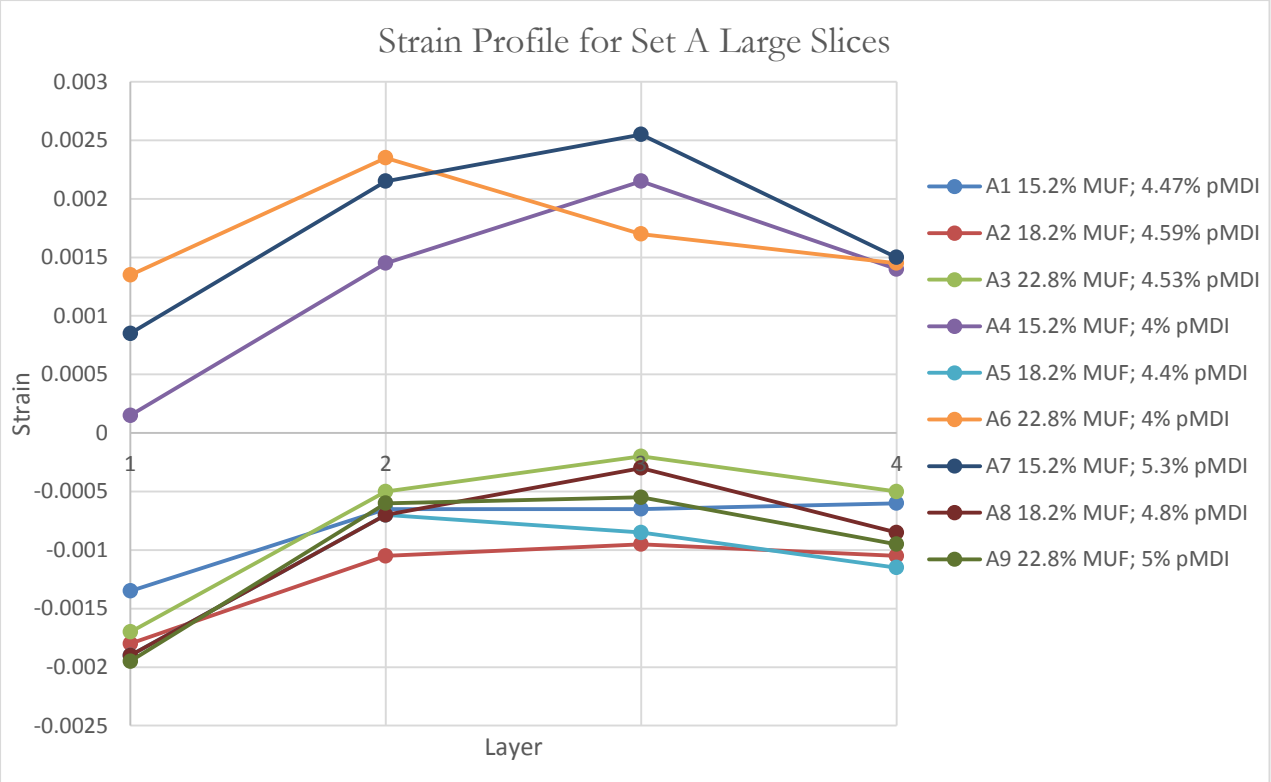

Figure 48: Strain profile for Set A based on large slices

Strain profiles for Set A board samples are shown in Figure 4-2 which are based on the results of large slices. From the figure, it can be seen that A4, A6 and A7 show overall increase in slice lengths while other boards show overall decrease in lengths after slicing. If a slice's length decreased after slicing, it means that this slice was in tension before cutting and vice versa. This phenomenon is shown in Figures 4-3 and 4-4. However, in theory, as the samples were held together before slicing, some slices in a board should show tension and some other slices should show compression since the board is static and overall forces have to be balanced. However, samples may lose moisture during slicing thus promoting shrinkage after slicing. This would generate a false decrease in the slice length and thus a false tensile stress. The opposite is also true as the samples may gain moisture after slicing thus promoting expansion after slicing. This would give a false increase in slice length and thus a false compressive stress. Since the experimental conditions were not ideal and air humidity factors do come into play, it was very difficult to control the moisture loss or gain during slicing and after slicing.

The trends presented in the figure are useful and thus were used for stress determination with known MOE values. It is noted that all boards showing overall positive strain were boards with low strand adhesive loading.

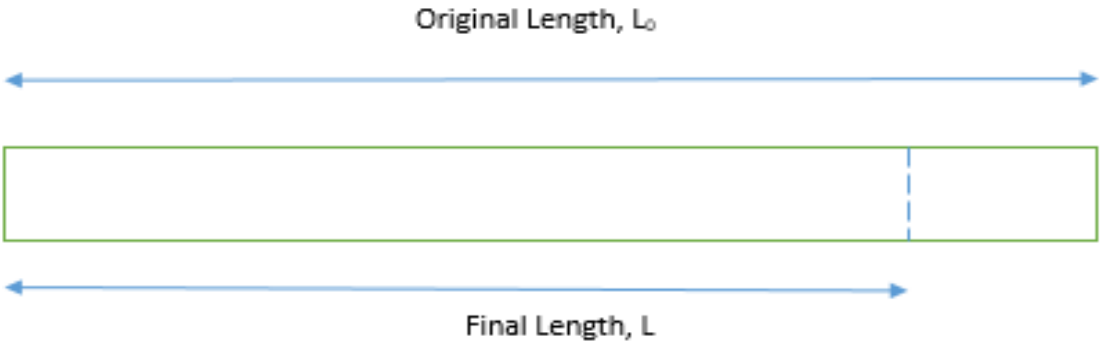

Figure 49: Compression in wood slice

If a slice is in tension/compression in a board, it would relieve its stresses after being sliced/removed from the board. For the board to be statically stable, the net forces on it would have to vanish according to Newton's laws.

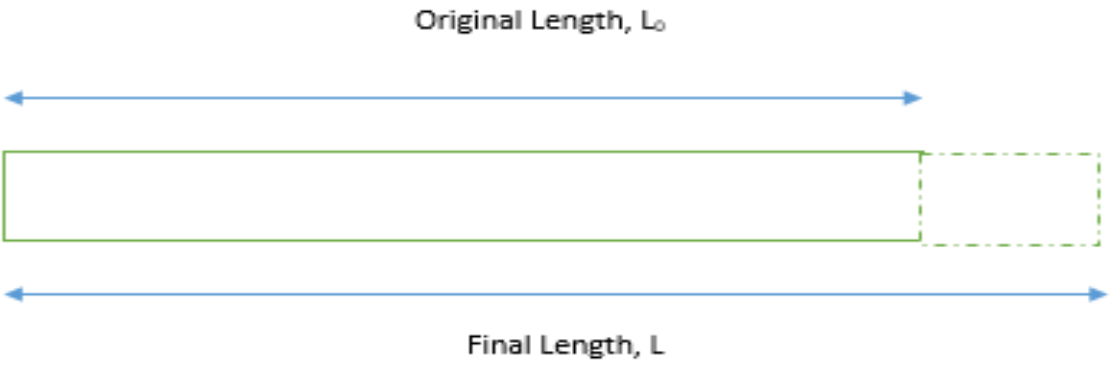

Figure 50: Expansion in wood slice

These stresses are present due to a combination of board processing factors like the recipe of board and hot pressing and environmental factors like relative humidity which governs how easily moisture can diffuse along the board to/from the environment.

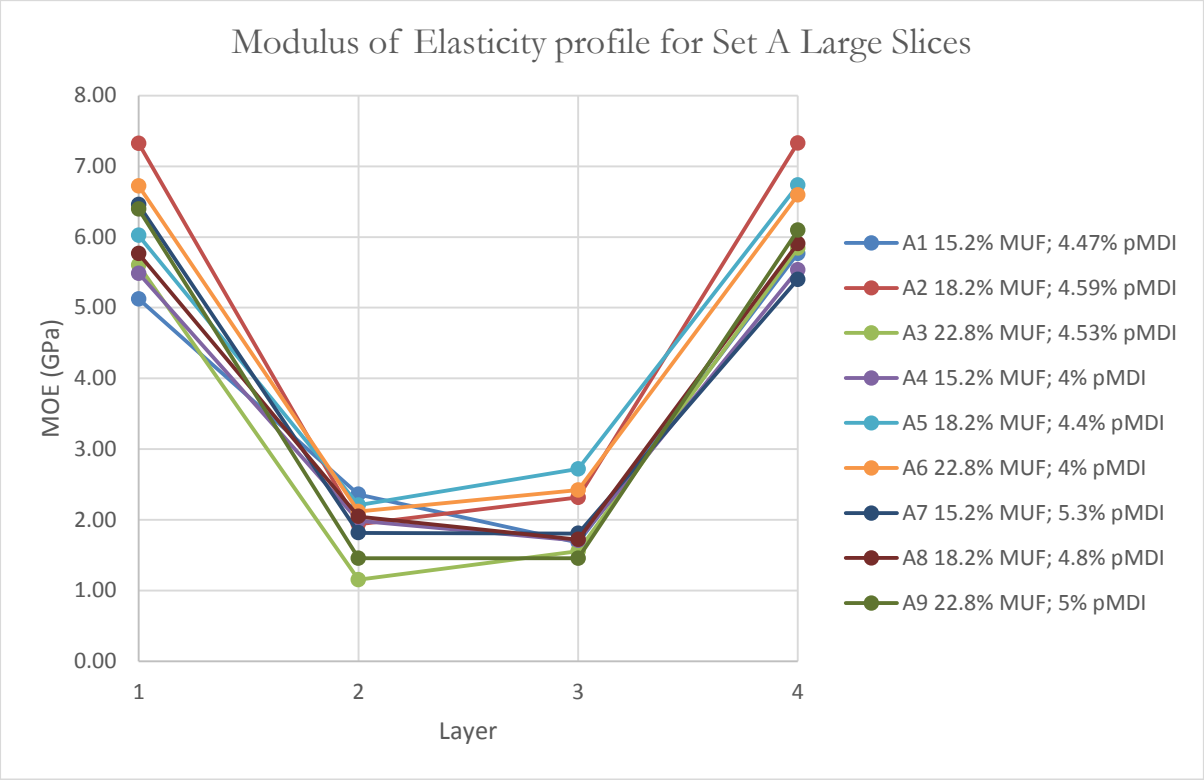

Figure 51: MOE profile for set A based on large slices

Modulus of elasticity (MOE), also known as "Young's Modulus", is a measure of a material's resistance to deformation while Modulus of Rupture (MOR) is a measure of a material's resistance to rupture at maximum loading. Modulus of rupture was also determined using a three-point bend test on the slices obtained from the FL section of the board (see Figure 3-3 in Chapter 3).

As explained earlier, these slices were the large four slices, top fibre layer (Layer 1), middle strand sawed into two pieces (Layer 2 & 3) and bottom fibre layer (Layer 4) from the FL section. The result of MOE are shown in Figure 4-5 while the results of MOR are shown in Figure 4-6. From these figures, both MOE and MOR profiles show a parabolic behavior as expected. The MDF fibre layers had high adhesive loading and were exposed to high temperatures during hot pressing, therefore had the highest mechanical properties (MOE and MOR). In comparison, the strand layers had lower adhesive loading and were exposed to lower temperatures during hot press, and thus had much lower MOE and MOR. In addition, the MOE and MOR increase with decrease in moisture content. The MDF fibre layers had lower moisture contents than the strand

layers thus the mechanical property difference is partially attributed to the moisture content variation.

From the MOE results, A2 board showed the highest average MOE (4.73 GPa) and A3 board showed the lowest average MOE (3.54 GPa). Although A2 board had lower fibre MUF loading (18.2%) than A3 board (22.8%), the board had lower average moisture content thus the high MOE can be attributed to this factor. Both boards had similar strand loading (4.53% and 4.59% pMDI solution), therefore, the A2 board recipe is the most effective to produce boards with high stiffness.

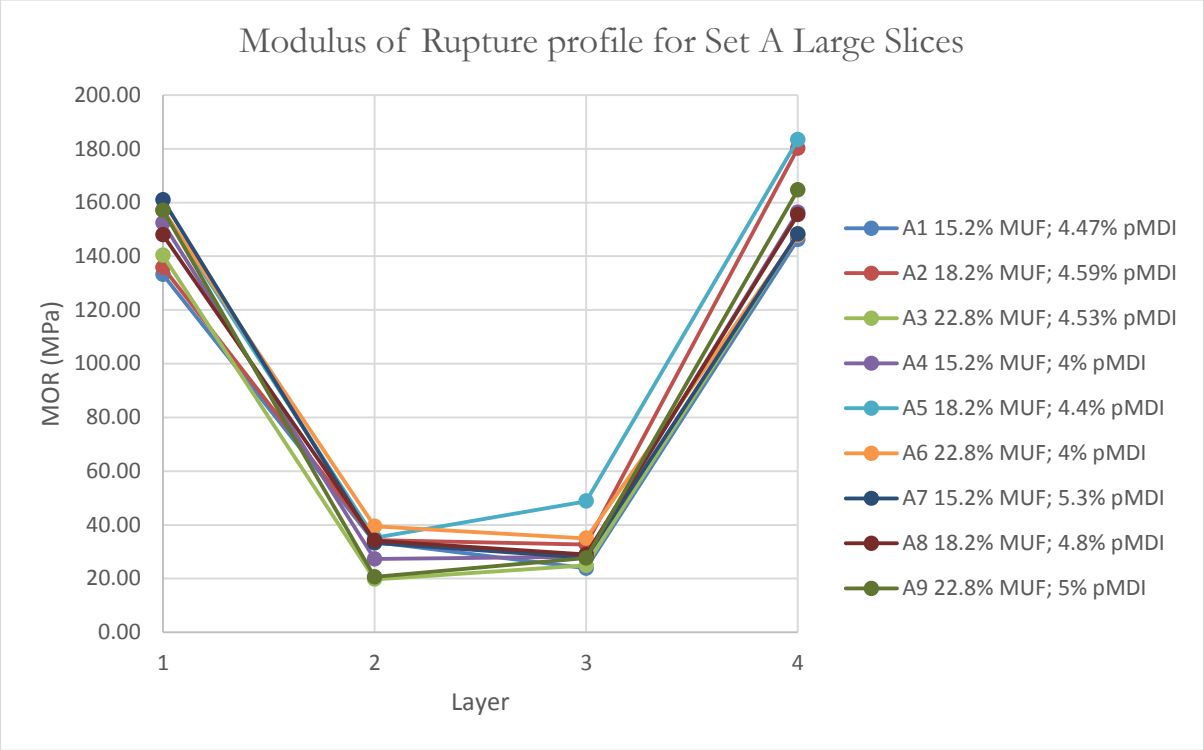

Figure 52: MOR profile for set A based on large slices

From the MOR result, board A5 shows the highest average MOR (106.12 MPa) with board A2 being a close second (95.77 MPa). A3 showed the lowest average MOR (83.31 MPa) and low MOE. The reason for board A5 having the high MOR was also related to its low average moisture content. It is interesting to find that the strand pMDI loading appears to have less effect on the MOE and MOR. Board A5 board also had a pMDI loading of 4.4% which was 0.2% less than board A2. Board A9 board had a higher pMDI loading of 5% but had low MOE and MOR.

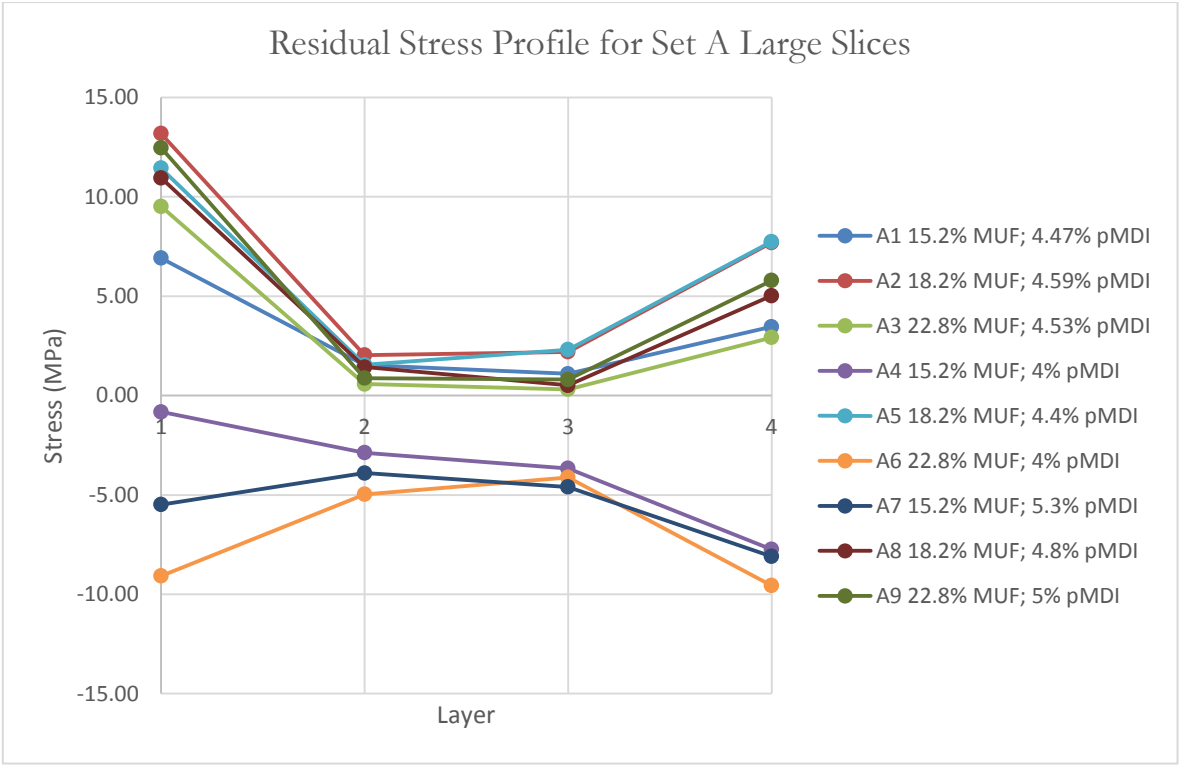

Figure 53: Residual stress profile for set A based on large slices

The most important factor affecting board warp is the residual stress distribution which are generated during hot pressing and remain in the board after the hot pressing. The residual stresses can only be observed either by removing the constraints (slicing) or board becomes distorted when different parts of the board bend in different directions. The residual stress of a slice was calculated based on its strain (ε_i) and MOE (E_i):

$$\sigma_i = - \varepsilon_i E_i$$

1. The negative sign on the right hand side is used to keep stress consistent with previous discussion. A slice had tensile residual stress if the slice shrank after slicing and compressive residual stress if the slice expanded after slicing.

The results of residual stresses determined based on the above method are shown in Figure 4-7. As the residual stress is directly related to strain, similar patterns of strain are observed for the stress distribution although the signs of the strain and stress are opposite. As mentioned in the previous section, significant errors occurred due to the errors in length measurements and the moisture loss or re-distribution during cutting and during the elapsed time before cutting. From

the results shown in Figure 4-7, it can be seen that A4, A6 and A7 board samples show overall compressive stresses after slicing while other board samples show tensile stresses.

Table 18: Mechanical properties for set A large slices

Sample no.	MUF Loading (weight, percentage over oven dry fibre)	pMDI Loading (weight, percentage over oven dry strands)	Average Modulus of Elasticity for whole board (GPa)	Maximum Residual Stress Difference (MPa)	Asymmetrical Stress Distribution (MPa)	Average Modulus of Rupture for whole board (MPa)
A1	151.7 g (15.2%)	76 g (4.47%)	3.73	5.82	3.46	84.19
A2	182 g (18.2%)	78 g (4.59%)	4.73	11.15	5.49	95.77
A3	227.5 g (22.8%)	77 g (4.53%)	3.54	9.21	6.60	83.31
A4	151.7 g (15.2%)	68 g (4%)	3.68	6.92	6.92	91.01
A5	182 g (18.2%)	75 g (4.4%)	4.42	9.89	3.70	106.12
A6	227.5 g (22.8%)	68 g (4%)	4.46	5.45	0.48	94.82
A7	151.7 g (15.2%)	90 g (5.3%)	3.87	4.20	2.61	92.57
A8	182 g (18.2%)	82 g (4.8%)	3.86	10.44	5.93	91.62
A9	227.5 g (22.8%)	85 g (5%)	3.85	11.66	6.68	92.48

Note that the adhesive loading values are based on solution of adhesives used.

The distribution of stresses through the board thickness is the most important factor for board distortion, and this is reflected by the maximum residual stress difference and the asymmetry of the stress. These are quantified in Table 4-2. Maximum residual stress difference is defined as the difference between the layer with the maximum positive stress (or the highest stress) and the one

with the most negative stress (or lowest stress). It is found that the residual stress profiles show a general parabolic profile but not as symmetrical. The asymmetrical stress distribution is defined as the difference between top layer stress and the bottom layer stress.

From the results presented in Table 4-2, Board A6 had the lowest asymmetrical stress distribution (0.48 MPa) and the second lowest maximum stress difference (5.45 MPa). A7 board had the lowest maximum stress difference (4.2 MPa) and the second lowest asymmetrical stress distribution (2.61 MPa). A1 board had both the moderate maximum stress difference and the asymmetrical stress distribution. On the other hand, A9 had the highest maximum stress difference at 11.66 MPa and the highest asymmetrical stress distribution (6.68 MPa).

4.2 Set A - Small Slices

4.2.1 Moisture Content Gradient and Average Moisture Content

The moisture content profiles through the board thickness from the small slices (cut using multi-saw) are shown in Figure 4-8 for all of the board samples. From the figure, it is found that the moisture content profiles for all of the board samples except for board A9 had similar 'bell' shape. In Figure 4-8, the x-axis shows the board layer; 1 and 5 being the top and bottom MDF layers which moisture contents were between 4.5% and 6% (excluding A9) while 2,3,4 are the middle strand pieces which had moisture content between 9% and 10%.

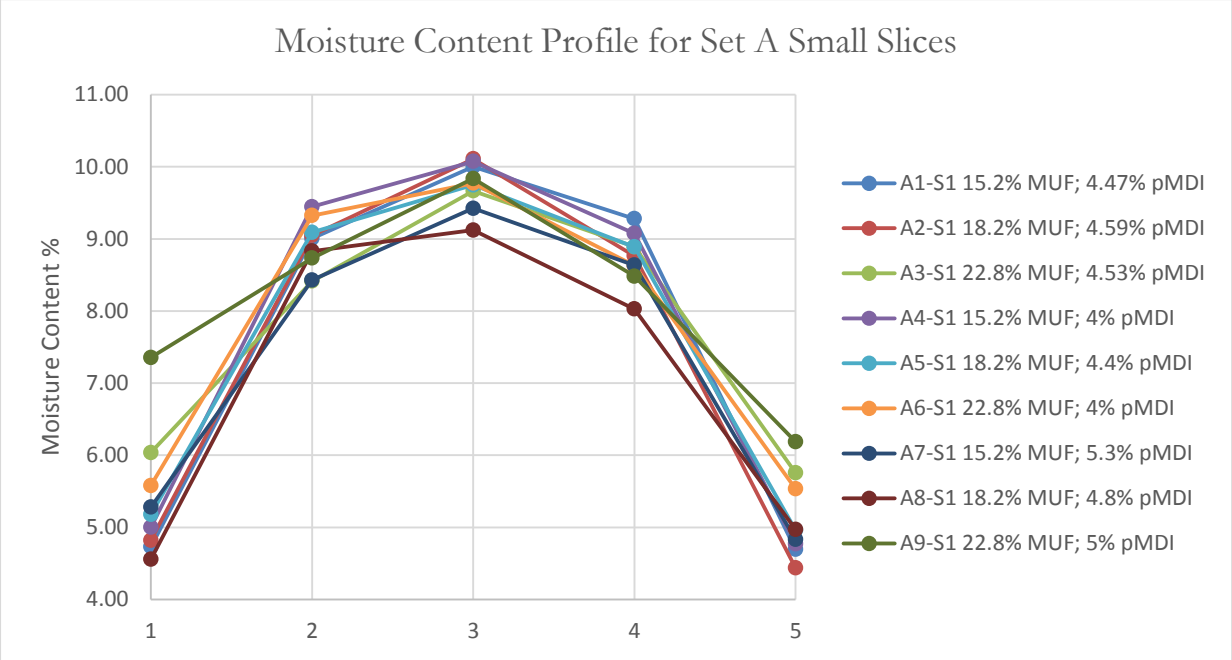

Figure 54: Moisture content profile for set A based on small slices

The average moisture contents of all the board samples are given in Table 4-3 which were obtained from 4 sections each having 5 slices.

Table 19: Average moisture content in set A board samples based on measured moisture contents of small slices

Sample Identification	MUF Loading (weight, percentage over oven dry fibre)	pMDI Loading (weight, percentage over oven dry strands)	Average Moisture content of board sample %(dry basis)
A1	15.2%	4.47%	7.65
A2	18.2%	4.59%	7.74
A3	22.8%	4.53%	10.30
A4	15.2%	4%	7.90
A5	18.2%	4.4%	7.83
A6	22.8%	4%	12.40
A7	15.2%	5.3%	7.52
A8	18.2%	4.8%	7.44
A9	22.8%	5%	8.07

Note that all the adhesive loading values are based on solution of adhesive used.

Average moisture content of board samples presented in Table 4-3 have similar trends as those given in Table 7 measured from larger slices. In Table 4-1, A2 and A5 had similar average moisture content (7.74% and 7.83% respectively) as these two boards had similar adhesive loadings both for MDF fibres (18.2%) and strands (4.59% for A2 and 4.4% for A5). Boards A3, A6 and A9, which had the highest adhesive loadings for MDF fibres (22.8%), showed the highest average moisture contents at 10.30%, 12.40% and 8.07% respectively. A1, A7 and A8 showed the lowest average moisture contents in which A1 and A7 had the lowest adhesive loadings for MDF fibres (15.2%) and A8 had adhesive loading of 18.2% for the MDF fibres. Therefore, there is a strong correlation between the board average moisture content and the adhesive loading of the MDF fibres.

4.2.2 PROFILES OF STRAIN AND RESIDUAL STRESS

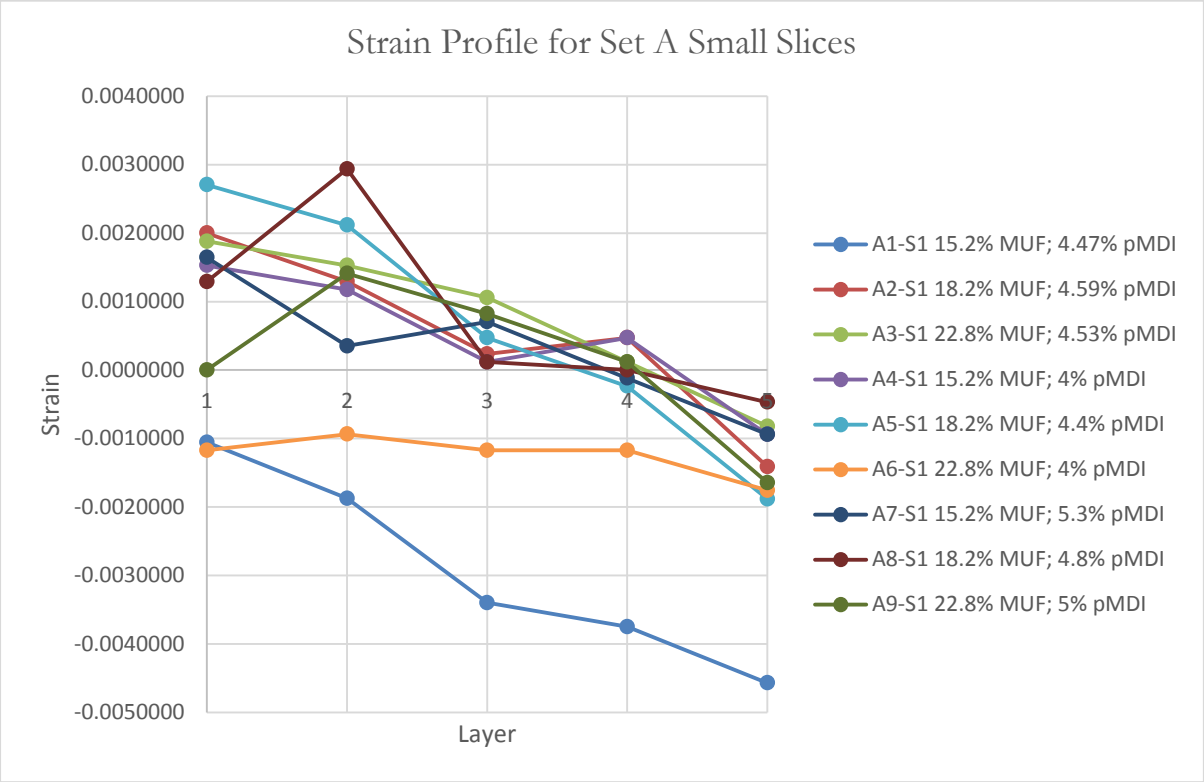

Figure 55: Strain profile for set A based on small slices

The strain profiles measured from small slices are shown in Figure 4-9 for all of Set A board samples. Boards A1 and A6 showed negative strains for all of the layers while other samples showed both positive and negative strains through the board thickness. In the latter samples, the strains tended decreasing from positive on the top to negative on the bottom layers. There is no clear trends between strain and adhesive loading of each for the MDF fibres and for the strands although it appears that the top layers tend to have positive strain or less negative strain while the bottom tends to have negative or low positive strains. The stress will be calculated based on the strains and the MOE of each layer.

The residual stresses were calculated the same way as those for large slices with a slight variation the following way:

1. The MOE values calculated for the larger slices were transferred to the corresponding smaller slices. The MDF layers (slice 1 and 5) used the MOE values from the top and bottom slices while three small strand slices (slices 2, 3 and 4) used MOE values obtained from the two large strand slices in determination of MOE values.

2. The maximum stress difference and the asymmetrical stress distribution were determined in the same way as that for the large slices from section S1 of each board sample.

Figure 56: Residual stress profile for set A based on small slices

The results residual stress profiles for all board samples are shown in Figure 4-10. As seen from the large slices, some boards show overall tensile stresses and some show overall compressive stresses while the remaining boards show both tensile and compressive stresses. The impact of residual stresses can be analysed by the maximum stress difference and asymmetrical stress distribution through the board thickness.

It is noted that the measurements of strains in smaller slices was more likely to result in higher errors than the larger slices during the multi-saw slicing and longer time between the board making and the slicing tests. Nevertheless, the results of maximum stress difference and asymmetrical stress distribution from the small slices are given in Table 4-4.

Table 20: Maximum stress differences and asymmetrical stress distribution for set A based on small slices

Sample Identification	MUF Loading (solution, wt.% on oven-dry fibres)	pMDI Loading (solution wt.% on oven-dry strands)	Maximum Residual Stress difference (MPa)	Asymmetrical stress distribution (MPa)
A1	151.7 g (15.2%)	76 g (4.47%)	21.94	-20.97
A2	182 g (18.2%)	78 g (4.59%)	24.97	-24.97
A3	227.5 g (22.8%)	77 g (4.53%)	15.34	-15.34
A4	151.7 g (15.2%)	68 g (4%)	13.59	-13.59
A5	182 g (18.2%)	75 g (4.4%)	28.95	-28.95
A6	227.5 g (22.8%)	68 g (4%)	9.84	-3.95
A7	151.7 g (15.2%)	90 g (5.3%)	15.70	-15.70
A8	182 g (18.2%)	82 g (4.8%)	10.22	-10.22
A9	227.5 g (22.8%)	85 g (5%)	12.06	-10.02

It can be seen in Table 4-4 that the results of maximum stress difference and asymmetrical stress distribution for all of the board samples had similar trends to those obtained from large slices (Table 4-2). A5 board had the highest difference of the maximum stresses (28.95 MPa) and the worst asymmetrical stress distribution (-28.95 MPa). The next worst boards are A1 and A2 which corresponding stress distribution indicators are 21.94 MPa and -20.97 MPa for A1 board, and 24.97 MPa and -24.97 MPa for A2 board. Board A6 had the lowest maximum stress difference (9.84 MPa) and the lowest asymmetrical stress distribution (-3.95 MPa). The other boards had moderate maximum stress difference (10.22 MPa to 15.70 MPa) and the asymmetrical stress distributions (-10.02 MPa to -15.70 MPa).

4.3 Set B – Large Slices

4.3.1 Moisture content gradients and Average Moisture Content

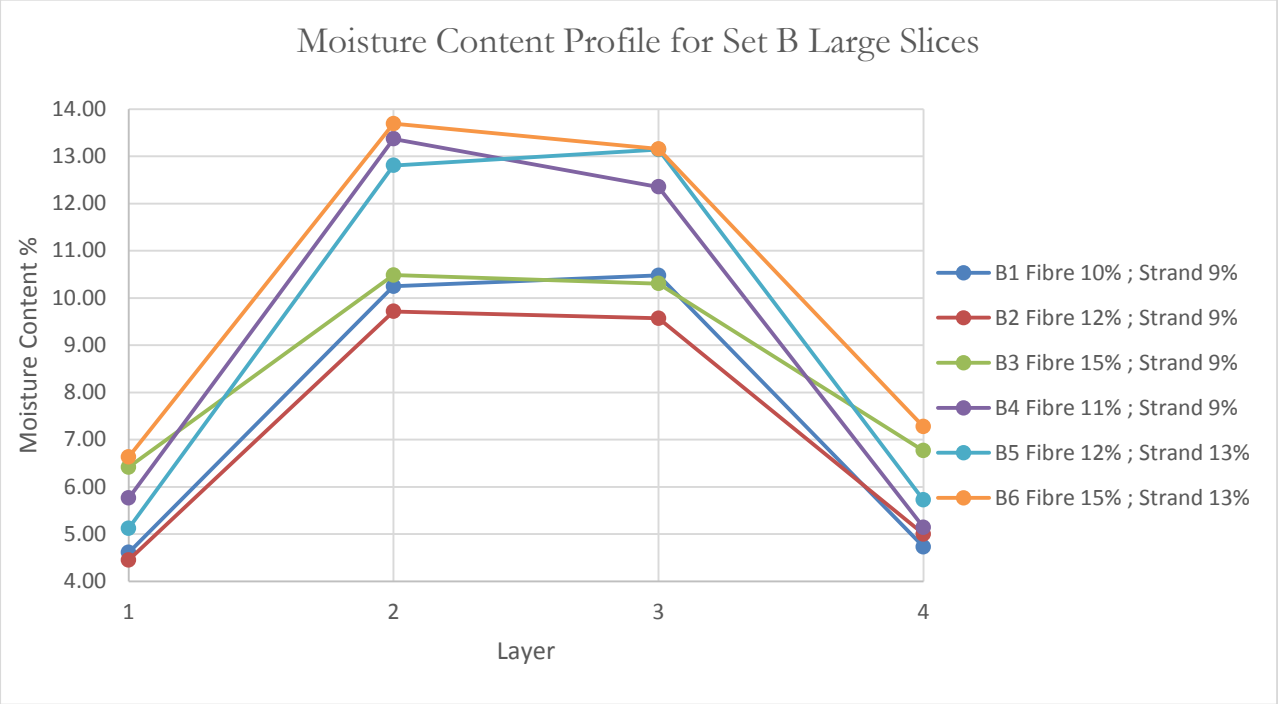

Figure 57: Moisture content profile for set B based on large slices

The moisture profile for the OD sections cut from Set B boards are shown in Figure 4-11. The moisture content gradients show clearly display how the added moisture before hot pressing strongly affects the moisture profile with boards B1, B2, B3 and B4 having same strand moisture (9%) but different moisture in the fibre layer. The moisture layer in board B6 is seen to be the highest since it has the highest fibre and strand moisture content at 15% and 13 % respectively. Board B4 shows unexpected results displaying strand moisture profile similar to board B6. This is probably due to B4 board somehow gaining additional moisture during the experiment procedure. The moisture content results for this set B large slices are recorded in Table 4-5.

Table 21: Average moisture content in set B board samples based on measured moisture content of large slices

Sample Identification	pMDI Loading (solution weight, and percentage over oven dry strands)	Moisture in fibre (weight, percentage over oven dry fibre)	Moisture in strand (weight, percentage over oven dry strands)	Average Moisture Content% of board samples (dry basis)
B1	72 g (4.2%)	100 g (10%)	153 g (9%)	7.52
B2	76 g (4.5%)	120 g (12%)	153 g (9%)	7.18
B3	80 g (4.7%)	150 g (15%)	153 g (9%)	8.49
B4	76 g (4.5%)	110 g (11%)	153 g (9%)	9.16
B5	78 g (4.6%)	120 g (12%)	221 g (13%)	9.20
B6	76 g (4.5%)	150 g (15%)	221 g (13%)	10.19

4.3.2 PROFILES OF STRAIN, STRESS AND MOE

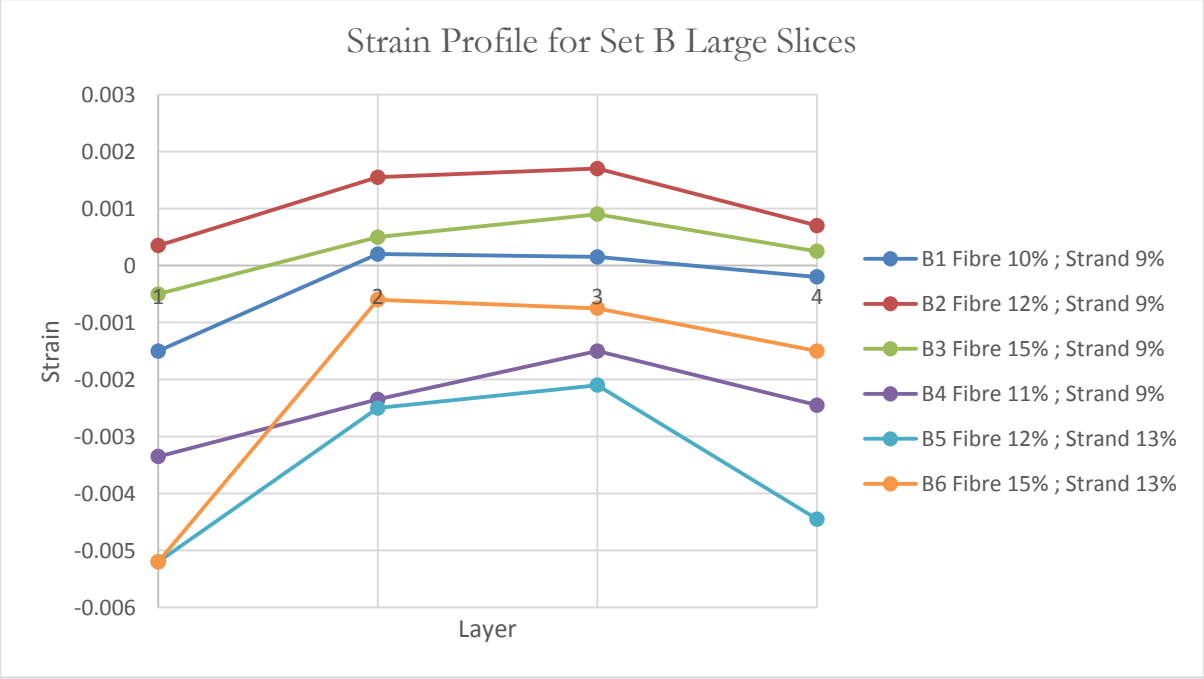

Figure 58: Strain profile for set B based on large slices

Strain profiles for Set B board samples are shown in Figure 4-12. There is much less overlap in strain profiles in Set B than observed in Set A. The profile suggests that strain becomes more positive with increase in moisture content of fibre but this is uneven as Board B3 shows a more negative profile in comparison to board B2 and again a decrease is seen in board B4 which is

very negative than boards B1, B2, B3. As mentioned before board B4 had some moisture absorption during the process and can be considered an outlier in the trend.

Strand moisture content seems to have more effect on the strain profile than fibre moisture content. This can be seen in the extremely negative profiles created by boards B5 and B6. In effect, addition in moisture should cause expansion in the wood and result in more positive strains. Strand moisture was increased to from 9% to 13% and board B6 with a higher fibre moisture shows a more positive strain profile than B5. Board B2 shows a more positive profile than B5 as does B3 in comparison to B6 so the strain profiles seem to be getting more negative as strand moisture content is increased. So, the results do show an indication of strain profiles becoming more positive as the moisture levels increase but this is highly uneven as the results differ depending on whether the fibre or strand moisture levels increase. This discussion is continued when the residual stress profiles are examined.

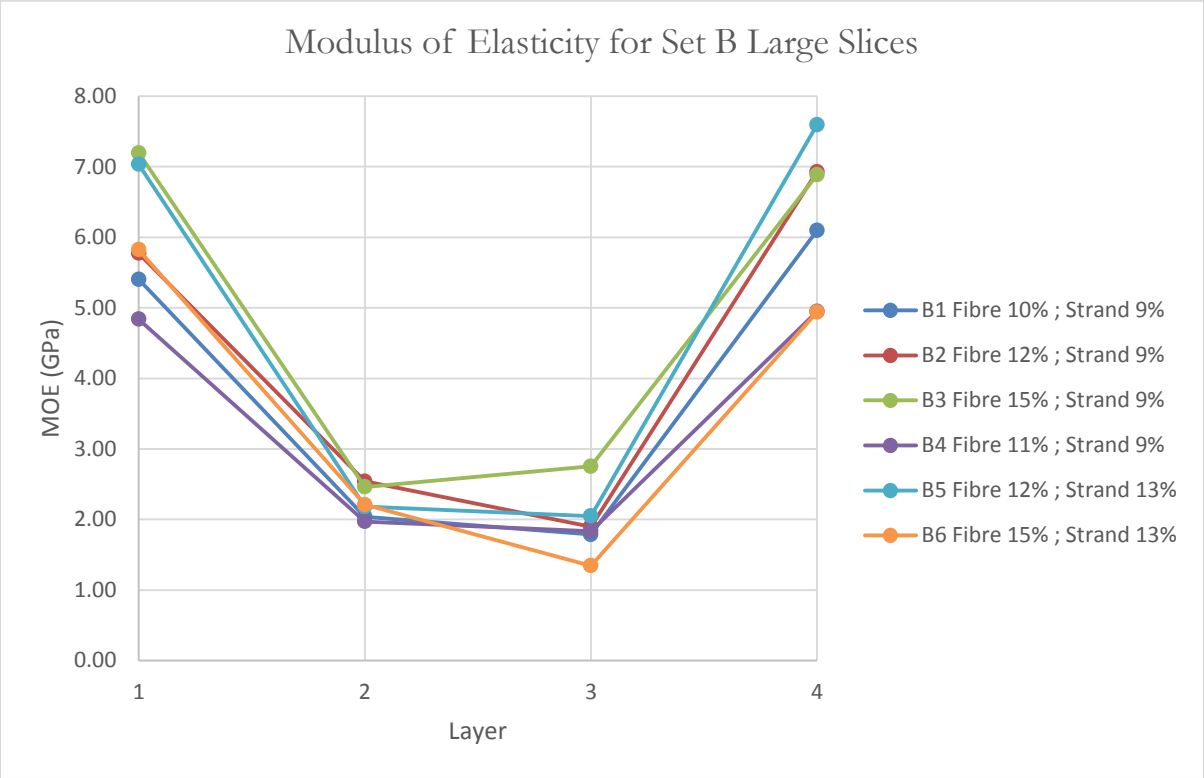

Figure 59: MOE profile for set B based on large slices

The MOE profiles are shown in Figure 4-13. As explained before, the highest MOE is observed in the fibre layers as they are exposed to high temperature during hot pressing. MOE is seen to be increasing as the fibre moisture levels increase since board B2 has a higher MOE profile than board B1 and board B3 has a higher MOE profile than board B2. Board B6 shows a very low MOE profile and only shows an average of 3.58 GPa which is the second lowest in the set while

boards B3 and B5 show the highest MOE profiles with averages of 4.82 and 4.71 GPa respectively. MOE is seen to be increasing as Moisture content is increased from 10% to 15% in boards B1 to B3 but this is not seen in board B6 which has a lower MOE profile and average compared to B5.

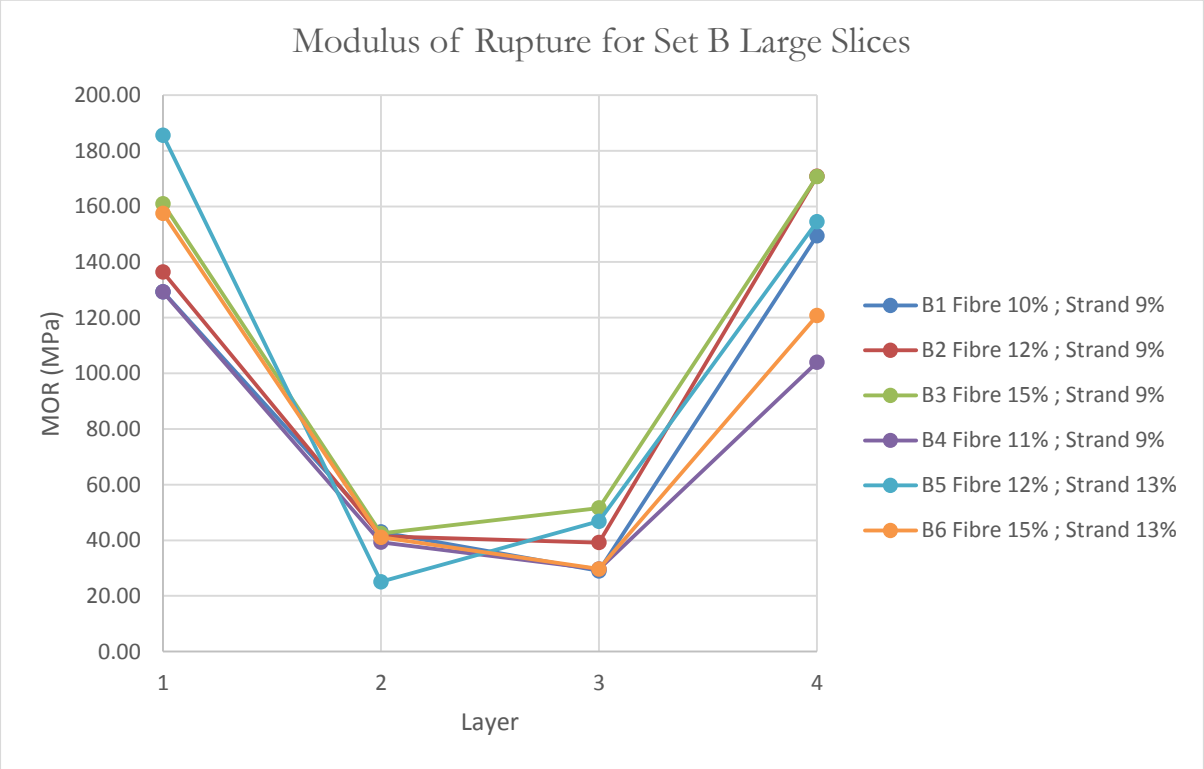

Figure 60: MOR profile for set B based on large slices

MOR profiles for Set B boards can be seen in Figure 4-14. The profiles show that the MOR value is increasing with fibre moisture content but this is only observed in boards B1, B2 and B3. B6 shows having a higher moisture content still shows a lower MOR profile than B5 and the second lowest. The highest MOR value is noted in board B3 with a value of 106.44 MPa and second highest in board B5 which has an MOR of 102.99 MPa which also has a high fibre and strand moisture content (12% and 13% respectively).

Figure 61: Residual stress profile for set B based on large slices

Figure 4-15 shows the Residual Stress profile for all boards in Set B. Board B2 is the most stable board since it has a very even profile with maximum stress difference being 2.83 MPa and asymmetrical stress distribution being 2.83 MPa. This makes it the least likely board to warp in the set. B6 is the most unstable board in this set since it has the highest maximum stress difference of 29.28 MPa and asymmetrical stress distribution of 22.88 MPa. B5 is also highly unbalanced with stress difference at 32.28 MPa but is the most symmetric having asymmetrical distribution of only 2.79 MPa. Moisture content addition in boards do play an important role in the residual stress profile since moisture content in strand over 9% seems to be making the board less symmetrical making it more likely to warp. Mechanical properties are summarised in Table 4-6.

Table 22: Mechanical properties for set B based on large slices

Sample Identification.	Moisture in fibre (weight, percentage over oven dry fibre)	Moisture in strand (weight, percentage over oven dry strands)	Maximum Residual Stress Difference (MPa)	Asymmetrical distribution (MPa)	Average MOE (GPa)	Average MOR (MPa)
B1	100 g (10%)	153 g (9%)	8.51	6.89	3.83	87.69
B2	120 g (12%)	153 g (9%)	2.83	2.83	4.28	96.96
B3	150 g (15%)	153 g (9%)	6.08	5.32	4.82	106.44
B4	110 g (11%)	153 g (9%)	13.46	4.09	3.4	75.54
B5	120 g (12%)	221 g (13%)	32.28	2.79	4.71	102.99
B6	150 g (15%)	221 g (13%)	29.28	22.88	3.58	87.25

4.4 Set B – Small slices

4.4.1 Moisture Content Profiles and Average Moisture Content

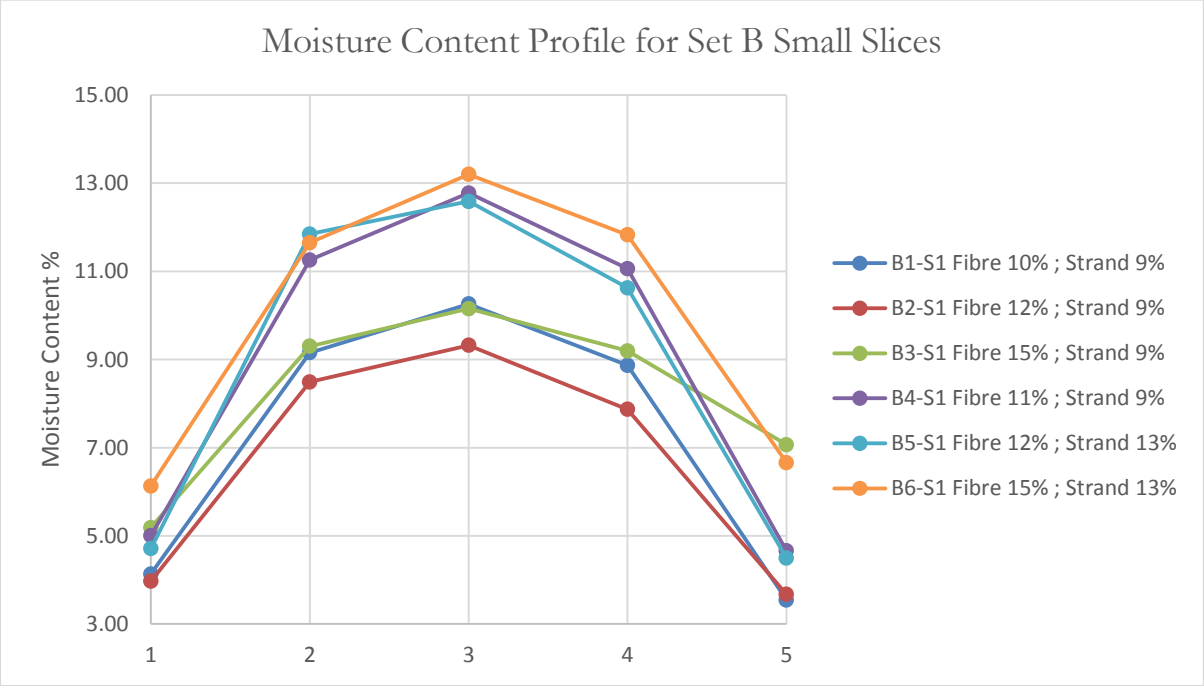

Figure 62: Moisture content profile for set B based on small slices

The moisture content profile for small slices is shown in Figure 4-16 for all the board samples. As with Set A the 'bell' shape is prominent in this Set B as well. All the boards' fibre layers have moisture content between 3% and 7% and strand layers have between 8% and 13%. Table 4-7 shows the average moisture distribution for the board. B1 having lowest fibre-strand moisture content combination shows the least average moisture distribution at 7.45% and B6 having the highest combination shows the highest average moisture content at 9.73%.

Table 23: Average moisture content in set A board samples based on measured moisture contents of small slices

Sample Identification	Moisture in fibre (weight, percentage over oven dry fibre)	Moisture in strand (weight, percentage over oven dry strands)	Average Moisture Content of board sample% (dry basis)
B1	100 g (10%)	153 g (9%)	7.45
B2	120 g (12%)	153 g (9%)	9.59
B3	150 g (15%)	153 g (9%)	8.39
B4	110 g (11%)	153 g (9%)	9.01
B5	120 g (12%)	221 (13%)	8.93
B6	150 g (15%)	221 (13%)	9.73

The results obtained from small slices also show a strong correlation between moisture added and moisture content since average moisture content% of board is increasing with increase in fibre and strand moisture. Board B3 shows a lower moisture content than boards B2 and B4 even though board B3 has the highest moisture content % than boards B2 and B4. So these results are less reliable than those obtained from large slices.

4.4.2 PROFILES OF STRAIN AND RESIDUAL STRESS

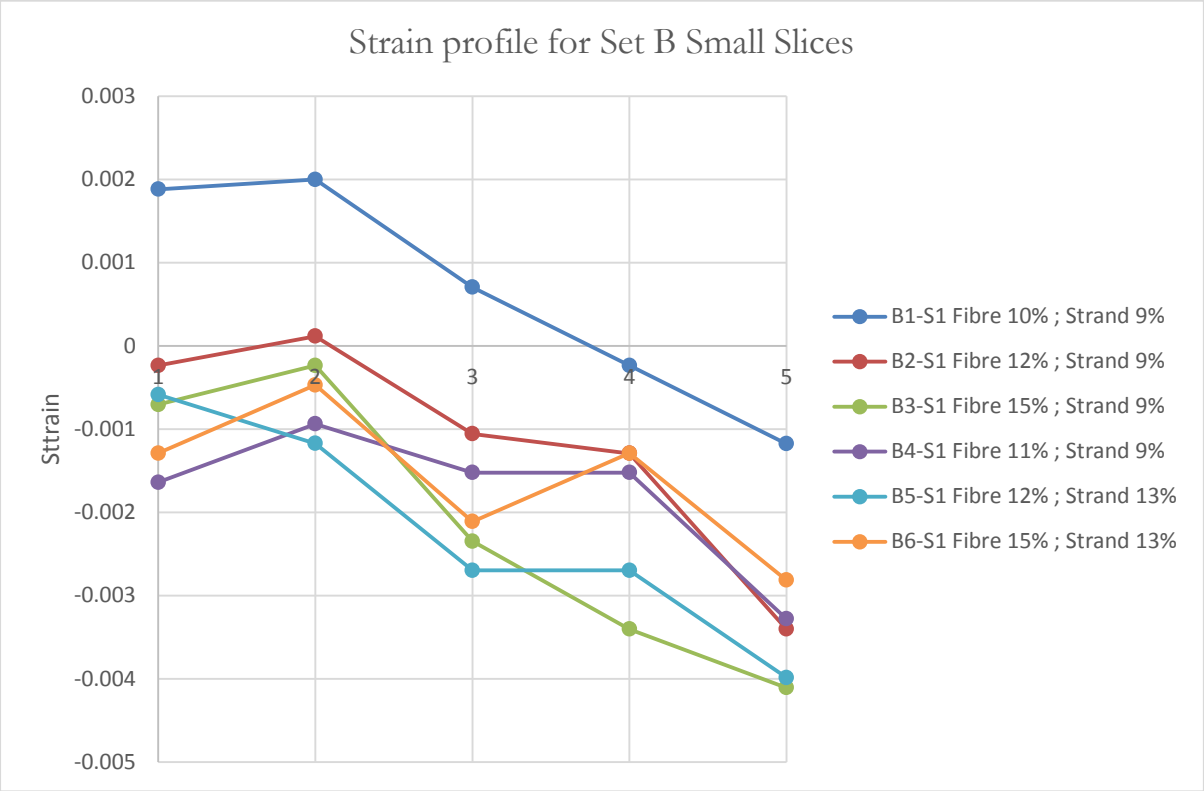

Figure 63: Strain profile for set B based on small slices

The strain profiles for all boards in Set B are shown in Figure 4-17. All of the profiles except that for board B1 shows a negative profile. Board B1 shows a positive strain in layer 1 and then a linear decrease over the next 4 layers finishing in a negative strain. These results do not agree with the strain profiles obtained from large slices of Set B since these suggest that the strain is getting progressively more negative as the moisture is increased although it agrees with Figure 4-12 that board B5 shows the most negative strain profile (with slight overlap). Hence these results are less reliable.

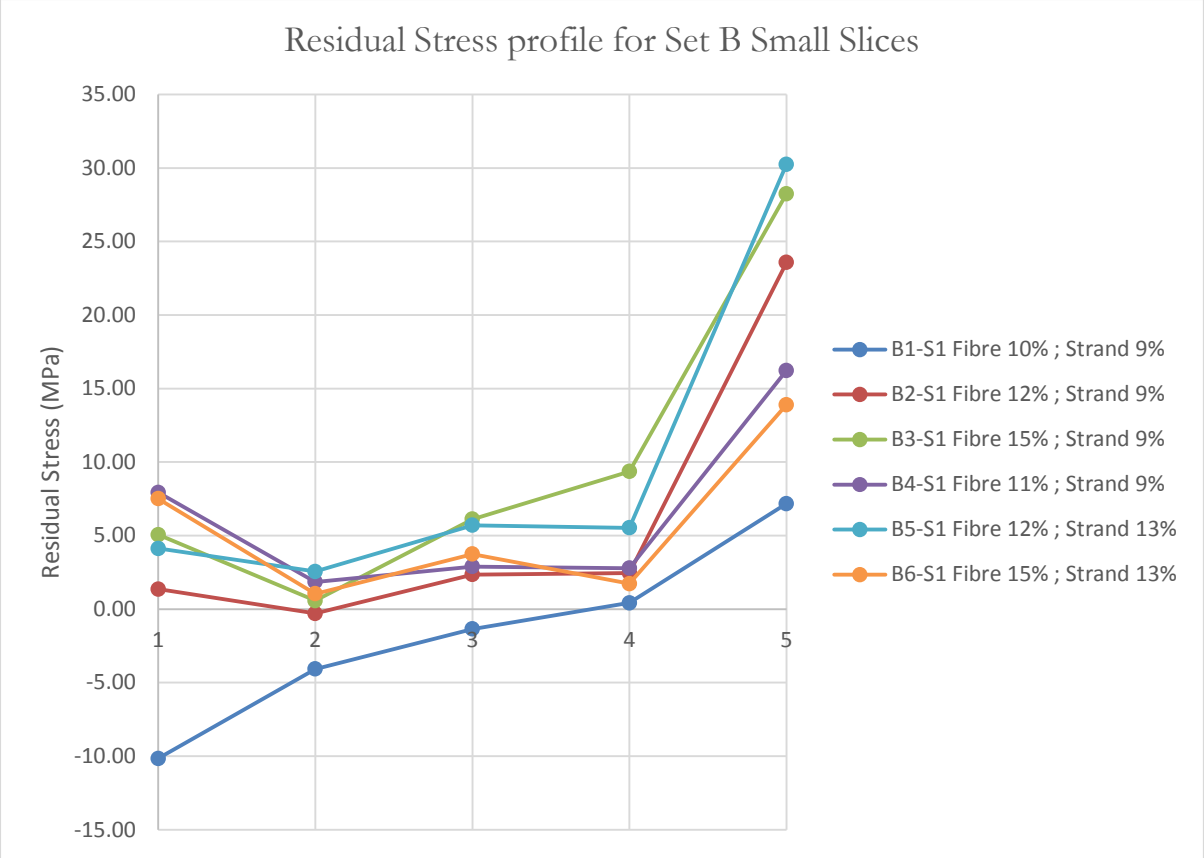

Figure 64: Residual stress profile for Set B based on small slices

Figure 4-18 shows the residual stress profiles obtained from small slices of Set B. The bottom fibre layer (Layer 5) shows high tensile stress while the top fibre layers show much less in all the samples. It is interesting to note that board B1 alone shows a profile that increases from compressive stress to tensile stress while all the other boards show tensile behaviour throughout their profile even though there is not much difference between boards B1, B2 and B3. The best in this set is B6 since it has the lowest stress difference (12.86 MPa) and is least asymmetrical distribution (-6.39 MPa). The worst behaviour is shows by B5 which is the least balanced and has the highest stress difference at 27.69 MPa and -26.12 respectively.

Table 24: Maximum residual stress difference and asymmetrical distribution for set B based on small slices

Sample Identification	Moisture in fibre (weight, percentage over oven dry fibre)	Moisture in strand (weight, percentage over oven dry strands)	Maximum Residual Stress difference (MPa)	Asymmetrical Distribution (MPa)
B1	100 g (10%)	153 g (9%)	17.33	-17.33
B2	120 g (12%)	153 g (9%)	23.87	-22.22
B3	150 g (15%)	153 g (9%)	27.67	-23.18
B4	110 g (11%)	153 g (9%)	14.39	-8.30
B5	120 g (12%)	221 (13%)	27.69	-26.12
B6	150 g (15%)	221 (13%)	12.86	-6.39

4.5 Set C – Large Slices

4.5.1 Moisture Content Gradients and Average Moisture Content

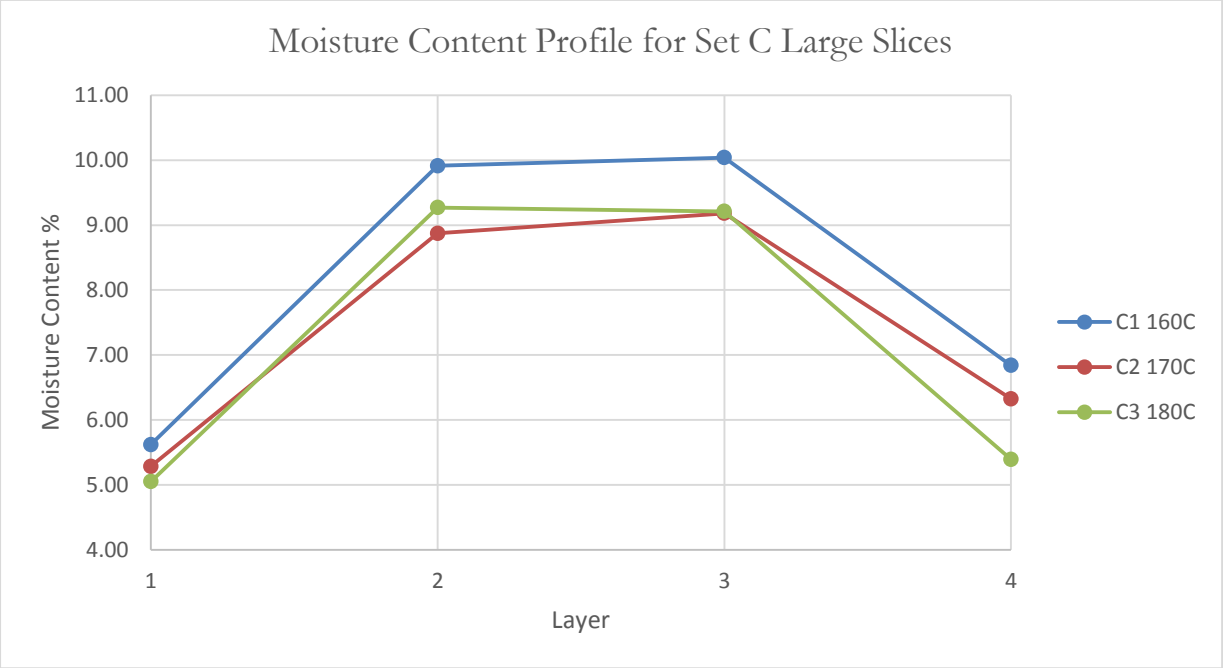

Figure 65: Moisture content profile in set C based on large slices

Figure 4-19 shows the moisture profiles for the three boards made for Set C and Table 4-9 contains average moisture distribution values. This set varied in hot press temperature only. The profiles in this set is similar to the curvature of the profiles followed by board samples in Set A and B. Fibre moisture is very close to 6% for both top and bottom layers while strand shows more lying between 8% and 10%. Board C1 has the highest amount of moisture distribution at an average of 7.47% while boards C2 and C3 seem to follow highly overlapping profiles with similar average moisture contents (6.88% and 6.71 % respectively). The reason for this is that there is moisture diffusion from the board during hot press and this rate is increased as the hot press temperature is increased.

Table 25: Average moisture content in set C based on measured moisture contents of large slices

Sample no.	Press Temperature (°C)	Average Moisture Content % of board sample
C1	160	7.47
C2	170	6.88
C3	180	6.71

4.5.2 Profiles of Strain, Stress and MOE

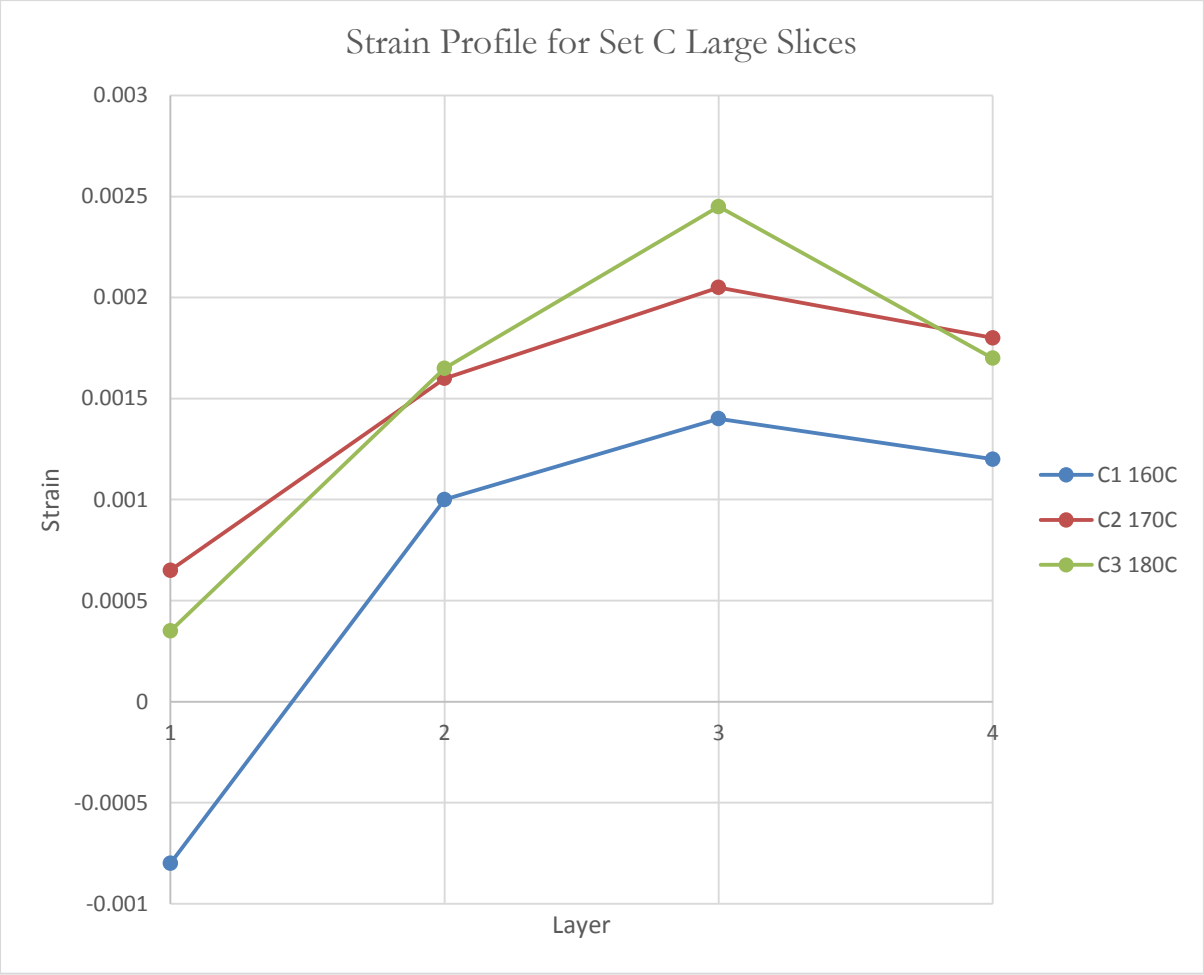

Figure 66: Strain profile for Set C based on large slices

In the strain profile in Figure 4-20, boards C2 and C3 show a very positive strain profile while C1 shows negative strain in Layer 1 which increases to a positive strain. It is the only one that shows the negative to positive transition indicating that the stresses in board C1 were not as well

relieved as boards C2 and C3. This is expected as strain gets more tensile after temperature increases and causes expansion which makes the stresses to be relieved. Also of interest is the overlap and similarity of curvature of boards. Board C1 has a lower temperature but has exactly the same shape Layer 2 onwards following a similar slope. Also, board C2 and C3 overlap slightly. This might suggest that a 10^0 Celsius increase in temperature from 160^0 Celsius to 170^0 might have a bigger difference on the board than a raise from 170^0 to 180^0 since the stress relief could possibly become saturated after 180^0 although more temperatures need to be investigated to confirm this.

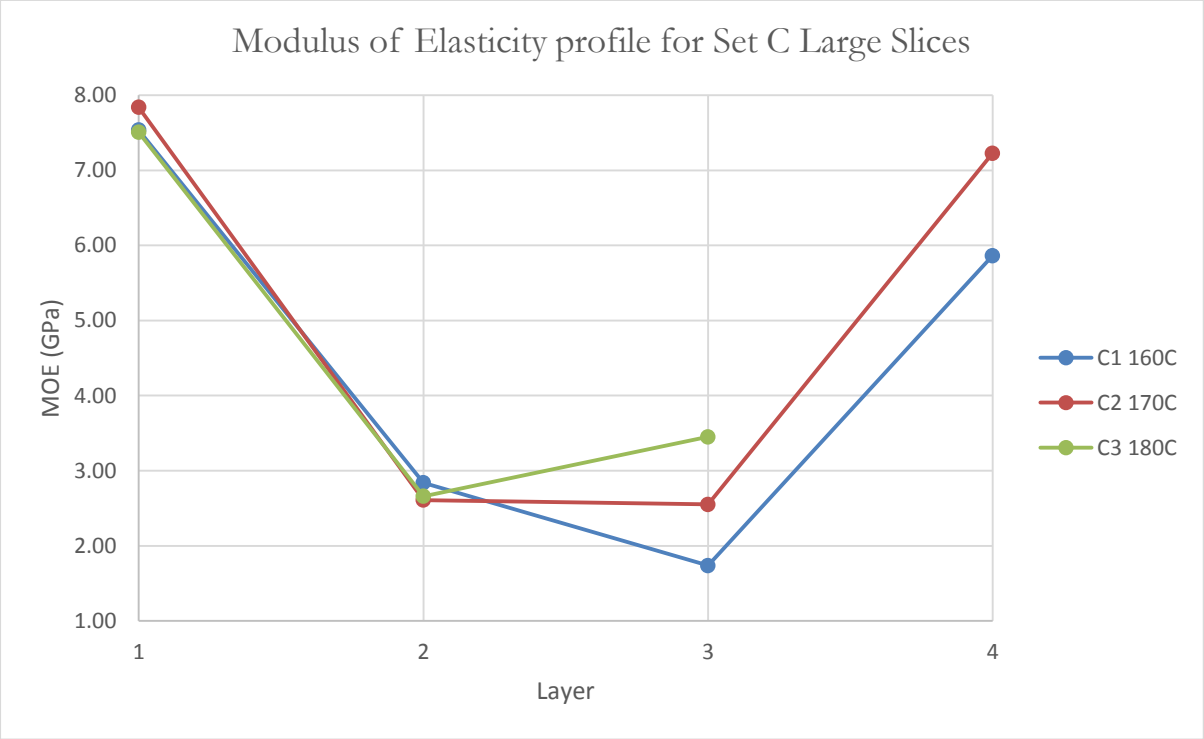

Figure 67: MOE profile for Set C based on large slices

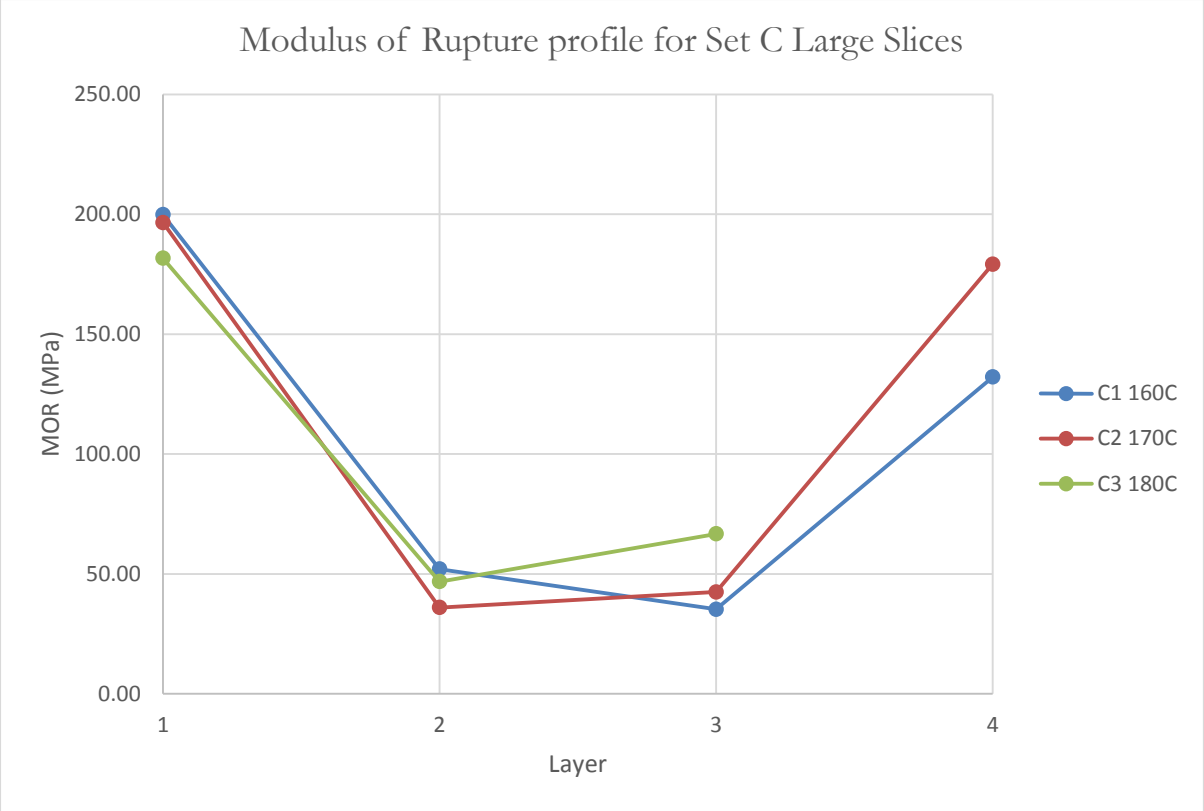

Figure 68: MOR profile for set C based on large slices

Note - C3-FL-4 was damaged during 3-point bend testing and so a data point for layer 4 in each of the profile graphs for board C3 would be missing. Also, a spare was not available for Instron testing. However strain was measured during making of the slices so a datapoint for that strain is present.

Figure 4-21 shows MOE profiles and Figure 4-22 shows MOR profiles for set C based on large slices. Its can be clearly seen that all three board samples almost follow a similar curve for both modulus of elasticity and rupture profiles. The three profiles have a high degree of overlap so it is difficult to predict a trend based on temperature although there is an observation that can be noted from the profiles. They all start at about the same value for Layer 1 but as further layers are investigated, boards C2 and C3 overtake board C1 in MOE and MOR values indicating that strength does increase with higher hot press temperature.

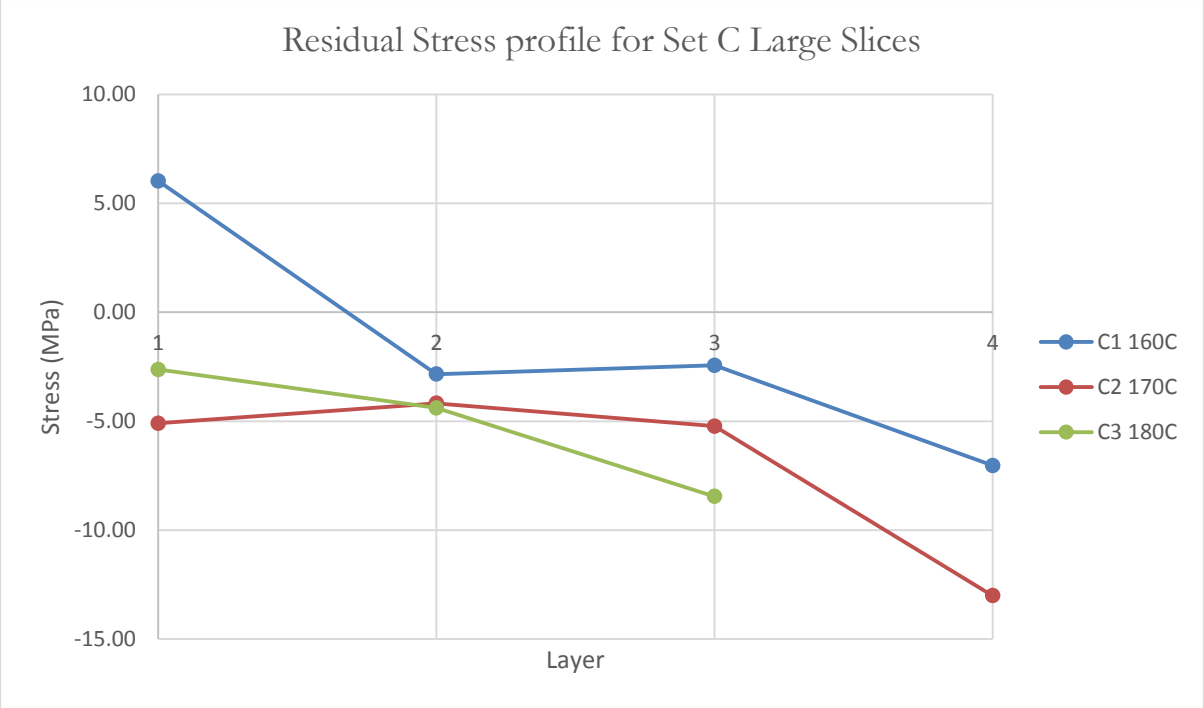

Figure 69: Residual stress profile for set C based on large slices

Figure 4-23 shows the residual stress profiles for Set C board samples. Board C1 shows tensile stress in the top fibre layer but decreased almost stepwise to a negative stress. One common feature that can be observed is that as the layers are investigated further, the stress is becoming more compressive. Boards C2 and C3 show the most compression. Their top layers are more compressive C1's top layer and consecutive layers continue to be more negative as compression increases. Table 4-10 shows that the maximum stress difference and asymmetrical distribution show that C1 is the most unstable being 13.07 MPa for both values. Residual stresses are caused by temperature gradients and this experiment set's case, they pertain to the difference between the hot press temperature and the temperature gradient created between the layers. The maximum strain difference and asymmetrical distribution make C3 the best and C1 the worst in this set. This is due to the fact that higher temperatures play a role in relieving residual stresses within the Triboard and add to its stability thus making it less likely to warp.

Table 26: Mechanical properties for set C based on large slices

Sample no.	Press Temperature (°C)	Average MOE for whole board (GPa)	Maximum Residual Stress Difference (MPa)	Asymmetrical distribution (MPa)	Average MOR for whole board (MPa)
C1	160	4.49	13.07	13.07	104.78
C2	170	5.06	8.83	7.92	113.53
C3	180	4.54	5.83	-2.63	98.37

4.6 Set C – Small Slices

4.6.1 Moisture Content Profiles and Average Moisture Content

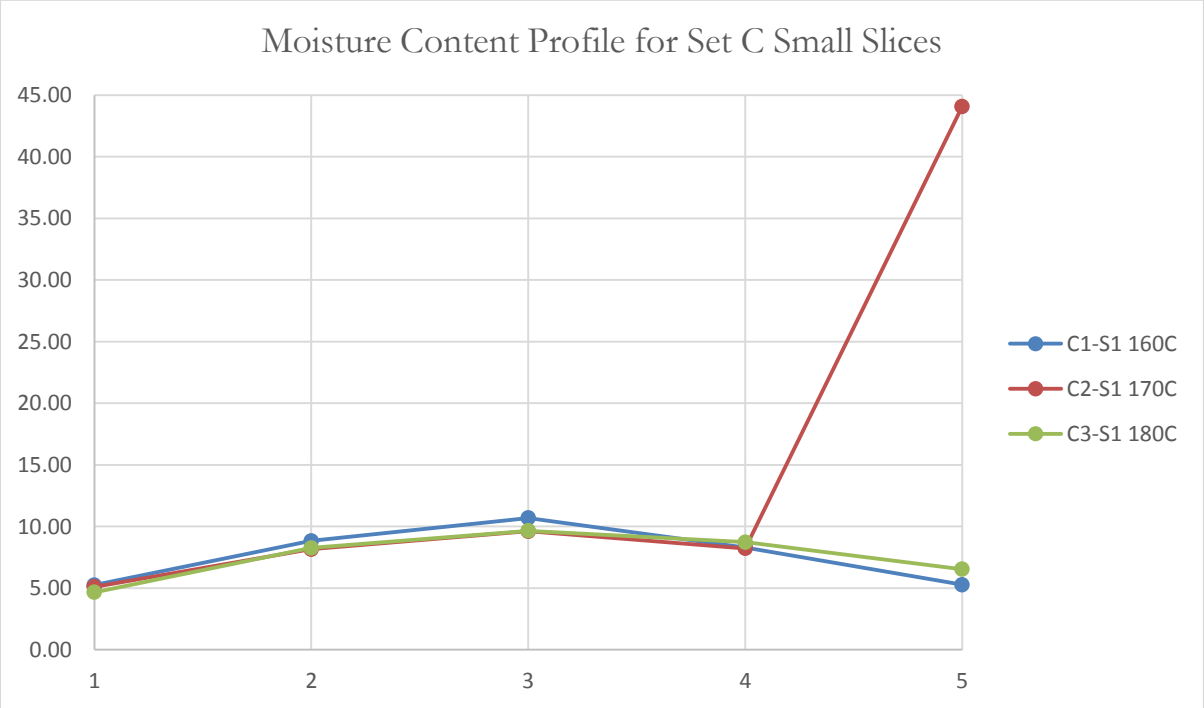

Figure 70: Moisture content profile for set C small slices

Figure 4-24 shows the moisture content profiles of Set C based on oven drying of small slices and Table 4-11 shows the average moisture contents for the boards. All three board moisture content profiles look very similar except board C2 bottom fibre layer which showed very high moisture content had an average moisture distribution for the board of 11.51% while boards C1

and C3 had a similar moisture content profiles. From these results, it is difficult to establish a relation between hot press temperature and moisture distribution of the board. It can be seen from Table 4-9 that large and small slices agree on the moisture content profiles, both suggesting that Moisture Content decreases with increase in hot press temperature.

Table 27: Average moisture content in set C board samples based on measured moisture contents of small slices

Sample no.	pMDI Loading on strand	Press Temperature (°C)	Average Moisture Content of board sample % (dry basis)
C1	88 g (5.2%)	160	8.20
C2	90 g (5.3%)	170	11.51
C3	86 g (5.1 %)	180	6.02

4.6.2 Profiles of Strain and Residual Stress

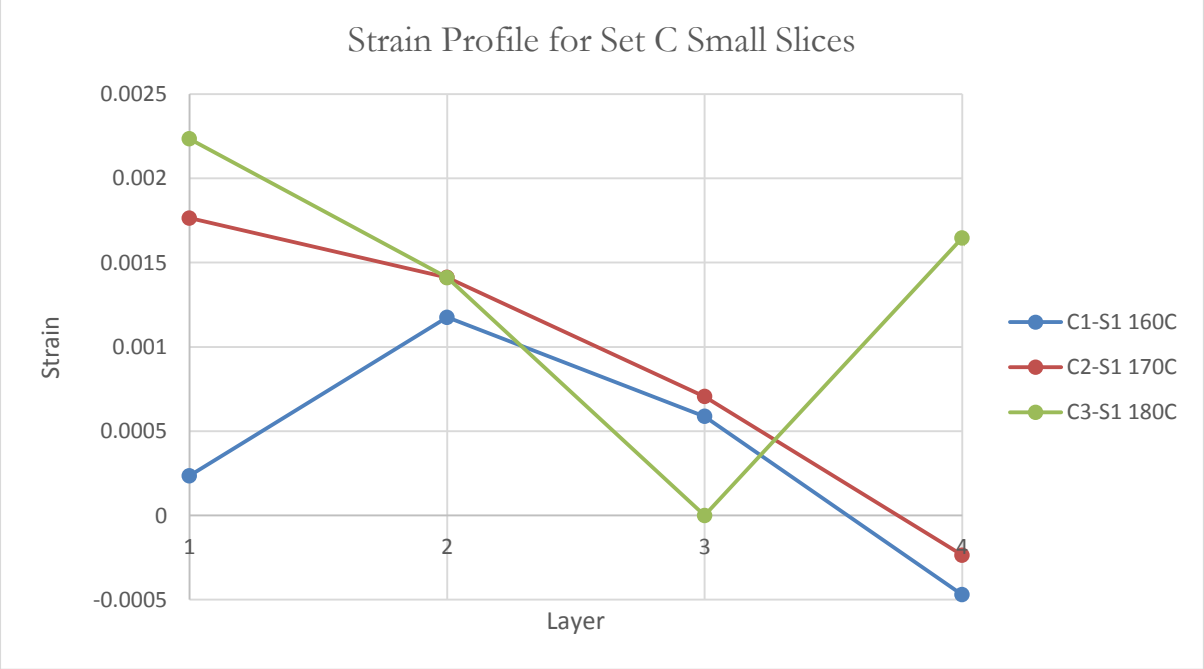

Figure 71: Strain profile for set C based on small slices

The strain profile for small slices for Set C boards are shown in Figure 4-25. These profiles are quite different from the strain profiles of large slices. Board C1, in Figure 4-20, shows a negative strain in top layer and then increases to tensile stress in layers 2, 3, and 4 whereas the small slices

show that board C1 has a slight positive strain and increases then decreases to a negative strain. This difference is also seen in C2 and C3 when both C2 and C3 are seen to be becoming more positive in large slices but more negative in smaller slices. The results in Figure 4-25 are less reliable since they do not show a trend as clear as Figure 4-20 for large slices and show more randomness.

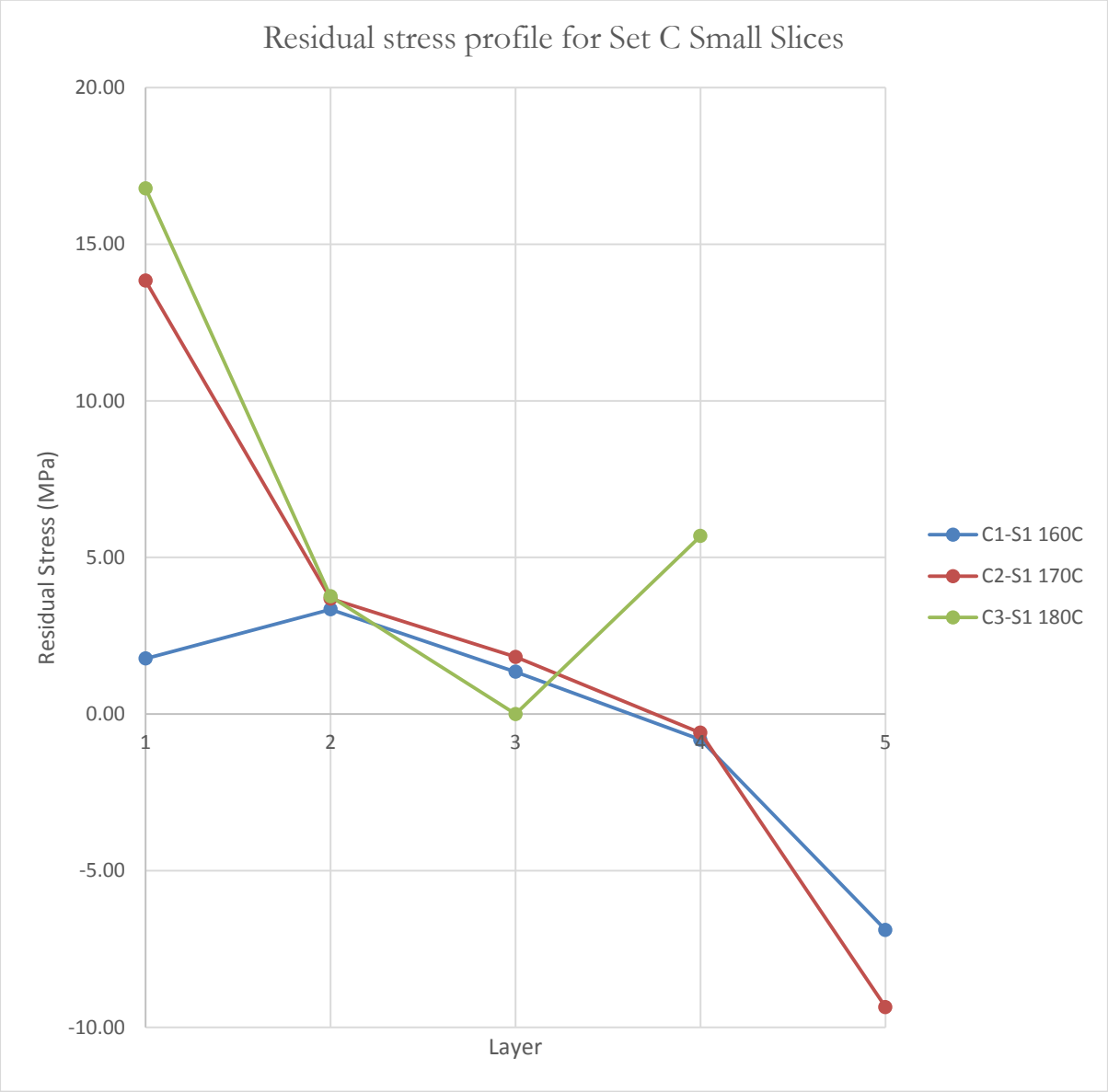

Figure 72: Residual stress profile for set C small slices

The residual stress profiles for small slices of Set C boards can be seen in both Figure 4-26. All three boards show a decrease in stress starting after high positive stress in Layer 1. The tensile stress increasing within the board due to temperature doesn't seem to agree with results in Figure

4-26 since there is high amount of overlap in stresses of Layers 2, 3 and 4. Large slices show a different behaviour where more compressive behaviour is noted rather than tensile although it is difficult to state that this is a trend as not enough temperatures were investigated in this experiment. According to Figure 4-26, board C1 had the most balanced stresses as it does not have slopes as sharp stays in between low tensile and compressive stresses in contrast to boards C2 and C3 which have very sharp decrease in stresses after the first layer. Table 4-12 shows the Maximum residual stress difference and asymmetrical distribution. Those results make board C1 the best (10.23 MPa and 8.66 MPa respectively) and board C2 the worst (23.19 MPa for both values) according to results obtained from small slices. Also, small slices show much less symmetry and higher strain differences in comparison to large slices which make them different from large slices results' and unreliable.

Table 28: Maximum stress difference and asymmetrical stress distribution for set C based on small slices

Sample Identification	pMDI Loading on strand	Press Temperature (°C)	Maximum Stress Difference (MPa)	Asymmetrical Distribution (MPa)
C1	88 g (5.2%)	160	10.23	8.66
C2	90 g (5.3%)	170	23.19	23.19
C3	86 g (5.1 %)	180	16.78	16.78

4.7 Set D – Large Slices

4.7.1 Moisture Content Gradient and Average Moisture Content

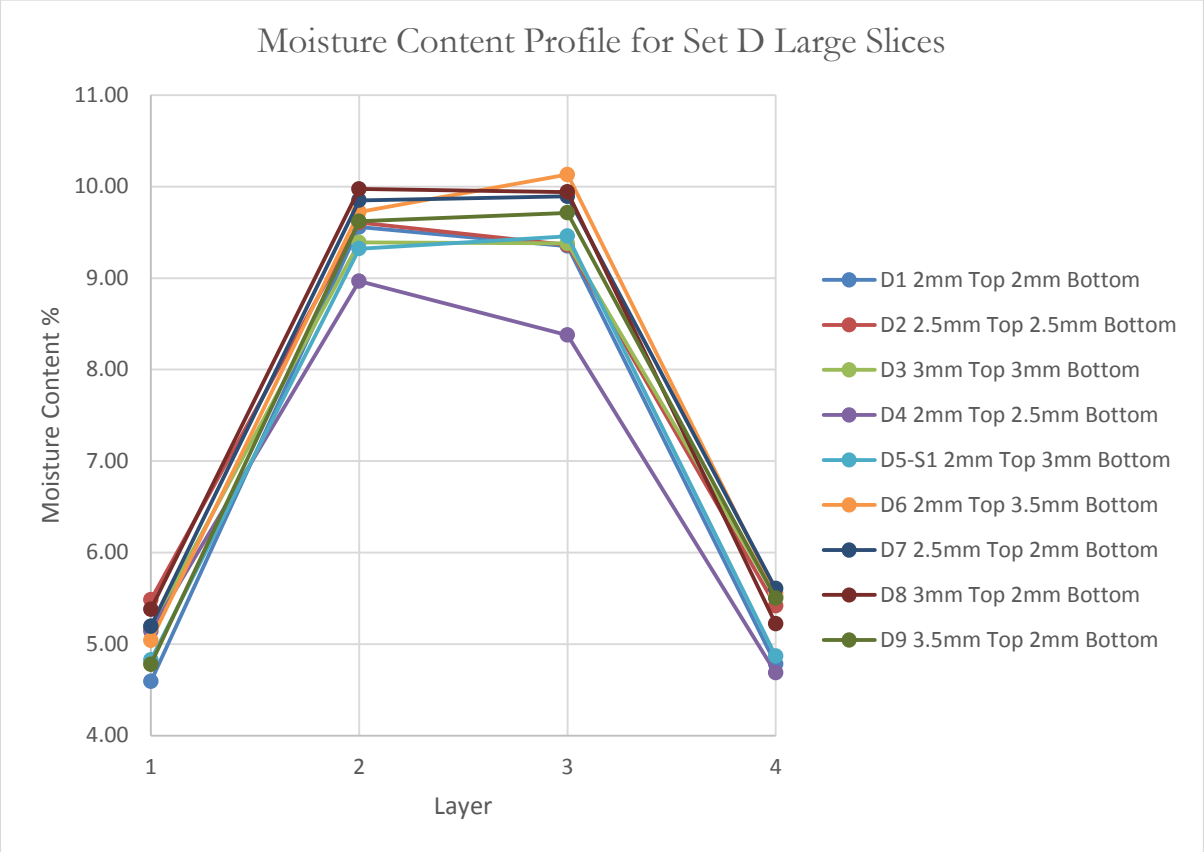

Figure 73: Moisture content profile for set D large slices

Figure 4-27 shows the moisture content profiles for Set D. There is a high degree of overlap between all the profiles which makes it difficult to spot a trend in terms of variation in fibre layer thickness. Average moisture content results in Table 4-13 shows that the moisture content% is observed to be going up with increasing fibre layer thickness in some samples. Moisture content does not show large variation and stays between 6.79% and 7.64%.

Table 29: Average moisture content in set D board samples based on measured moisture contents of large slices

Sample Identification	MDF layer thickness (mm)	Average Moisture Content for sample board % (dry basis)
D1	L1–L2*: 2 - 2	7.07
D2	L1-L2: 2.5 – 2.5	7.47
D3	L1–L2: 3 – 3	7.37
D4	L1–L2: 2 – 2.5	6.79
D5	L1-L2: 2 – 3	7.12
D6	L1–L2: 2 – 3.5	7.61
D7	L1–L2: 2.5 – 2	7.64
D8	L1-L2: 3 – 2	7.63
D9	L1–L2: 3.5 – 2	7.40

*L1 = top MDF layer; L2 = bottom MDF layer.

4.7.2 Profiles of Strain, Stress and MOE

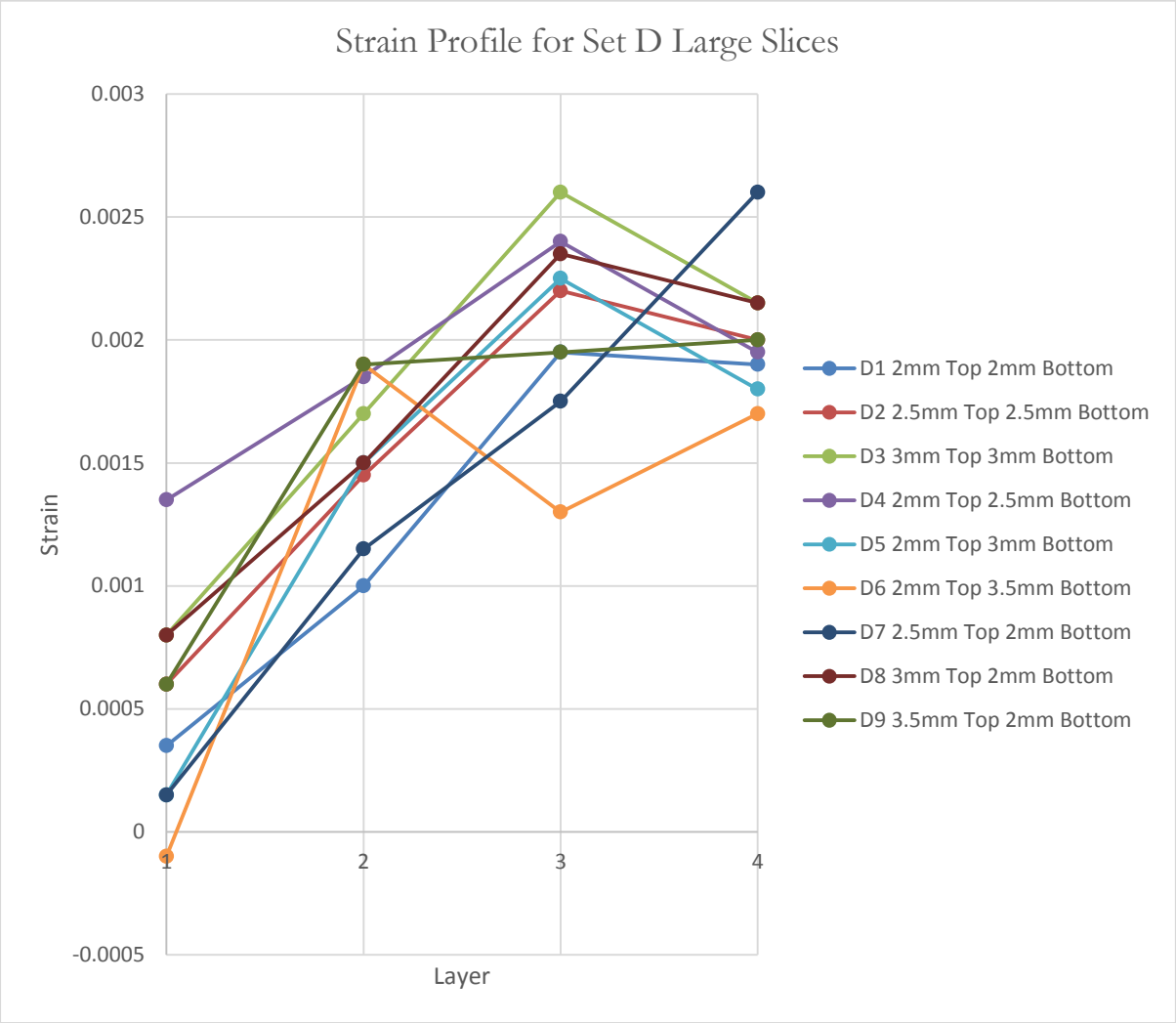

Figure 74: Strain profile for set D based on large slices

Figure 4-28 shows the strain profiles for Set D board samples. The strain seems to be clearly increasing as the fibre layer thickness is increased (per layer) and overall the strain is positive for all board samples. This trend is more prominent in board samples D1, D2 and D3 since there are increases in thicknesses on both top and bottom layers for these while other samples only have one-layer increase in thickness. In Figure 4-28, there is only layer 1 of D6 which shows a negative strain while all other layers of all other samples show highly positive strain. Also Layer 4 in some boards shows much higher strain regardless whether it has the same or different thickness than Layer 1.

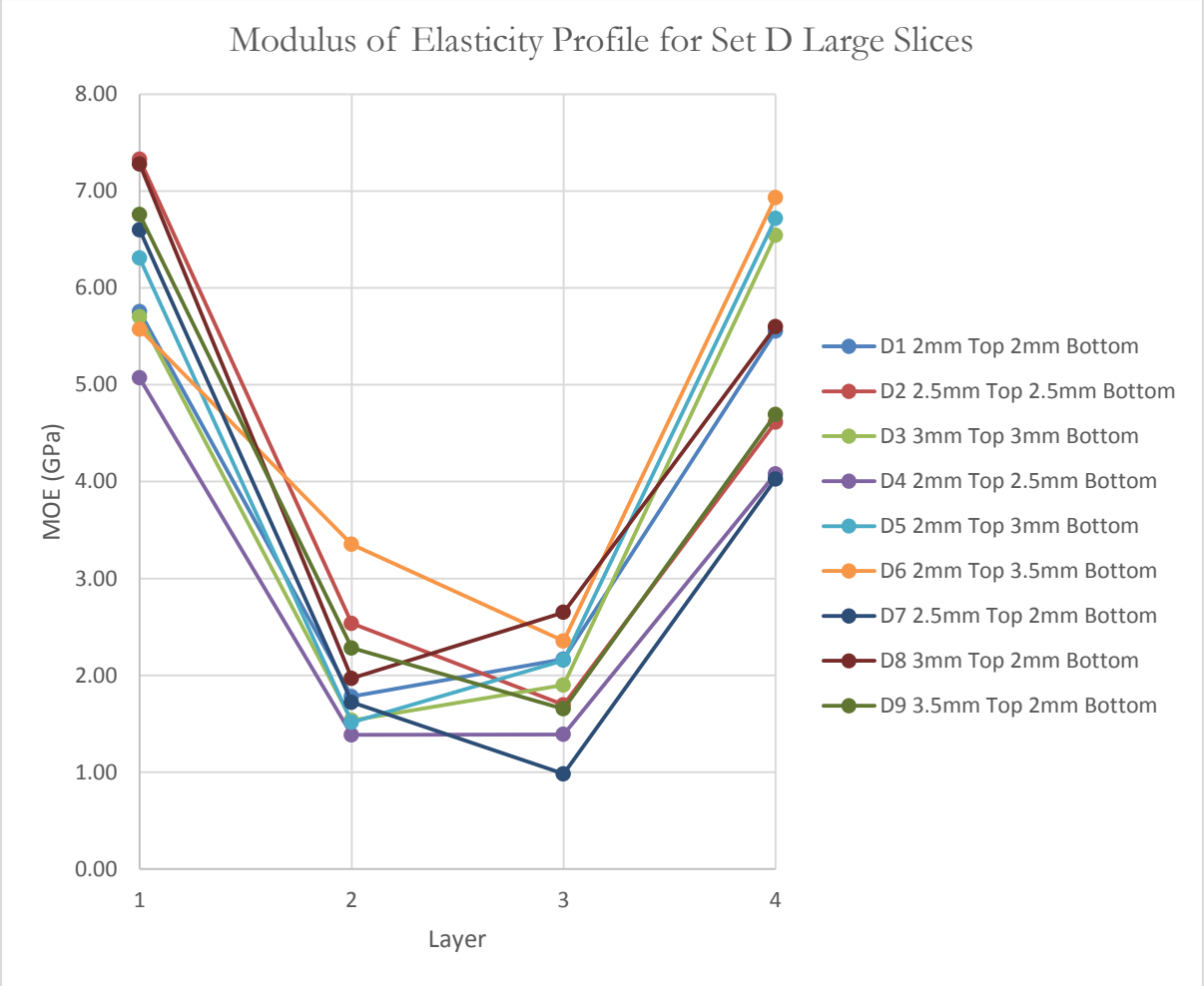

Figure 75: MOE profile for set D based on large slices

Figure 4-29 shows the MOE profiles for Set D boards and Table 4-14 shows the mechanical properties of Set D board samples based on large slices. The average MOE average for board D6 (2 mm MDF on top and 3.5 mm on the bottom) is observed to be the highest at 4.55 MPa and board D4 (2 mm MDF on top and 2.5 mm on the bottom) shows the lowest at 2.98 MPa. Also boards with layer thicknesses lower than these two has higher average MOE values, so it is difficult to follow a trend on basis of layer thickness. This is also due to the fact that there is a certain randomness in the average MOE values. There is a rise and then a fall in the MOE values as the thickness is increased and decreased in the layers sequentially. For example, in board D2 there is an increase in the layer thickness of 1 mm per layer from board D1 and there is an increase in MOE value but then there is a decrease as another 1mm per layer increased in board D3. This means that additional thickness in the MDF layers is not necessarily promoting strength.

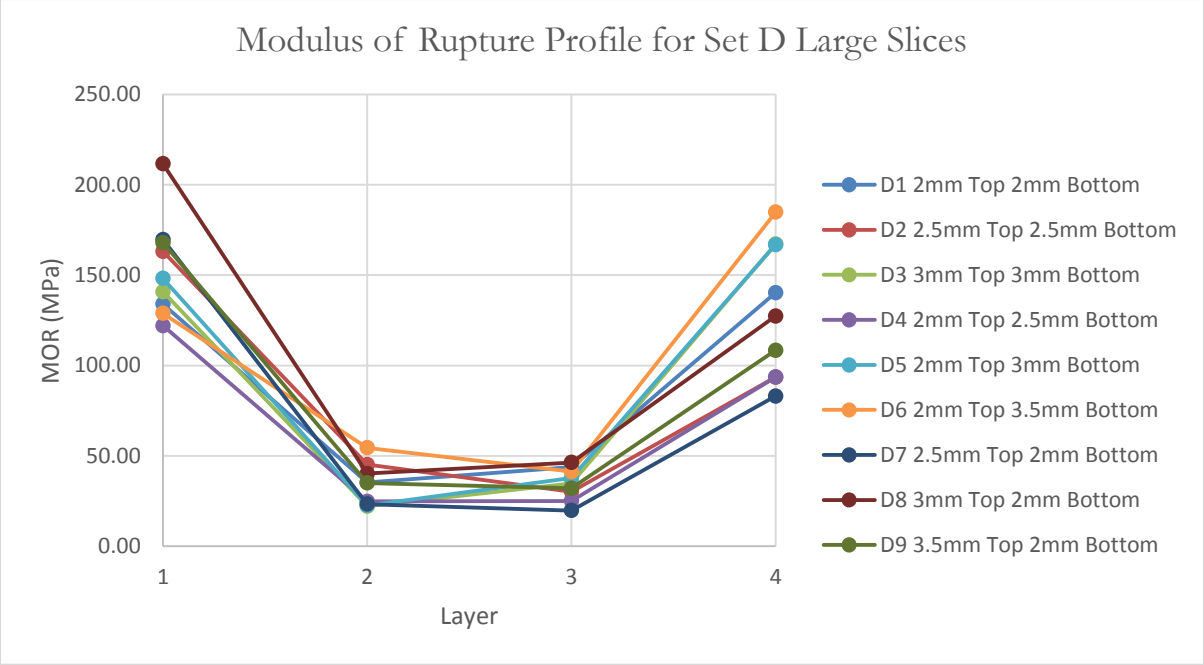

Figure 76: MOR profile for set D based on large slices

The MOR profiles for Set D can be seen in Figure 4-30. A similar observation can be made in case of MOR results. Overlapping profiles are observed and it is difficult to predict a trend and a randomness is prominent in MOR values recorded in Table 4-14. Highest MOR is observed in D8 of 106.36 MPa and lowest in D4 of 66.36 MPa.

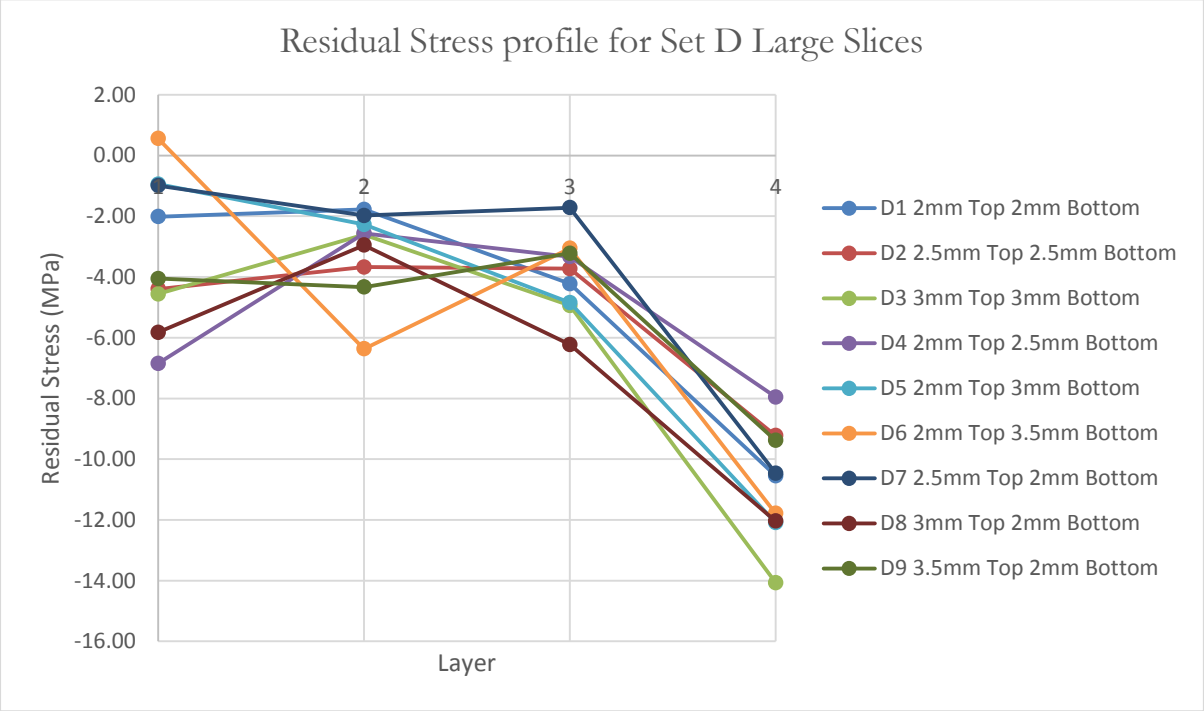

Figure 77: Residual stress profiles for set D based on large slices

The residual profiles observed in Figure 4-31 display increasingly compressive behaviour. Bottom fibre layers show high compressive stress but top fibre layer shows much less compressive/more tensile stress. Board D4 is the most stable board in this set since it shows the lowest residual stress difference and least asymmetrical distribution (5.39 MPa and 1.11 MPa respectively) and board D6 is the worst as it has the highest residual stress difference and highest asymmetrical distribution (12.34 MPa). As explained earlier, the MOE values are randomly scattered and this also affects the residual stress difference and asymmetrical distribution method of assessment whether the board is stable or not.

Table 30: Mechanical properties for set D based on large slices

Sample Identification	MDF layer thickness (mm)	Average MOE for whole board (GPa)	Maximum Residual Stress Difference (MPa)	Asymmetrical Distribution (MPa)	Average MOR for whole board (MPa)
D1	L1–L2*: 2 - 2	3.81	8.77	8.53	88.34
D2	L1-L2: 2.5 – 2.5	4.04	5.55	4.83	82.99
D3	L1–L2: 3 – 3	3.92	11.46	9.51	91.24
D4	L1–L2: 2 – 2.5	2.98	5.39	1.11	66.36
D5	L1-L2: 2 – 3	4.17	11.15	11.15	93.83
D6	L1–L2: 2 – 3.5	4.55	12.34	12.34	102.36
D7	L1–L2: 2.5 – 2	3.33	9.48	9.48	73.94
D8	L1-L2: 3 – 2	4.37	9.09	6.22	106.36
D9	L1–L2: 3.5 – 2	3.85	6.16	5.33	85.8

*L1 = top MDF layer; L2 = bottom MDF layer.

4.8 Set D – Small slices

4.8.1 Moisture Content profile

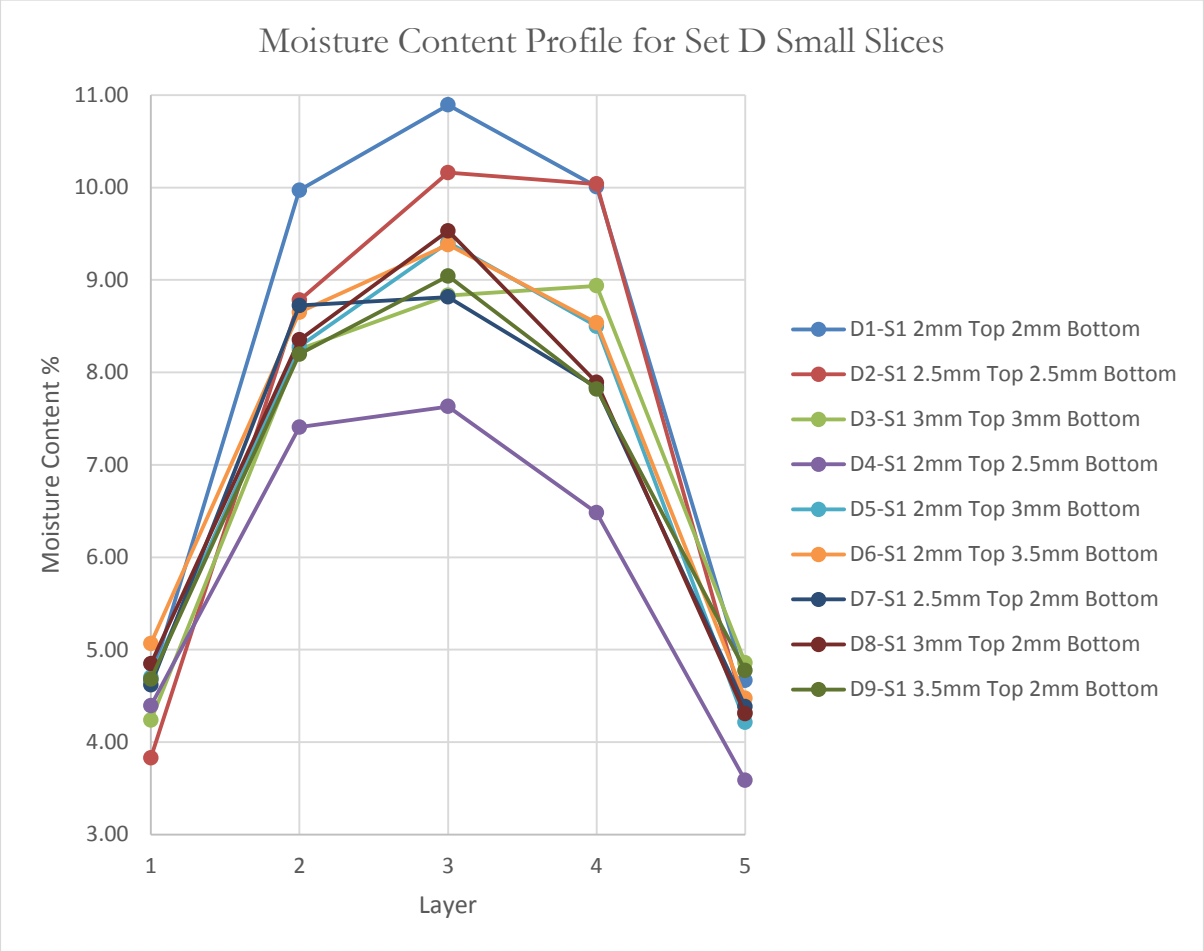

Figure 78: Moisture content profile for set D based on small slices

Figure 4-32 shows the moisture content profiles for Set D based on small slices. A thicker MDF layer should prevent moisture diffusion outside. The results do not seem to support this since all the boards have similar overlapping profiles with the moisture content for all boards lying between 3.5% and 5% for both top and bottom fibre layers. Looking at the Table 4-15, a slight decrease in moisture content is seen as the layer thickness is increased from 2 to 2.5 mm but increases again as the layer thickness is increases so results are ambiguous.

Table 31: Average moisture content in set D board samples based on measured moisture contents of small slices

Sample no.	MDF layer thickness (mm)	Average Moisture Content % for sample board (dry basis)
D1	L1–L2*: 2 - 2	7.22
D2	L1-L2: 2.5 – 2.5	7.27
D3	L1–L2: 3 – 3	9.23
D4	L1–L2: 2 – 2.5	6.50
D5	L1-L2: 2 – 3	7.13
D6	L1–L2: 2 – 3.5	9.26
D7	L1–L2: 2.5 – 2	7.02
D8	L1-L2: 3 – 2	9.52
D9	L1–L2: 3.5 – 2	6.99

Looking at average moisture content% in Table 4-15, it increases as the thickness goes up as observed in D1, D2 and D3 (increase in both top and bottom layers) and also in D4, D5 and D6 (increase in only bottom layer) as the layer moisture content% increases as the thickness of the layer increases while D7, D8 and D9 have an increase and then a decrease in D9. However, these results differ from those obtained from large slices as noted in Table 4-13 since moisture content varies from 7.07% to 7.64% in large slices but in small slices moisture content varies from 6.50% to 9.52%.

4.8.2 Strain and Stress Profiles

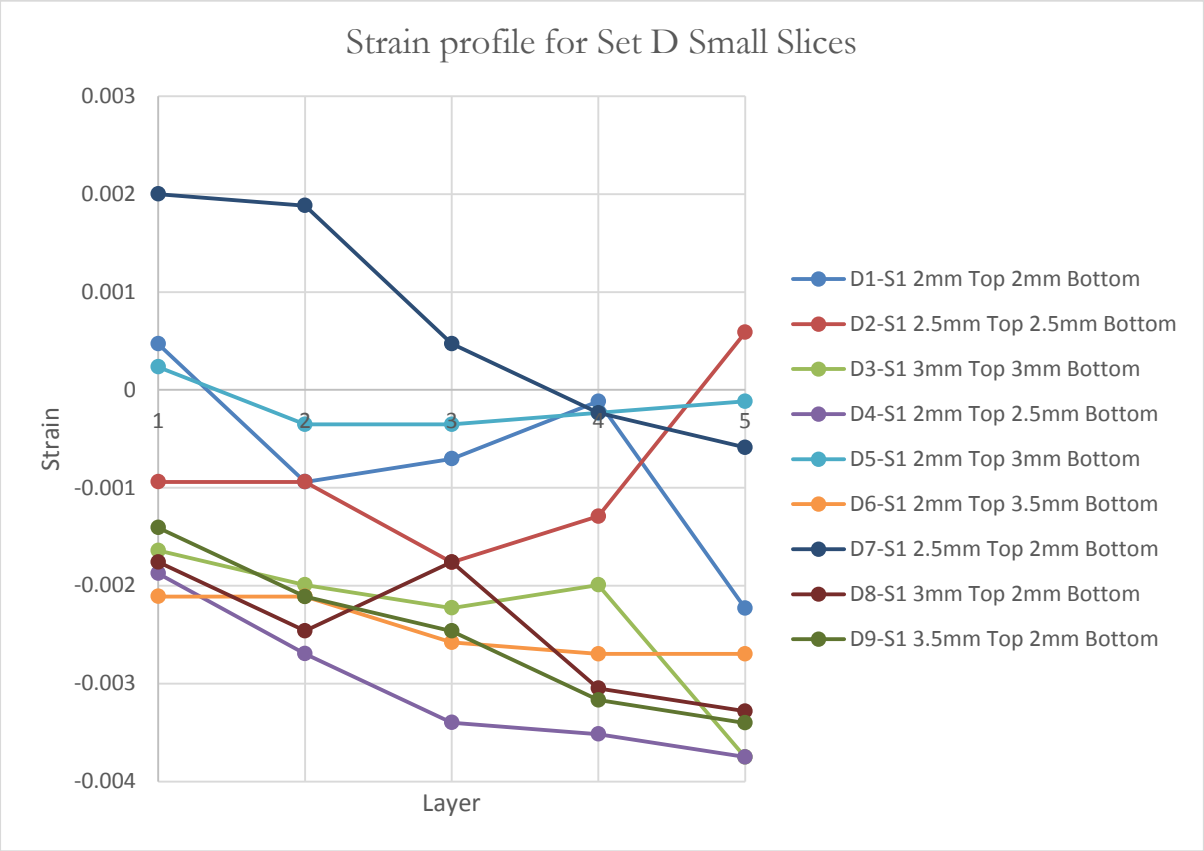

Figure 79: Strain profiles for set D based on small slices

Figure 4-33 shows the strain profiles for Set D board samples based on small slices. There is major contrast in strain profiles obtained for large and small slices. The strain profiles in Figure 4-28 show an almost linear increase in strain of the slices while Figure 4-33 pertaining to small slices show more of a low to high negative strain transition. Bottom fibre layers show more negative strain while top layers show less negative or more positive strain although the transition from top to bottom layers is not very smooth. D5 shows very little strain compared to the others (observe in Figure 4-33 that the profile for D5 is almost a straight line on the x-axis; strain is negligible at -0.0002) while D4 shows the most negative strain in this set.

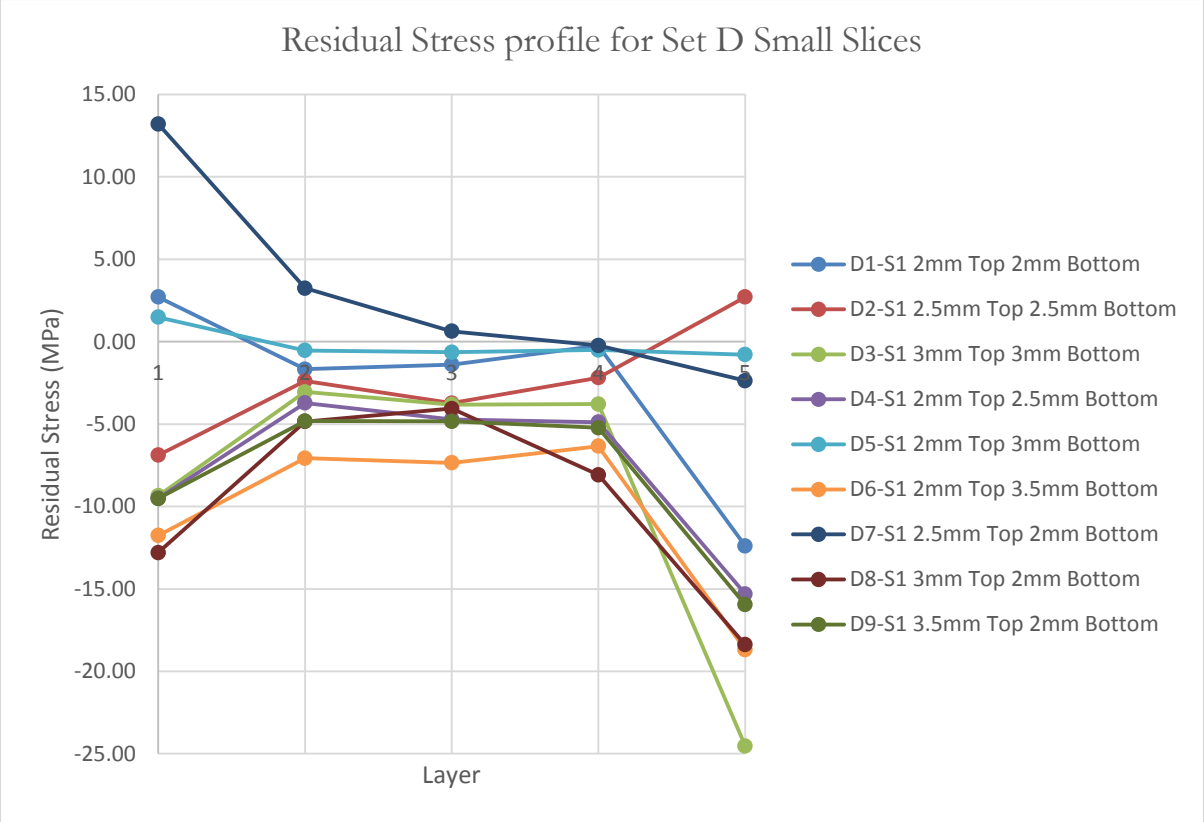

Figure 80: Residual stress profile for Set D based on small slices

Figure 4-34 shows the Residual Stress profile for Set D based on small slices and Table 4-16 shows the maximum residual stress differences and asymmetrical distributions of board samples. Board D5 shows the least stress difference in this set and the least asymmetrical distribution at 2.27 MPa for both making it the best in Set D. Board D3 is the worst since it has the highest stress difference and along with it the highest asymmetrical distribution (21.49 MPa and 15.18 MPa respectively). These results are different from those of Set D obtained from large slices but the best thickness variation in the MDF layer would be to have the bottom layer 0.5 mm to 1 mm thicker than the top MDF layer.

Table 32: Maximum residual stress and asymmetrical distribution of set D based on small slices

Sample no.	MDF layer thickness (mm)	Maximum Residual Stress Difference (MPa)	Asymmetrical distribution (MPa)
D1	L1–L2*: 2 - 2	15.09	15.09
D2	L1-L2: 2.5 – 2.5	9.59	-9.59
D3	L1–L2: 3 – 3	21.49	15.18
D4	L1–L2: 2 – 2.5	11.58	5.79
D5	L1-L2: 2 – 3	2.27	2.27
D6	L1–L2: 2 – 3.5	12.35	6.93
D7	L1–L2: 2.5 – 2	15.58	15.58
D8	L1-L2: 3 – 2	14.32	5.58
D9	L1–L2: 3.5 – 2	11.14	6.44

CHAPTER 5

CONCLUSIONS AND FUTURE WORK

From this masters project, the best and worst conditions/recipes can be obtained based on both large and small samples sizes that were tested. These have been assessed with profiles of residual stress of those samples. In addition, explanation and analysis are performed on the best sample that could possibly be applied to the current JNL Triboard recipe for the least warp. Finally, future work is recommended to further reduce Triboard warping.

5.1 A COMPARISON OF THE BEST AND WORST SAMPLES FROM EACH SET BASED ON LARGE SLICES

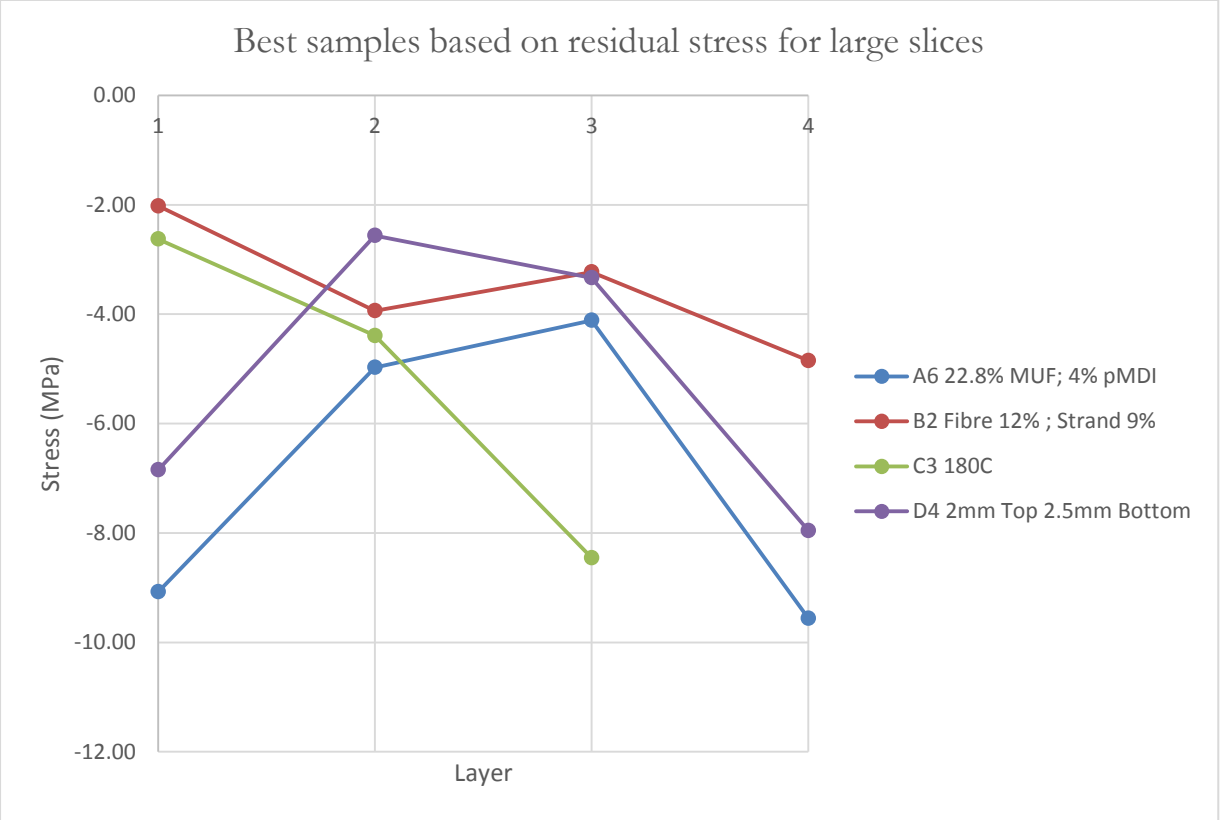

Figure 81: Best samples based on residual stress for large slices

Based on the residual stress profile, the best samples are those for which the stresses are most symmetrical or the difference between the maximum stress and the minimum stress is the

lowest. From this criteria, the best samples are A6, B2, C3 and D4, each representing one series of experiments, and their residual stress profiles shown in Figure 5-1.

based on measurements obtained from large slices. Board A6 is regarded as the best sample based on symmetrical profile of the residual stresses although it shows the most compressive stresses on two surface layers (layer 1 and layer 4). Board B2 has the lowest difference between the maximum stress and the minimum stress within the board as shown in the figure. The profile for Board C3 is not complete (due to slice getting damaged during mechanical testing) but it still gives better results compared to C1 and C2 which had much higher stress differences and higher asymmetrical distributions. Board D4 is also regarded as one of the best samples as it also gives the best symmetrical stress profile although it was not as good as Board A6. This indicates that boards A6 and D4 are most likely to have the least warp. The detailed values for stress differences and asymmetrical distribution are given in Table 5-1.

Table 33: Maximum residual stress difference and asymmetrical distribution of best samples based on large slices

Sample no.	Variation in Triboard recipe	Maximum Residual Stress Difference (MPa)	Asymmetrical distribution (MPa)
A6	**Adhesive loading**: 22.8% MUF; 4% pMDI	5.45	0.48
B2	**Moisture change:** Fibre 12%; Strand 9%	2.83	2.83
C3	**Hot press Temperature:** 180^0C	5.83	-2.63
D4	**Fibre Layer Thickness:** 2 mm Top; 2.5 mm Bottom	5.39	1.11

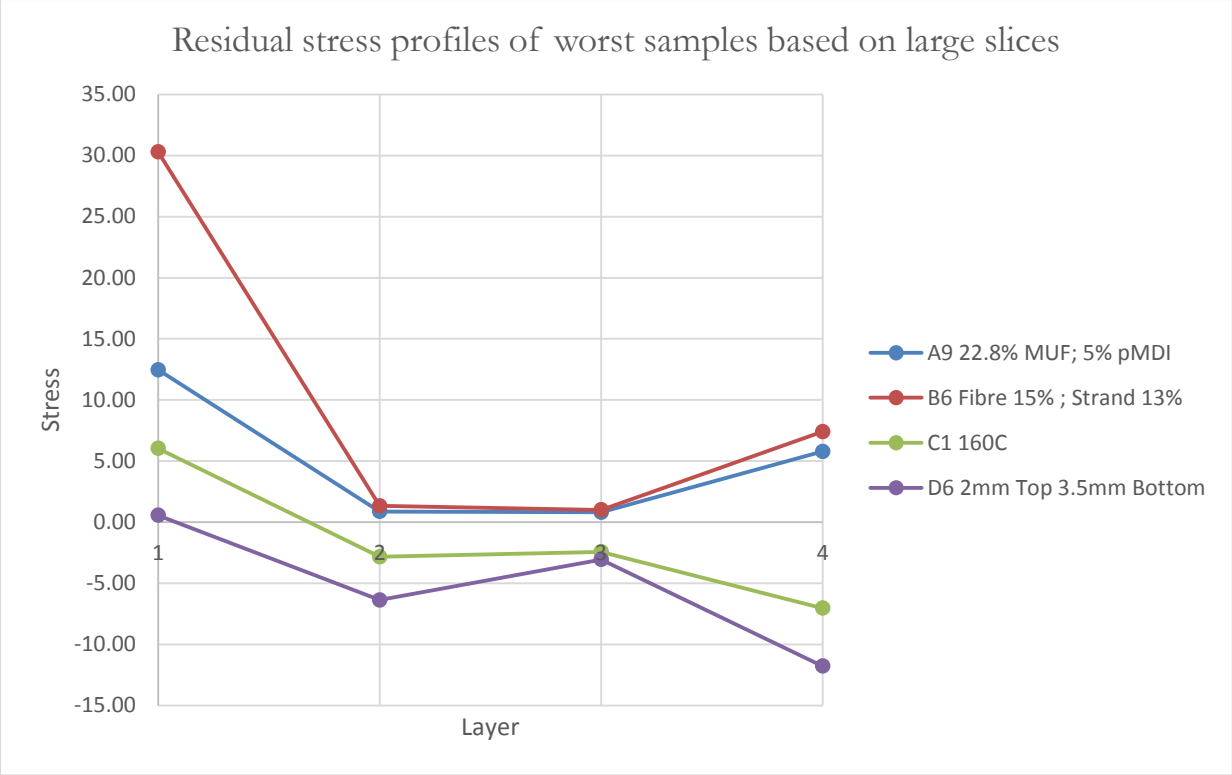

Figure 82: Worst samples based on residual stress for large slices

Figure 5-2 and Table 5-2 show the residual stress profiles for board samples A9, B6, C1 and D6, again each representing one series of experiments, which are regarded as the worst samples with the same criteria as described in previous section of this chapter. Board B6 displays worst behaviour as it has the highest residual stress difference and very poor symmetry (stress difference between two surface layers was 23 MPa). Therefore, this board with the highest moisture content both in the fibres (15%) and in the strands (13%) is most likely to warp. C1 is the worst sample for the set C series of experiments in which the effect of hot pressing temperature was examined. This worst board was made at the lowest hot pressing temperature of 160^0C. Among the four worst samples shown in Figure 5-2, Board A9 has the least difference between the two surface layers and the lowest difference between the maximum stress and the minimum stress, however, the Board A9 is still the worst in this series of experiments in which the adhesive loading was tested. Board A9 is still the worst in this series of experiments in which the adhesive loading was tested. Board A9 has a high adhesive loading for the strands at 5% pMDI.

Table 34: Maximum stress difference and asymmetrical distribution of worst samples based on large slices

Sample no.	Variation in Triboard recipe	Maximum Stress Difference (MPa)	Asymmetrical distribution (MPa)
A9	**Adhesive loading**: 22.8% MUF;5% pMDI	11.66	6.68
B6	**Moisture change:** Fibre 15%; Strand 13%	29.28	22.88
C1	**Hot press Temperature:** 160^0C	13.07	13.07
D6	**Fibre Layer Thickness:** 2 mm Top; 3.5 mm Bottom	12.34	12.34

5.2 A COMPARISON OF THE BEST SAMPLES FROM EACH SET BASED ON SMALL SLICES

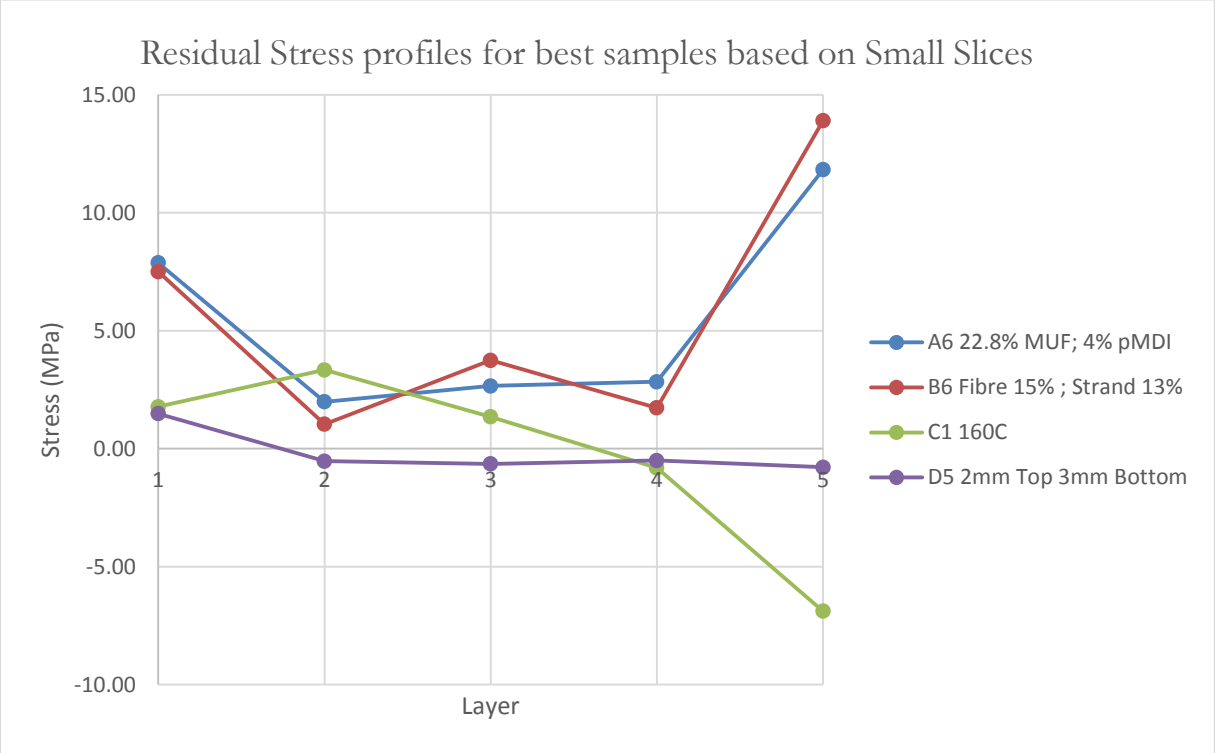

Figure 83: Best samples based on residual stress for small slices

Figure 5-3 and Table 5-3 show the residual stress profiles for sample boards that were considered the best based on the criteria described in Section 5.1 from the small slice tests, each sample representing one recipe series. By comparing the results in Figure 5-1 and those in Figure 5-3, it is found that small slices gave a different result from the large slices. However, Board A6 is regarded as the best sample from both tests of large slices and small slices. Board A6 from small slices tests show that both tests of large slices and small slices. Board A6 from small slices tests show that the maximum compressive stress in its first layer was about 8 MPa and shows a gradual decrease and then an increase in the bottom layer with over 12 MPa stress making it the most stable and symmetrical in Set A. The A6 board sample is the only one that is in agreement with Set A large/small slices.

A similar profile is seen for Board B6 where layer 1 shows tensile stress of about 8 MPa and steadily increases up to a tension in layer 5 of close to 15 MPa making it the most stable and symmetrical in Set B. Board B6 has the highest moisture content both in the fibre layer and in the strand layer.

Board C1 shows high compressive stress in Layer 5 of about -7 MPa and the highest tensile stress of 2 MPa in Layer 1 while hot press temperature was at 160^0 C which was the lowest temperature investigated.

Board D5 shows almost a flat profile having very low tensile stress in Layer 1 and very low compressive stress in Layer 5, and thus this board has the lowest stress difference and the most symmetrical stress distribution. By considering the results of both large slices and small slices, it is most likely that the stability of the boards can be improved with the top fibre layer being 0.5 to 1 mm thinner than the bottom fibre layer. However, the difference should not be greater than 1mm although the exact reason for this is unknown.

Table 35: Maximum stress difference and asymmetrical distribution of best samples based on small slices

Sample no.	Variation in Triboard recipe	Maximum Residual Stress Difference (MPa)	Asymmetrical Distribution (MPa)
A6	**Adhesive loading**: 22.8% MUF; 4% pMDI	9.84	-3.95
B6	**Moisture change:** Fibre 15%; Strand 13%	12.86	-6.39
C1	**Hot press Temperature:** 160^0C	10.23	8.66
D5	**Fibre Layer Thickness:** 2 mm Top; 3 mm Bottom	2.27	2.27

5.3 EXPLANATION BASED ON LAB RESULTS WITHIN SETS

It is possible to gain some insight into the Triboard warping problem based on the results obtained from the experimental work done at AICA in October 2015. Four parameters were investigated including adhesive loading, moisture content before hot-press, hot-press temperature and fibre layer thickness. Although warping could not be observed due to the small size of the board, its stability was measured using two values namely maximum stress difference and asymmetrical distribution.

In Set A, where effect of adhesive loading was observed, board A6 with 22.8% MUF loading on MDF layer gave the most stable board with a stress difference of 5.45 MPa and asymmetrical distribution of 0.48 MPa whereas board A5 gave the least stable board and had an MUF loading of 18.2% on MDF layer. In contrast, JNL uses 12% MUF on the fibre layer. The results from Set A are highly conclusive of higher MUF loading producing a more stable board.

Set B investigated the effect of moisture added to fibres and strands pre-pressing. The results are in agreement with the company recipe since the best board produced was Board B2 from the large slices tests, which had a fibre moisture of 12% and strand moisture of 9%. This board had a stress difference and asymmetrical distribution of 2.83 MPa. JNL's recipe uses 11% moisture content in fibres 8% moisture content in strands.

Set C results show that a hot press temperature of 180^0C produced the most stable board with a maximum stress difference of 5.83 MPa and asymmetrical distribution of 2.63 MPa. The lowest temperature investigated was 160^0C. This temperature produced the most unstable board in this set since its maximum stress difference and asymmetrical distribution of 13.07 MPa. This was mainly due to the boards internal stresses relieved at a higher temperature. Another factor to keep in mind is the press cycle time. JNL uses a temperature of 170^0C for 412 seconds while in these experiments, a press cycle time of 500 seconds was used.

Set D explored the effect of fibre layer thickness on Triboard stability while keeping constant core strand thickness. Board D4 recipe gave the most stable board with 2 mm on top layer and 2.5 mm on bottom layer. The maximum stress difference was 5.39 MPa and asymmetrical distribution was 1.11 MPa which made it the most balanced board in Set D. The worst board in Set D was board D6 which had 2 mm fibre on top layer and 3.5 mm fibre on the bottom layer. It had a maximum stress difference and asymmetrical distribution of 12.34 MPa. So having too much difference between top and bottom layer fibre layers could seriously change direction of

warping. This is in agreement with tests conducted by JNL (Trial Report). JNL managed to get an upward curve (positive warp) on their Triboard samples with an additional 2 kg on top of the layer. The results from Set D support the fact that fibre layer on top should be at the most 1mm thinner than the bottom fibre layer. Table 5-4 shows a comparison of recipes that is currently employed by JNL plant and those that produced the most stable board.

Table 36: A comparison of recipes based on JNL Triboard and experiment sets

Company Recipe	Best Recipe based on Masters project
12% MUF Loading on Fibre layer	Board A6 – 22.8% MUF on Fibre layer
Press cycle time = 412 seconds Hot press temperature = 170^{0}C	Board C3 - Press cycle time = 500 seconds Hot press temperature = 180^{0}C
Fibre MC% prior to hot press = 11% Strand MC% prior to hot press = 8%	Board B2 - Fibre MC% prior to hot press = 12% Strand MC% prior to hot press = 9%
Fibre thickness =2.1 mm per side	Top Fibre layer thickness = (Bottom fibre layer thickness – up to 1mm)

5.4 MOISTURE CONTENT PROFILES OF SAMPLES

- In Set A, it has been observed that fibre layer moisture content and the board average moisture content increased with increase in adhesive (MUF) loading from the results of large slices. Board A7 (15.2% MUF) showed the lowest amount of average moisture content while board A3 (22.8% MUF) showed the highest average moisture content. Results from small slices show the same trend although the actual values of moisture contents were different from those of large slices.
- In Set B, board prepared with a higher moisture content show a higher average moisture content and higher moisture content gradient during hot pressing. Boards B1, B2 and B3 show a low moisture content and the rest show a high moisture content. Board B4 remains an anomaly since it shows a high average moisture content while the fibres had lower initial moisture content. Results from both large and small slices show similar results.
- For Set C, the moisture content profiles of small and large slices do not agree. The results obtained from large slices show that Boards C2 and C3 had almost the same moisture content profile while Board C1 had a higher moisture content profile. This indicates that more moisture was lost during hot pressing at higher temperatures. For the small slices the moisture contents of all slices were almost similar except for Board C2 which shows a sharp increase in moisture content value in the bottom fibre layer.
- For Set D, results are ambiguous since with an increase in layer thickness there is an increase in average moisture contents in both large and small slices in some cases but not for all samples. Theoretically, a thicker fibre layer should reduce moisture diffusion more effectively than a thinner fibre layer since there is more matter for the moisture to penetrate. However, some sample did not show this trend which is highly possible to be due to the delay in testing samples after slicing.
- Warp is observed in a sample when the residual stresses are strong enough to overcome the structural integrity of the sample. It was difficult to observe any warping in the samples made I the experiments owing to the small board size. The Triboards which have been outlined as the best ones differ whether they are based on large or small slices but the large slices give more reliable results since they were sliced within a shorter period of time after the boards were prepared.

5.5 RECOMMENDATIONS AND FUTURE WORK

JNL has conducted studies studying the effects of shipping, improved wrapping, storage of panels and effect of varying MDF fibre layer thickness during the Triboard processing on Triboard stability. It has been found that only varying the fibre thickness had positive impact. From this masters project, recommendations are proposed as follows for future work on understanding and reducing the Triboard warping:

1. Humidity conditioning of Triboards so that the boards moisture content is close to equilibrium moisture content before warping and then wrapping.
2. Confirmation of best recipes at the plant and these are:
    a. Increasing adhesive loading for fibres (Board A6);
    b. Increase hot press temperature to 180^0C and the hold-up time (Board C3);
    c. Increase the bottom fibre layer thickness by 0.5-1 mm.
3. Incorporation of water/steam spray immediately after hot-pressing so that the surface moisture content will be increased and post-press moisture loss will be reduced.